



Contribution of Mitochondria to Insulin Secretion by Various Secretagogues

Petr Ježek,ⁱ Blanka Holendová,ⁱⁱ Martin Jabůrek, Andrea Dlasková, and Lydie Plecítá-Hlavatá

Abstract

Significance: Mitochondria determine glucose-stimulated insulin secretion (GSIS) in pancreatic β -cells by elevating ATP synthesis. As the metabolic and redox hub, mitochondria provide numerous links to the plasma membrane channels, insulin granule vesicles (IGVs), cell redox, NADH, NADPH, and Ca^{2+} homeostasis, all affecting insulin secretion.

Recent Advances: Mitochondrial redox signaling was implicated in several modes of insulin secretion (branched-chain ketoacid [BCKA]-, fatty acid [FA]-stimulated). Mitochondrial Ca^{2+} influx was found to enhance GSIS, reflecting cytosolic Ca^{2+} oscillations induced by action potential spikes (intermittent opening of voltage-dependent Ca^{2+} and K^{+} channels) or the superimposed Ca^{2+} release from the endoplasmic reticulum (ER). The ATPase inhibitory factor 1 (IF1) was reported to tune the glucose sensitivity range for GSIS. Mitochondrial protein kinase A was implicated in preventing the IF1-mediated inhibition of the ATP synthase.

Critical Issues: It is unknown how the redox signal spreads up to the plasma membrane and what its targets are, what the differences in metabolic, redox, NADH/NADPH, and Ca^{2+} signaling, and homeostasis are between the first and second GSIS phase, and whether mitochondria can replace ER in the amplification of IGV exocytosis.

Future Directions: Metabolomics studies performed to distinguish between the mitochondrial matrix and cytosolic metabolites will elucidate further details. Identifying the targets of cell signaling into mitochondria and of mitochondrial retrograde metabolic and redox signals to the cell will uncover further molecular mechanisms for insulin secretion stimulated by glucose, BCKAs, and FAs, and the amplification of secretion by glucagon-like peptide (GLP-1) and metabotropic receptors. They will identify the distinction between the hub β -cells and their followers in intact and diabetic states. *Antioxid. Redox Signal.* 36, 920–952.

Keywords: pancreatic β -cell metabolism, insulin secretion, redox signaling, mitochondrial Ca^{2+} transport, branched-chain ketoacid oxidation, fatty acid-stimulated insulin secretion, ATP-sensitive K^{+} channel, TRPM channels, GLP-1

Introduction

Mitochondria as metabolic and redox hub

MITOCHONDRIA HAVE BEEN recognized for seven decades as the metabolic and redox hub, not only providing cells with ATP but also with a plethora of metabolites and signaling mechanisms. Mitochondria cannot be ignored

in the majority of studies working toward understanding physiological and pathological mechanisms at the subcellular level. For pancreatic β -cells, the ultimate physiological role of mitochondria lies in the notoriously known elevation of ATP synthesis upon glucose-stimulated insulin secretion (GSIS). However, mitochondrial redox signaling is one of its recently discovered roles (104, 194), as well as the transport

Department of Mitochondrial Physiology, Institute of Physiology of the Czech Academy of Sciences, Prague, Czech Republic.

ⁱORCID ID (<https://orcid.org/0000-0002-2720-9395>).

ⁱⁱORCID ID (<https://orcid.org/0000-0002-3904-8189>).

© Petr Ježek *et al.*, 2021; Published by Mary Ann Liebert, Inc. This Open Access article is distributed under the terms of the Creative Commons License [CC-BY] (<http://creativecommons.org/licenses/by/4.0>), which permits unrestricted use, distribution, and reproduction in any medium, provided the original work is properly cited.

of Ca^{2+} across the inner mitochondrial membrane (IMM), synchronized with Ca^{2+} oscillations evoked by action potential firing, which are caused by the predominantly intermittent opening of voltage-dependent Ca^{2+} channels (Ca_V); in rodents, these are mostly L-type channels (Ca_L) (31, 91, 210, 212, 213).

The additional Ca^{2+} release is superimposed onto the primary Ca^{2+} oscillations incoming from the endoplasmic reticulum (ER) (49, 280) and other Ca^{2+} stores, such as insulin granule vesicles (IGVs) or lysosomes. By stimulating matrix dehydrogenases and adenylyl cyclase, the elevated matrix Ca^{2+} plays an important amplifying role during the first and second GSIS phase and during amplification mechanisms of insulin secretion, notably in incretin- (glucagon-like peptide [GLP-1]- and gastric inhibitory peptide [GIP]-) and metabotropic receptor signaling (71, 218).

We found that insulin secretion stimulated by branched-chain ketoacids (BCKAs) (194) and partly by fatty acids (FAs) (98, 103) essentially relies on mitochondrial retrograde redox signaling. Due to the relatively low content of cytosolic glutathione (17, 135–137, 270), the redox milieu of pancreatic β -cells promotes the signal spreading from mitochondria up to the targets within the plasma membrane, which can further switch-on Ca_V opening and action potential firing, followed by IGV exocytosis. It is unknown whether the redox signal spreading is enabled by a H_2O_2 diffusion or by a redox relay, for example, *via* peroxiredoxins, thioredoxins, or glutaredoxins, abundant in pancreatic β -cells (97, 204). In any case, β -cells appear to be a perfect redox system, ideally suited for redox signal conduction (105, 274). Nevertheless, the redox state is highly compartmentalized (17, 208).

Also, the specific metabolism of β -cells under fasting and fed conditions contributes *via* changes and the concomitant effects of NADH/NADPH homeostasis, as well as *via* the transport of various specific metabolites, for example, coenzyme A-esters (CoA-esters) of FAs, malonyl-CoA, and long-chain acyl-CoA as stimulating insulin secretion (196), formed from the matrix acetoacetate exported to the cytosol (52).

ATP-sensitive K^+ channel as prerequisite for triggering of GSIS

Recently, we reported that GSIS essentially relies on the physiological cytosolic redox signaling provided by H_2O_2 produced by NADPH oxidase 4 (NOX4) upon glucose intake, followed by the branching of the glucose-6-phosphate (G6P) flux toward the pentose phosphate pathway (PPP) (Fig. 1) (194). The two PPP enzymes produce NADPH, and the elevation of their activities causes an instant elevation of H_2O_2 formation by NOX4. This new paradigm of the requirement of increased ATP plus increased H_2O_2 for insulin secretion in response to glucose was concluded from experiments in which NOX4-knockout mice (NOX4KO) or mice with NOX4, ablated specifically in pancreatic β -cells (NOX4 β KO mice), exhibited a completely suppressed first GSIS phase, whereas the second phase was only moderately attenuated (194).

The first phase was rescued by NOX4 overexpression in pancreatic islets (PIs) isolated from NOX4 β KO mice or by H_2O_2 addition (194). Moreover, the ATP-sensitive K^+ channel (K_{ATP}) (8) could not be closed after the glucose addition to the patch-clamped INS-1E cells silenced for

NOX4 (194). In contrast, INS-1E cells having vestigial ATP synthase lacking DAPIT and thus having crippled ATP synthesis still maintained GSIS (134).

The textbook paradigm stressed the key role of glucose triggering of the first GSIS phase [reviewed, *e.g.*, in Refs. (104, 210)]. Glycolysis followed by the oxidative phosphorylation (OXPHOS) and elevated synthesis of ATP has been considered to be the only required condition, similar to the exclusive role of K_{ATP} . In The Synergy of Membrane Channels section, we will discuss that even 100% closure of the ensemble of K_{ATP} is not enough for GSIS triggering. In contrast, certain forms of the maturity-onset diabetes of the young (MODY), that is, of monogenic type of diabetes mellitus, are exemplar cases supporting the important role of K_{ATP} .

Thus, homogeneous mutations in *Kcnj11* (a gene encoding the KIR6.2 subunit of K_{ATP} , when the KIR6.2 tetramer forms the physical channel) and more heterogeneous mutations in the *Abcc8* gene (encoding the regulatory subunits sulfonylurea receptor 1 [SUR1]) reduce the ability of ATP to cause channel closure (9). These mutations impair ATP binding at KIR6.2 or how ATP binding translates into the pore closure, respectively (128, 161, 232). They may enhance MgADP activation of SUR1 by increasing the affinity of the nucleotide-binding domains for nucleotides (185). Both mutations can increase the unliganded channel open probability, which leads to a decrease in both ATP and possible sulfonylurea block (11, 199). However, note also that in different MODY types different gene mutations occur (*e.g.*, glucokinase gene *GCK* or genes encoding transcription factors *HNF1 α /4 α* , *PDX*), all affecting insulin secretion.

In this review, all the above-described aspects of the mitochondrial physiology of pancreatic β -cells will be discussed, including the “logical summation” principle of metabolic plus redox stimulation for the mitochondrial source of H_2O_2 , which besides GSIS plays an essential role in insulin secretion stimulated by BCKAs (194) and partially by FAs (103). Without detailed knowledge of the redox system of pancreatic β -cells and their sensing of glucose or other secretagogues, the health issues that develop due to type 2 diabetes (107, 248) cannot be understood. Hence, we collected up-to-date knowledge on mitochondria as key players in the physiology of pancreatic β -cells and the pathology of diabetes.

Mechanisms of Insulin Secretion

Plasma membrane depolarization in pancreatic β -cells

The synergy of membrane channels. Quite recently, an explanation was suggested as to why a 100% closed K_{ATP} population is still insufficient to induce the threshold depolarization (–50 mV) of plasma membrane potential (V_p), required for Ca_V opening and thus for switching on action potential firing (119, 221). V_p should be shifted far more than enabled by the 100% K_{ATP} closure alone. This additional V_p shift can be facilitated by numerous “synergic” channels (210), namely by the opening of nonspecific calcium channels (NSCCs), such as transient receptor potential melastin (TRPM) channel-2 (TRPM2) (79, 123, 210, 285), or by the concerted action of chloride channels (45). Moreover, TRPM2 channels are activated by H_2O_2 (79, 84, 123, 223), hence they could theoretically also contribute to the “logical sum” of the redox plus metabolic (ATP) signal.

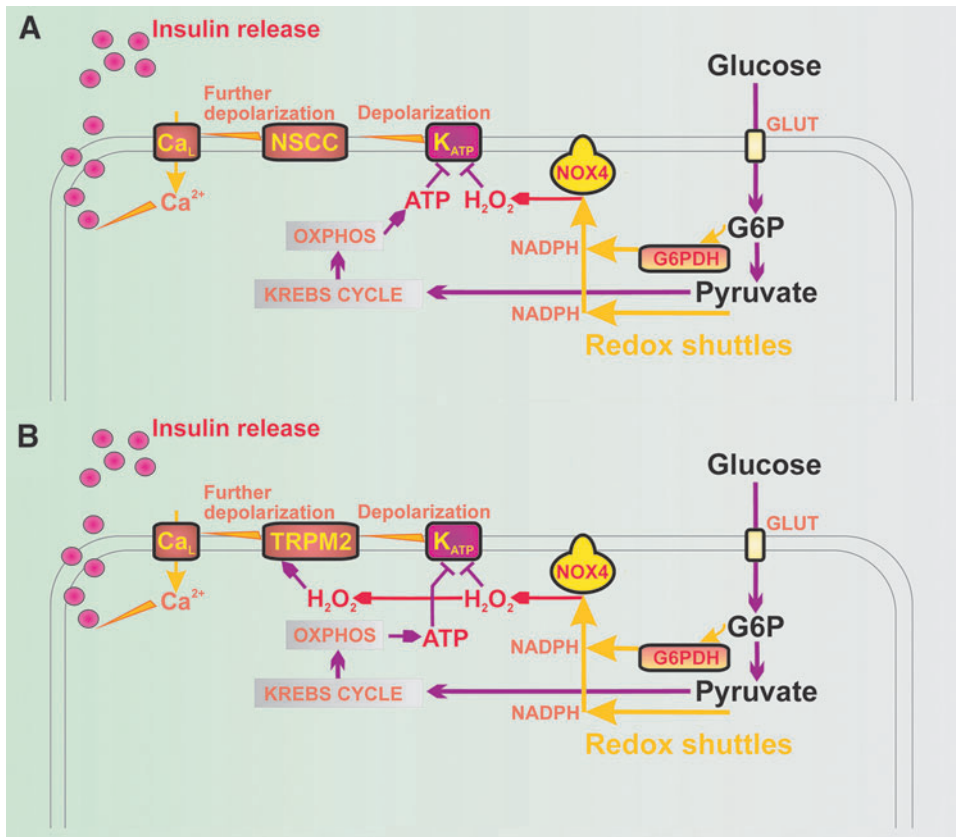


FIG. 1. Redox signaling triggers GSIS in parallel with ATP. (A) Hypothetical model based on Plecita-Hlavata *et al.* (194), in which only K_{ATP} is redox-regulated; K_{ATP} closure is only possible when H_2O_2 and ATP are elevated. (B) Extended hypothetical model, in which TRPM2 is also redox-activated. For an explanation, see the Introduction section and the Plasma Membrane Depolarization in Pancreatic β -Cells section. G6PDH, glucose-6-phosphate dehydrogenase; GSIS, glucose-stimulated insulin secretion; K_{ATP} , ATP-sensitive K^+ channel; TRPM, transient receptor potential melastin.

These “synergic” channels provide a small background inward current that cannot depolarize with an open K_{ATP} , but it is able to do so with a predominantly closed K_{ATP} ensemble since the NSCC conductance is then comparable to the small conductance provided by the remaining open K_{ATP} channels (K_{ATP} properties, Figs. 1 and 2). Also, the indirect inhibition of K_{ATP} by H_2O_2 was observed in smooth muscle cells (283).

The plasma membrane of β -cells possesses up to 60 channels belonging to 16 ion channel families (210, 280), with a distinct pattern in humans (101). Since the ~ 130 mM $[K^+]_{in}$ concentration inside the β -cell is much greater than outside ($[K^+]_{out} \sim 5$ mM), there would be an equilibrium resting V_p^{equi} of -82 mV, if only there was a K^+ -channel conductance. The actual $V_p^{resting}$ is -75 mV (49); hence, NSCCs and other channels should provide this shift since NSCCs conduct any Na^+ , Ca^{2+} , and K^+ . Evidence came from the observed depolarization reversal after the withdrawal of Ca^{2+} and Na^+ at a 10 mM concentration of glucose ($[glucose]$ in mouse β -cells (213). Without this NSCC conductance, the established V_p would only be equal to V_p^{equi} and the shift to -50 mV, required for Ca_v opening (212), would not take place, despite the 100% closed K_{ATP} ensemble (19, 119, 221, 239, 249, 280).

Besides there being a redox-activated TRPM2 channel (79, 123, 223), there are also the Ca^{2+} - and cAMP-activated TRPM4 and TRPM5 channels in rodent β -cells (119), plus the heat-activated transient receptor potential vanilloid 1 (TRPV1, capsaicin receptor), TRPV2, TRPV4, or transient receptor potential canonical 1 and 3 (TRPC1, TRPC3) channels. TRPC3 provides an additional shift upon G-protein-coupled receptor (GPR) 40 receptor activation by

FAs (276). Similarly, Cl^- channels (SLC12A, SLC4A, SLC26A, GABA_A, GABA_B, and glycine receptor Cl^- -channel) (45) and others (210) were implicated in V_p shifts, particularly volume-regulated anion channels (VRACs; *e.g.*, the leucine-rich repeat containing 8-isoform A; LRRC8A) (45, 246). TRPM2 is also activated by nicotinic acid dinucleotide phosphate (NAADP) (247), elevated upon GSIS (160, 285). Interestingly, TRPM2 was also reported to interact with peroxiredoxin 2, from which it can receive a redox signal (168, 186).

Action potential firing begins at $[glucose] > 6$ mM in mouse β -cells (49), stimulated by reaching a depolarization of up to -50 mV. Above -50 mV, Ca_v opening [predominantly Ca_L with minor contribution of R-, N-, and P/Q-type Ca^{2+} channels (228)] is intermittent with the opening of the voltage-dependent K^+ channels (K_v) in mice (150) or calcium-dependent K^+ channels (K_{Ca}) in humans (49) since K_v (K_{Ca}) opening terminates Ca^{2+} entry, but their time-dependent deactivation allows a new 30–40 ms spike (210). Also, Na^+ channels participate in upstrokes in a 30% β -cell population (289). Spikes return to a plateau V_p of -50 to -40 mV, the level of which is also adjusted by the two-pore K^+ channels TASK-1 and TALK-1 (50, 264). At 10 mM $[glucose]$, periods of a high and low frequency of action potential spikes exist, including burst and silent interburst phases (210).

The latter is explained by a transient ATP consumption by sarco/ER- Ca^{2+} -ATPase (SERCA) and plasma membrane Ca^{2+} -ATPase (PMCA), that is, ATPases removing Ca^{2+} (252, 253). At >20 mM glucose, ATP synthesis is thought to overcome its consumption, leading to a permanent action

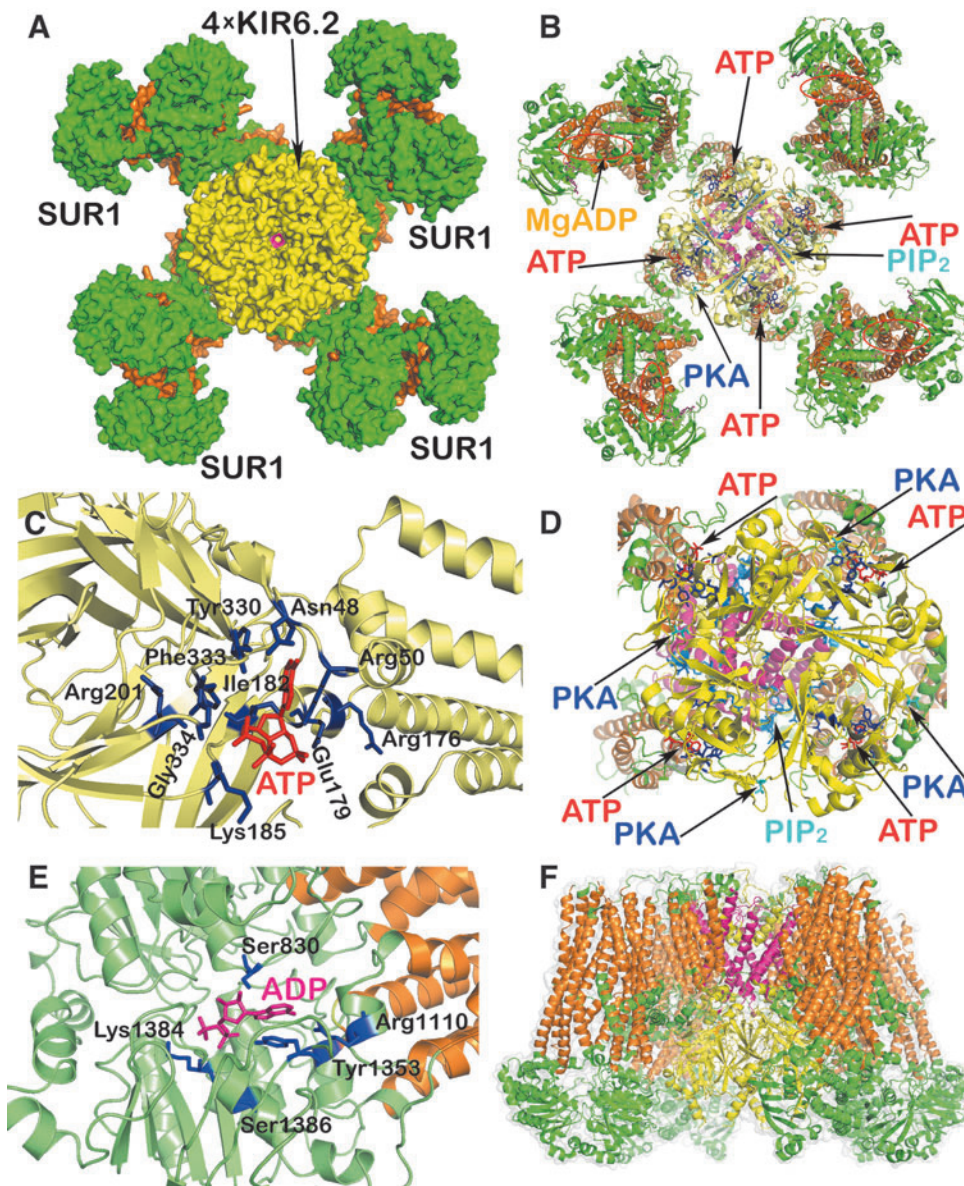


FIG. 2. K_{ATP} channel structure and regulation. Structures of both types of subunits of hetero-octameric K_{ATP} have been resolved, that is, the SUR1 (a product of *Abcc8* gene) and the pore-forming subunit, a potassium inward rectifier, KIR6.2 (*Kcnj11* gene) (101, 142, 159, 210). The displayed model of K_{ATP} channel was derived from the cryo-EM structure of the pancreatic ATP-sensitive K^+ channel SUR1/Kir6.2 in the presence of ATP and glibenclamide, pdb code 5twv (159), and cryo-EM structure of human K_{ATP} bound to ATP and ADP in quaternary form, pdb code 6c3o (131). The structure was visualized using the PyMOL Molecular Graphics System, Version 1.8 Schrödinger, LLC. (A) K_{ATP} channel from the intracellular site. (B) Visualization of the ATP and PIP_2 binding sites on the Kir6.2 subunits, Mg^{2+} -ADP binding pocket on the SUR1 subunits, and PKA interaction site within the Kir6.2. (C) Detail of the binding domain for ATP (in red) on the Kir6.2 subunit with interacting amino acid residues (in dark blue). (D) Detail of the Kir6.2 with ATP and PIP_2 binding domains and PKA interaction site. (E) Detail of the SUR1 Mg^{2+} -ADP binding site (in pink) with interacting amino acid residues (in dark blue). (F) Side view of the K_{ATP} channel; color coding: intracellular regions of Kir6.2 subunits in yellow, transmembrane domains in dark pink; intracellular domains of SUR1 subunits in green, transmembrane helices in orange. Four Kir6.2-subunits cluster together, forming the core of the $\sim 18 \times 13$ nm entire structure (166). The cytoplasmic Kir6.2 surface contains the ATP-binding site, implicated in the channel closing, exposed 2 nm below the membrane. An overlapping PIP_2 binding site stabilizes the open state. Upon PIP_2 release, the open probability decreases (14, 166, 234). The channel is closed as soon as the first ATP-binding site is occupied, one of four ATP-binding sites (179). Sensitivity to PIP_2 is regulated by the palmitoylation of Cys166 (277). Mg^{2+} -free ATP decreases the duration of channel openings, while periods of closing are longer (36), whereas $MgADP$ acts in the other direction (118). Artificial K_{ATP} openers (diazoxide) and K_{ATP} blockers, such as sulfonylureas (glibenclamide bound to SUR1), act independent of high ATP (233). Of the eight sites of four SUR1 subunits, each one bears an $MgATP$ - plus $MgADP$ -binding site. At the NBF1 of the former, $MgATP$ is hydrolyzed to $MgADP$, activating K_{ATP} at NBF2 and increasing the ATP-sensitive K^+ -conductance. This provides lower excitability and sensitivity to ATP inhibition (179). Already 5–15 μM ATP (IC_{50} 10 μM ; $\sim 25 \mu M$ with Mg^{2+}) closes the channel in inside-out patches, in which the medium affects the cytosolic side (35, 262). In contrast, in intact resting β -cells, much higher [ATP] is required to close K_{ATP} . IC_{50} of ~ 0.6 mM was found for the whole-cell patch-clamp mode (242). This low sensitivity is adjusted by the PKA phosphorylation of Thr224 (144) and Ser372, which increases the K_{ATP} open probability (16). Any further closing only occurs at higher [ATP] or even hypothetically requires H_2O_2 . NBF, nucleotide-binding fold; PIP_2 , phosphatidylinositol 4,5-bisphosphate; PKA, protein kinase A; SUR1, sulfonylurea receptor 1.

potential firing (49), upon which 100% of K_{ATP} channels close (210). The amplitude becomes reduced by 15 mV after ~ 3 min.

The resulting pulsatile Ca^{2+} entry elevates the cytosolic Ca^{2+} concentration $[Ca^{2+}]_c$. The accumulated Ca^{2+} pool acts simultaneously on the protein exocytotic machinery and thus stimulates the pulsatile Ca^{2+} -dependent exocytosis of IGVs (213, 214, 260). In human PIs, the threshold is -60 mV, the frequency of action potential spikes is higher, whereas 5 ms spikes are grouped into shorter ~ 2 s groups and their termination upon lowering glucose is slow (211). As for the [glucose] dependence in mice, 50% of K_{ATP} closing was already reported at 3 mM, keeping V_p constant; while at 5 mM 93% and at 10 mM 97% of K_{ATP} channels were closed (251). Thus, V_p depolarization is due to the closure of remaining $\sim 7\%$ K_{ATP} in mouse PIs when [glucose] is increased above 5 mM (235).

In mouse β -cells, Ca_v isoforms $Ca_v1.2$ and $Ca_v1.3$ are responsible for 50%, $Ca_v2.1$ for 15%, and $Ca_v2.3$ for 25% of the whole-cell Ca^{2+} current, which is activated at -50 mV (228). Interestingly, R-type $Ca_v2.3$ channels were reported to open exclusively during the second phase of GSIS (109). The protein kinase A (PKA) phosphorylation of $Ca_v1.2$ and $Ca_v1.3$ enhances their activity (122). Note that different groups of channels, not only Ca_v , are involved in action potential spikes in different species, cultured cells or even within individual cells of PIs (210), which is outside the scope of this review.

The deactivation of Ca_v is switched predominantly by the opening of $K_v2.1$ in rodents (150, 213) or $K_v2.2$ and $K_{Ca}1.1$ channels (BK channels) in humans (49, 101). A delayed rectifier K^+ current is induced at positive V_p down to -30 mV (215). The opening of $K_v2.1$ channels repolarizes V_p and thus closes Ca_v channels. The ablation of $K_v2.1$ reduced K_v currents by $\sim 80\%$ and prolonged the duration of the action potential, secreting more insulin. Mice with ablated $K_v2.1$ exhibited lower fasting glycemia, but elevated insulin, and improved GSIS (100). Interestingly, glucose, glyceraldehydes, and 2-ketoisocaproate (KIC) were reported to increase K_v currents (284).

Ca^{2+} oscillations. Besides synergy with other channels, Ca_v opening intermittent with K_v opening leads to V_p oscillations (action potential firing) (91), which induce primary oscillations in $[Ca^{2+}]_c$ (210). The latter is further modulated by a Ca^{2+} efflux from the ER (49, 280), lysosomes, IGVs, or mitochondria (see the Mitochondrial Ca^{2+} Signaling in Pancreatic β -Cells section). However, the ER Ca^{2+} efflux cannot be initiated without the preceding primary Ca_v -mediated Ca^{2+} influx. The two components are superimposed, that is, fast cytosolic Ca^{2+} oscillations with 2–60 s periods and slow Ca^{2+} oscillations with periods reaching up to several minutes (15, 73). The resulting complex Ca^{2+} oscillations finally induce pulsatile insulin secretion. One can predict more IGVs to be secreted with a higher time-integrated cytosolic Ca^{2+} concentration.

Basic mitochondrial contribution to insulin secretion

ATP supply and its regulation in pancreatic β -cells. Undoubtedly, increasing ATP synthesis by OXPHOS with increasing [glucose] is the first prerequisite for GSIS (152,

156). OXPHOS respiration is determined as the oxygen consumption rate (OCR). The OCR of cultured β -cells or PIs, incubated with low (insulin nonstimulating) [glucose], increases after further glucose elevation (193). Simultaneously, mitochondrial IMM potential $\Delta\Psi_m$ also increases, indicating that the OCR increase is not due to uncoupling (protonophoric action), but stems from faster ATP synthesis, while the respiratory proton pumps are fully coupled *via* the protonmotive force ($\Delta p = \Delta\Psi_m + \Delta pH$) to the H^+ backflow through the ATP synthase.

OXPHOS can be semiquantified, when accounting for the ratio (R_r) of OCR to OCR_{Oligo} . OCR_{Oligo} values of nonphosphorylating respiration are set by oligomycin, blocking the ATP synthase, hence driven by the H^+ leak. For rat INS-1E cells, the ratio R_r exhibits a sharp increase between 3 and 8 mM [glucose] with AC_{50} at ~ 3.5 mM and saturation at >8 mM [glucose] in INS-1E cells (193). This AC_{50} roughly corresponds to the half-maxima of the surplus in the total cell ATP and in the insulin secretion rate (116). For human healthy and diabetic PIs, AC_{50} of 4.4 and 5.5 mM were found, respectively (47).

The parameter A_r , where $A_r = (OCR - OCR_{Oligo})/OCR_{FCCP}$, follows a very similar relationship to AC_{50} (193), reflecting the fraction of the maximum respiration (OCR_{FCCP}) capacity used for ATP synthesis. The extent of this sharp increase in R_r or A_r perfectly correlates with the [glucose] range for which 50%–100% closure of the K_{ATP} ensemble proceeds, despite different ranges for rat *versus* mice *versus* human PIs (see The Synergy of Membrane Channels section). With oligomycin, the closure of the K_{ATP} ensemble in INS-1E cells is incomplete (194).

When a major fraction of ATP synthase molecules are incapable of synthesizing ATP in INS-1E cells, such as upon silencing of the subunit DAPIT, GSIS is virtually unchanged, although elevations of ATP were only $\sim 10\%$ of those in nontransgenic cells (134). This interpretation stems from the reasoning that the second leg required for GSIS (*i.e.*, redox signaling) was preserved, and the established lower ATP was able, together with H_2O_2 , to close K_{ATP} (or simultaneously open TRPM2).

With isolated rat PIs, elevations from resting 2 mM up to insulin-stimulating 4 mM [ATP] (at 10 mM [glucose]) were found (43), while AC_{50} at ~ 3 mM was reported for the total ATP rise and 50% K_{ATP} closure in mouse PIs, not correlating with AC_{50} of ~ 12 mM for GSIS (210). Perhaps specific AC_{50} for the first phase should be considered. In α -toxin-permeabilized PIs, the 84% K_{ATP} closure occurred already at 1 mM ATP (251). The perfusion of human PIs with up to 7.5 mM [glucose] leads to $\sim 30\%$ of maximum GSIS (267), with insulin release observed beginning at 3 mM (89). In humans, blood glycemia of 7.5 mM stimulates a fivefold increase in insulin (266). Note that there is no sudden increase in glucose after a meal in humans, instead glycemia increases over ~ 30 min from ~ 5 to 8 mM (61).

Description of the diabetic phenotype is out of scope in this review [but cf. Refs. (5, 17, 107, 248)]. Type 2 diabetes etiology originates not only from the impaired molecular mechanisms of insulin secretion but also from low-grade inflammation causing insulin resistance and promoting β -cell oxidative stress, ER stress, and cell death. Pancreatic β -cells first attempt to compensate the glucotoxic metabolic demand by enhancing their mass, which also elevates insulin

production. Still, their exhaustion induces further pathogenesis, impaired β -cell biogenesis, leading to dedifferentiation and dysfunction (20). This further deteriorates insulin secretion. During the β -cell mass expansion phase of the type 2 diabetes development, the first GSIS phase is often missing, whereas the second phase is enhanced and prolonged, so higher time-integrated insulin release exists. This was therefore termed hyperinsulinemia (117).

Regulations of ATP synthase by ATPase inhibitory factor 1. Searching for factors that adjust the [glucose] range to the sensing one (3–8 mM in INS-1E cells), we found ATPase inhibitory factor 1 (IF1) to be a key element (115, 116) (Fig. 3). This regulation adds to well-known settings of the sensing [glucose] range due to other factors, including the proper K_m of rodent glucose transporter GLUT2/SLC2A2 (human GLUT1/SLC2A1), K_m , and the lack of product inhibition for glucokinase, existing smooth fluxes of glycolysis that supply the Krebs cycle, followed by the efficient supply

of substrates (NADH, succinate) for the respiratory chain and OXPHOS (227, 290). Note that glucokinase is considered a glucose sensor. This notion is supported by its importance since inactivation of both glucokinase alleles leads to the maturity-onset diabetes of the young type 2 (MODY-2). Nevertheless, this causes defective K_{ATP} regulation (205).

IF1 was thought to be able to only inhibit the reverse mode of the ATP synthase, in which H^+ ions are pumped into the intracrystal space (ICS) across the c-subunit-ring of the membrane F_O moiety, whereas the energy is supplied by ATP hydrolysis to ADP ongoing at the F_1 moiety. This is unlikely in primary cells; in cancer cells, this mode is mixed with the regular ATP synthesis (269).

However, evidence was found for the inhibition of ATP synthesis by IF1 *in vivo* (115, 116). A mild partial inhibition of a fraction of the ATP synthase (Fig. 3) may just set the proper glucose-sensing range in pancreatic β -cells. With silenced IF1 in INS-1E cells, the insulin secretion dependence on [glucose] was shifted far left with $AC_{50} \sim 1$ mM (115). A similar shift with increasing [glucose] was observed for the

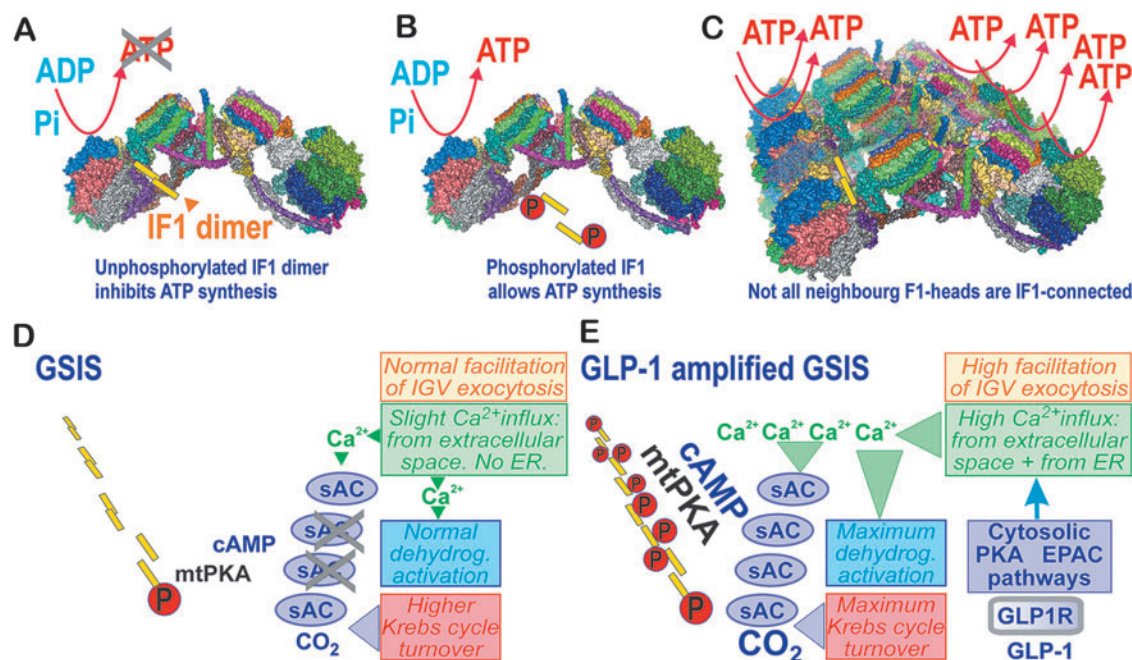


FIG. 3. IF1 adjusts glucose-sensing concentration range being hypothetically regulated by PKA upon GSIS and its amplification by GLP-1. (A, C) Inhibitory binding of nonphosphorylated IF1 dimer within structure of ATP synthase dimer (A) and four adjacent ATP synthase dimers (C), within model of crista segment. (B) Inability of phosphorylated IF1 to bind and inhibit ATP synthase. (D) Hypothetical phosphorylation of small fraction of IF1 molecules upon GSIS, when mild activation of the soluble adenylyl cyclase within mitochondrial matrix (mt-sAC) produces proper cAMP levels, required to adjust the accurate proper IF1 phosphorylation by the mitochondrial matrix PKA. Mt-sAC is activated by the increased CO_2 due to a higher Krebs cycle (glucose metabolism) turnover upon GSIS and also the concomitant cytosolic Ca^{2+} oscillations relayed to the matrix cause oscillations in $[Ca^{2+}]_m$ superimposed onto the steady-state increasing $[Ca^{2+}]_m$ levels (cf. the Contribution of Mitochondrial Ca^{2+} to Insulin Secretion section). (E) Hypothetical higher IF1 phosphorylation state upon GLP-1 amplification of GSIS. Here, in addition to the situation described in (D), the mt-sAC population could be more activated due to higher CO_2 , resulting from the additional activation of matrix dehydrogenases, which are superactivated (mt-sAC as well) by more integrally intensive $[Ca^{2+}]_m$ oscillations superimposed onto the steady-state increasing $[Ca^{2+}]_m$ levels. They are determined by cytosolic Ca^{2+} oscillations with a prolonged duration of bursts onto which the Ca^{2+} efflux from ER stores is also superimposed (cf. the Mitochondrial Ca^{2+} Homeostasis upon Receptor-Augmented Insulin Secretion section). As a result, hypothetically, a higher fraction of the matrix IF1 population should be phosphorylated and hence ATP synthesis could be more intensive. ER, endoplasmic reticulum; GLP-1, glucagon-like peptide 1; IF1, ATPase inhibitory factor 1; SAC, soluble adenylyl cyclase.

glucose-induced surplus in total cell ATP, which was always higher in IF1-silenced cells (fivefold higher at 1 mM; about twice at 7 mM [glucose]), reflecting a mild inhibition of ATP synthesis in control cells. In contrast, the IF1 overexpression in INS-1E cells inhibited GSIS, so that the maximum saturated insulin release was about half, whereas AC_{50} was slightly right-shifted to 4.5 mM (116). A more profound shift to ~ 7 mM was observed for the [glucose] dependence of cell surplus ATP levels, which were about halved at 1 mM and $\sim 25\%$ at 7 mM glucose (116). These results reflected the ATP synthase inhibition *in vivo* by the excessive (over-expressed) IF1.

Structural aspects of IF1 interaction with ATP synthase *versus* cristae morphology. ATP synthase dimers are organized in arrays or rows along the crista rims (Fig. 3C), while actually determining the morphology of cristae. If we can approximate the two neighboring dimers by the revealed structure of the tetrameric porcine ATP synthase (80), we can also speculate on the actual IF1 localization *in vivo*.

The IF1 dimers bridge the two F_1 moieties, however, not those within a single ATP synthase dimer, but between two neighboring dimers (Fig. 3A–C) (80). These connections (bridges) *via* the dimeric IF1 are lifted above the membrane of the crista edge. The membrane at this edge is bent into a sharp rim purely due to the single F_0 -dimer structure. IF1 is attached to the bottom of the interface between the α - and β -subunit, where it meets with the γ -subunit of the F_1 moiety (74, 80). Speculatively, one may assume that both the F_1 moieties bridged with the IF1 dimer cannot synthesize ATP. In this instance, not all dimers along the ATP synthase row of dimers could be connected by the IF1-IF1 bridges since if this was the case, no ATP synthesis could exist; all F_1 moieties would be inhibited.

Moreover, the IF1 dimerization is prevented when IF1 is phosphorylated on Ser39 by PKA (68, 69). Also, fast degradation *via* the factor IEX1 was reported (230). Therefore, not only the regulation of IF1 expression *versus* degradation (53) but also PKA signaling provides fine-tuning of ATP synthesis. We hypothesize that the multifaceted natural regulation of IF1 and/or all ATP synthase subunits (including mtDNA-encoded) sets the proper activity within the ensemble of ATP synthases, which provides the properly adjusted rate of ATP synthesis in pancreatic β -cells. This complex regulation predetermines the glucose sensing that starts between 3 and 4 mM (strictly dependent on the elevated NOX4-redox signal) in INS-1E cells or isolated mouse PIs.

When the fraction of phosphorylated IF1 increases within the matrix, an even higher rate of ATP synthesis can be achieved, as simulated by IF1 silencing or additions of dibutyryl-cAMP, which increased cytosolic ATP levels (115). Also, GSIS was upregulated after the dibutyryl-cAMP treatment, but the upregulation ceased in IF1-knockdown cells, indicating that the IF1 phosphorylation enabling higher ATP synthesis was the important component of this mechanism. The dibutyryl-cAMP treatment also compensated the suppressing effect of IF1 on the cytosolic ATP and on the total released insulin amount (116).

Mitochondrial PKA pathways in pancreatic β -cells. PKA either phosphorylates suitable protein residues exposed to the cytosolic face of the outer mitochondrial membrane (OMM;

PKA_{OMM}) or even proteins of the mitochondrial matrix (mtPKA) (78, 292). The latter implies the existence of sensors leading to cAMP signaling in the matrix (187, 287). Thus, adenylyl cyclase mt-sAC (soluble adenylyl cyclase), phosphodiesterase mtPDE2A2 (2), and also mtPKA (286), were identified to be localized in the matrix. Indeed, the GPR receptor activator forskolin induced the phosphorylation of matrix proteins, such as IF1 (68, 69). cAMP cannot freely diffuse into the matrix, and no cAMP carrier is known (2); hence, the matrix cAMP pool is independent of the cytosolic one (44, 46). The ICS-localized or peripheral intermembrane space-localized PKA_{IMS} might phosphorylate the Complex IV COXIV-1 subunit, which prevents its inhibition by ATP and hence enhances respiration and OXPHOS (39). For PKA_{IMS}, one could expect the cytosolic cAMP to penetrate at least to the peripheral intermembrane space.

Matrix mt-sACs are hypothetically activated by elevated matrix Ca^{2+} , while experiments reported mt-sAC activation by bicarbonate, which increased matrix cAMP (34, 132). Nevertheless, no mtPKA activation under these conditions was found (132). Since CO_2 is increasingly released when the Krebs cycle turnover is elevated, mt-sAC activation could occur upon the metabolic stimulation of insulin secretion. Similarly, increasing responses of matrix $[Ca^{2+}]_m$ to cytosolic Ca^{2+} oscillations and Ca^{2+} efflux from the ER (Fig. 3D, E) may activate the matrix mtPKA (3), the existence of which was found in *Drosophila* (286). Thus, OXPHOS is facilitated in the mitochondria of numerous tissues due to the Hsp70-mediated import of the NDUFS4 subunit of Complex I, initiated by phosphorylation, as well as by the phosphorylation of IF1 (69, 115, 116). The observed release of the PKA catalytic subunits by the increased ROS is also noteworthy (216, 243).

Mitochondrial Ca^{2+} Signaling in Pancreatic β -Cells

Contribution of mitochondrial Ca^{2+} to insulin secretion

Stimulation of matrix dehydrogenases and OXPHOS machinery by mitochondrial Ca^{2+} . The stimulation of matrix dehydrogenases upon GSIS is one of the most plausible benefits provided by the Ca^{2+} influx into the matrix *via* the mitochondrial calcium uniporter (MCU) complex (41, 70, 71) (Fig. 4). The FAD-glycerol-3-phosphate dehydrogenase, localized on the outer IMM surface, is then instead influenced by the cytosolic Ca^{2+} penetrating into the intramembrane space or ICS (4, 165, 219, 252). Ca^{2+} activation was also reported for mt-sAC (34, 44, 46), which hypothetically leads to the phosphorylation of IF1 (69, 115, 116) by a putative matrix mtPKA (3, 132). mtPKA releases the IF1-mediated inhibition of the ATP synthase, thus enhancing ATP synthesis (69). A link to Ca^{2+} was suggested for the observation of 50% GSIS suppression upon ablation of the GTP-providing succinyl-CoA (S-CoA) synthetase, whereas the ablation of its ATP-providing form accelerated GSIS (126). We conclude that the mitochondrial Ca^{2+} transport represents a key factor of GSIS dependence on mitochondria.

Mitochondrial Ca^{2+} transport upon GSIS. The mitochondrial matrix content of bound Ca^{2+} and the free Ca^{2+} concentration $[Ca^{2+}]_m$ (124) are finely regulated by the $\Delta\Psi_m$ -driven Ca^{2+} influx *via* the MCU complex (41), which is balanced by the Ca^{2+} influx, conducted by the $Ca^{2+}/2Na^+$

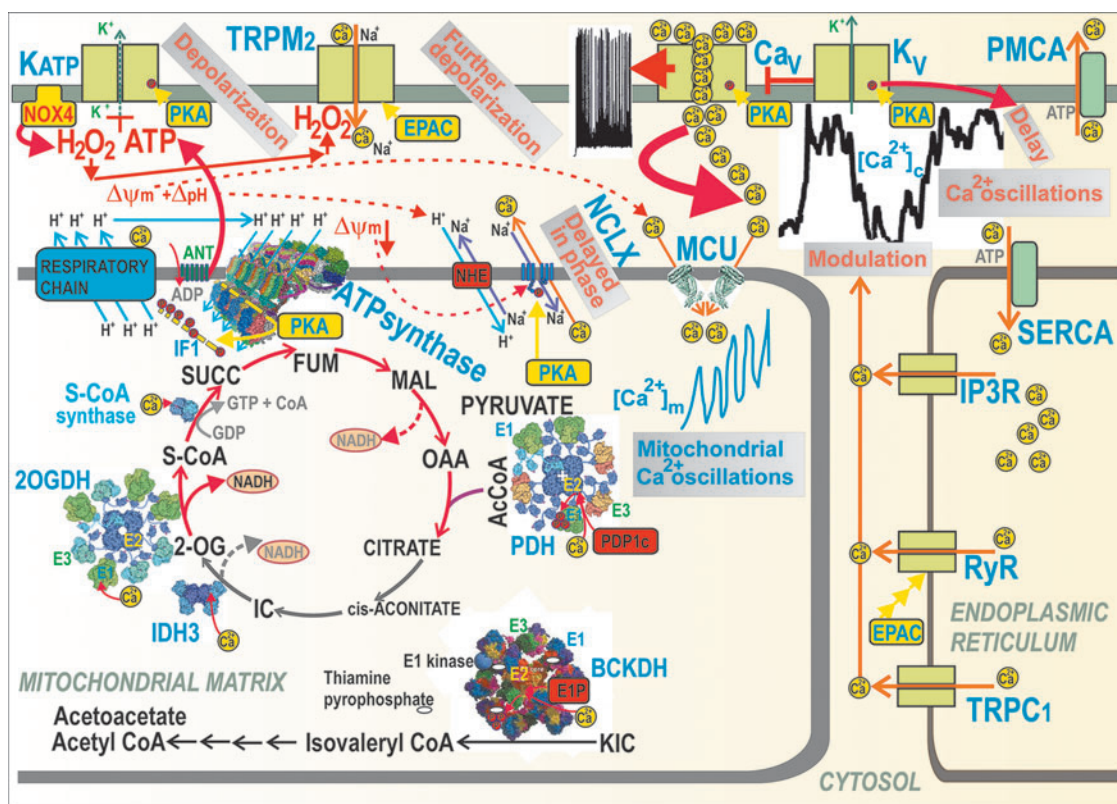


FIG. 4. Mitochondrial versus cytosolic Ca^{2+} oscillations and their ability to activate matrix dehydrogenases. Action potential firing is reflected by cytosolic Ca^{2+} oscillations, which determine the steady-state increase in matrix $[\text{Ca}^{2+}]_m$ with superimposed $[\text{Ca}^{2+}]_m$ oscillations and concomitant activation of matrix dehydrogenases. Activation due to the PKA pathway is also indicated, demonstrating phosphorylation (red circles) of (i) IF1 hypothetically forming bridges (yellow) between the neighboring dimers of the ATP synthase within a row of dimers (four dimers are depicted with the indicated H^+ backflow that leads to ATP synthesis); (ii) NCLX promoting activation via the $\Delta\psi_m$ decrease; (iii) K_{ATP} channels (setting their sensing of ATP to $\sim 1 \text{ mM}$ [ATP]); (iv) Ca_v channels, thus activating them. Similarly, the EPAC2A pathway (“EPAC”) reportedly activates TRPM2 and RyR. The dashed arrows, pointing to NADH, illustrate the sites where NAD^+ is made from NADH due to pyruvate redox shuttles (Fig. 5). Ca_v , voltage-dependent Ca^{2+} channels; EPAC, exchange proteins directly activated by cAMP; FUM, fumarate; IC, isocitrate; MAL, malate; NCLX, mitochondrial sodium calcium exchanger; RyR, ryanodine receptor; SUCC, succinate.

antiporter (mitochondrial sodium calcium exchanger [NCLX]) (38). The latter is driven by ΔpH via the Na^+/H^+ antiporter (plausibly NHE6/SLC9A6). Hypothetically, LETM1 may also ensure $\text{Ca}^{2+}/2\text{H}^+$ antiport, thus extruding Ca^{2+} from the matrix (202).

Mitochondrial Ca^{2+} participates in the first GSIS phase (70) and in GSIS potentiation by GLP-1 (71, 218). A sudden [glucose] elevation in primary β -cells induces the concomitant Ca_v -dependent $[\text{Ca}^{2+}]_c$ oscillations, which are relayed to delayed steady-state increases in mitochondrial $[\text{Ca}^{2+}]_m$ up to saturation (252, 253). The observed $[\text{Ca}^{2+}]_m$ oscillations, superimposed onto the linearly increased $[\text{Ca}^{2+}]_m$, are roughly in phase with $[\text{Ca}^{2+}]_c$ oscillations. The higher the frequency of the action potential spike within a burst, the higher $[\text{Ca}^{2+}]_m$ amplitude was reached (252). These changes induced a biphasic increase in the ATP/ADP ratio with its second phase after 5 min (124, 252, 253).

The mechanism behind this is probably enabled by slightly retarded NCLX responses, in which Ca^{2+} influx exceeds the Ca^{2+} efflux during these transients and during the entire nearly linear $[\text{Ca}^{2+}]_m$ increase up to saturation. The major effect of such integrally elevated $[\text{Ca}^{2+}]_m$ is in the well-

known Ca^{2+} activation of mitochondrial dehydrogenases (4, 164, 165, 219, 252) [doubted in Drews *et al.* (48)] (Fig. 4).

One cannot identify the above-described second phase in the ATP/ADP increase with the second GSIS phase, nevertheless in MCU-deficient β -cells, such a second-phase-ATP/ADP-increase was missing (252, 253). The $[\text{Ca}^{2+}]_m$ responses were slightly shifted up upon NCLX silencing (253). Insulin release from primary β -cells, monitored using Zn^{2+} as a surrogate, was stimulated either by high [glucose] independent of MCU deficiency (which led to delayed responses) or by K_{ATP} closing with tolbutamide, which ceased upon MCU deficiency (252). Hence, the activation of dehydrogenases was also delayed and was probably responsible for the observed second-phase ATP/ADP increase.

The overexpression of the Ca^{2+} -binding protein S100G in the matrix of INS-1E cells prevented $[\text{Ca}^{2+}]_m$ increases responding to $[\text{Ca}^{2+}]_c$, blocked the glucose stimulation of respiration and ATP, thus reflecting the prevention of OXPHOS upon impaired $[\text{Ca}^{2+}]_m$ responses (271). Typical $[\text{Ca}^{2+}]_m$ elevations up to 880 nM dropped to 530 nM. In primary β -cells, S100G overexpression specifically attenuated the second GSIS phase, while the first phase did not decrease (271). This

reflects a delay required for the full-extent activation of matrix dehydrogenases. In a more exaggerated way, this effect is also manifested during GSIS amplification by GLP-1 (90, 258).

Experiments suggested the essential requirement of MCU for GSIS in mice with an ablated MCU-pore, specifically in pancreatic β -cells (70). The insulin release was suppressed the first 5 min following the glucose administration, but after that, the time-integrated insulin release was equal to controls. Thus, in-phase MCU-mediated increases in $[Ca^{2+}]_m$ concomitant with $[Ca^{2+}]_c$ oscillations upon GSIS or GLP-1 amplification of GSIS (see the Mitochondrial Ca^{2+} Homeostasis upon Receptor-Augmented Insulin Secretion section) are among the precise mitochondrial machinery, which is required for optimum ATP synthesis.

The MCU complex is composed of the regulatory scaffolds MCU regulator 1 (MCUR1), the essential MCU regulator element (EMRE), and three isoforms of Ca^{2+} -channel/sensors, termed mitochondrial calcium uptake proteins 1, 2, and 3 (MICU1,2,3) (127, 191). Mitochondrial Ca^{2+} transporters are well known to respond to Ca^{2+} released from the ER. This is reflected by the silencing of either MCU or MICU1, which reduced $[Ca^{2+}]_c$ oscillations and respiration rates and also decreased ATP production and GSIS (4). MCU was found to be activated by kaempferol (22).

A higher $\Delta\Psi_m$ allosterically blocks NCLX, hence Ca^{2+} efflux, and thus increases $[Ca^{2+}]_m$ (129). Mechanistically, this requires the interaction of Ser258 with positively charged residues of NCLX, which is disrupted by PKA phosphorylation, hence NCLX becomes insensitive to $\Delta\Psi_m$, and thus active. For pancreatic β -cells, this regulation implies a low NCLX activity at low [glucose] but high activity upon insulin-stimulating [glucose] (129). Speculatively, this allosteric effect may be behind the oscillation of $[Ca^{2+}]_m$ since each cycle of MCU-mediated Ca^{2+} influx may transiently or locally decrease $\Delta\Psi_m$, whereas the concomitant fraction of imported Ca^{2+} partially upregulates OXPHOS, hence adds to $\Delta\Psi_m$, which in turn would activate NCLX. The regulation of OXPHOS by cytosolic Ca^{2+} penetrating into the ICS probably occurs *via* the Ca^{2+} -induced activation of Complex IV subunit Cox4.1, which disrupts its feedback inhibition by ATP (39, 114, 203). The impact on GSIS is yet to be studied.

Synchronization of cytosolic and mitochondrial Ca^{2+} upon GSIS. Within rodent islets, cooperation between β -cells exists. Synchronization of the electrical activity of the plasma membrane potential within the ensemble of cells in the islet results in synchronization of their cytosolic Ca^{2+} oscillations and other events (99, 111, 218). A few percent of pacemaker-like β -cells provides such synchronization. These cells were termed hub cells. Since it has been recognized that the second GSIS phase exists in PIs, but not in the β -cells isolated from islets, this cell cooperation was considered to substantiate the second phase. But, the delayed kinetics of the insulin granules (104) plus intercellular synchronization act in parallel.

Of course, major synchronization takes place within the individual β -cells. *At first*, the initial rise in ATP plus H_2O_2 upon elevating glucose sets the triggering event for Ca_v channels by closing K_{ATP} , whereas H_2O_2 can hypothetically also activate TRPM2 channels. With other NSCCs or other synergic channels, depolarization reaches up to the -50 mV

threshold of V_p , ultimately activating action potential firing due to the intermittent opening of Ca_v channels and K_v channels.

Second, the pulsatile Ca^{2+} influx from the exterior causes *cytosolic Ca^{2+} oscillations*. Specifically at intermediate [glucose], such as ~ 10 mM, Ca^{2+} oscillations might be terminated because of the transient exhaustion of cytosolic ATP by PMCA and SERCA (252, 253), thus creating silent interburst phases (210) [see the lag between burst $[Ca^{2+}]_c$ phases in Fig. 4—part of the records published in Plecita-Hlavata *et al.* (194)]. Moreover, under the activation of receptors, such as GPR (inositol-1,4,5-triphosphate receptor-diacylglycerol [IP3-DAG] signaling) or GLP-1 receptor (PKA and EPAC2 pathways), an additional amplifying Ca^{2+} efflux, is induced from the ER, *via* Ca^{2+} channels of TRPC1, ryanodine receptor (RyR), or IP3 receptor (IP3R). This ER Ca^{2+} efflux modulates and superimposes onto the existing cytosolic Ca^{2+} oscillations.

Third, cytosolic Ca^{2+} oscillations are relayed to the matrix, causing *oscillations in $[Ca^{2+}]_m$* superimposed onto the *steady-state increasing $[Ca^{2+}]_m$ levels* (252, 253). This is hypothetically allowed by the in-phase delayed Ca^{2+} efflux mediated by the NCLX Ca^{2+}/Na^+ antiporter, behind the instantly acting MCU. NCLX is inhibited by a higher $\Delta\Psi_m$, but due to higher ATP synthesis and concomitant H^+ backflow *via* the ATP synthase c-ring, $\Delta\Psi_m$ is partially diminished, leading to NCLX activation (129). The Ca^{2+} uniport *via* MCU is driven by the $\Delta\Psi_m$ component of the protonmotive force Δp , whereas the electroneutral $Ca^{2+}/2Na^+$ antiport by NCLX is driven by the Na^+ -gradient, established by the Na^+/H^+ antiporter (NHE6), which is then driven by the ΔpH component of Δp .

Fourth, besides the matrix mt-sAC, the resulting $[Ca^{2+}]_m$ elevation activates *matrix dehydrogenases* (42, 164, 218) in the set pace, specifically: (i) the 8-MDa multienzyme complex of pyruvate dehydrogenase (PDH), in which Ca^{2+} binds to heterodimers of the E2 PDH subunit and the catalytic subunit of pyruvate dehydrogenase phosphatase (PDP1c) within the core of the complex, which leads to the PDP1-mediated dephosphorylation of E1 subunits. The PDH-complex contains a hollow core of numerous dihydrolipoate acetyltransferase subunits (E2), plus 12 E3-binding subunits (E3BP). E3BP attaches subunits of pyruvate decarboxylase (E1) and dihydrolipoate dehydrogenase (E3). Since the phosphorylated E1 causes the inhibition of the overall PDH reaction, the Ca^{2+} -activated dephosphorylation is therefore the key event for the PDH activation (42).

(ii) BCKA-dehydrogenase (BCKDH) complex is activated by mechanism similar to (i), in which Ca^{2+} activation of the E1P-phosphatase occurs, which dephosphorylates the E1 subunit, which is otherwise inhibited by the phosphorylation enabled by the BCKDH-E1-kinase, and this is in turn inhibited by the cofactor thiaminepyrophosphate. Since the thiaminepyrophosphate-mediated kinase inhibition is strengthened by Ca^{2+} , hence Ca^{2+} activates BCKDH (180). Moreover, there is a direct Ca^{2+} -induced activation for (iii) Ca^{2+} binding to the E1 subunit of the 2-oxoglutarate dehydrogenase (2OGDH) multienzyme complex; (iv) Ca^{2+} binding to $\beta\gamma$ -subunit interfaces of the hetero-octameric NAD^+ -dependent isocitrate dehydrogenase 3 (IDH3) (42), and (v) Ca^{2+} activates the GTP-producing S-CoA synthase by as yet unknown mechanism (126).

Mitochondrial Ca^{2+} homeostasis upon receptor-augmented insulin secretion

Signaling by GLP-1 receptor for the amplification of GSIS. Produced in intestinal L-enterocytes, GLP-1 from the bloodstream activates its receptor (GLP1R) on the plasma membrane of pancreatic β -cells (170). GLP1R activation preferentially stimulates G-proteins $G_{\alpha s}$, but also $G_{\alpha q}$ or $G_{\alpha_{11}}$ (Fig. 10), and recruits β -arrestin, depending on a biased agonism differently to different agonists, such as exendin-4 and oxyntomodulin (238, 275).

A scaffold protein β -arrestin promotes signaling *via* $G_{\alpha s}$ to cAMP, but also to CREB (238), extracellular regulated kinase ERK1,2 (169), and insulin receptor substrate 2 (IRS-2). This activates β -cell growth, differentiation, and β -cell identity maintenance (238). The major $G_{\alpha s}$ stimulation spreads signals *via* enhanced cAMP (65, 133, 177) and the initiation of PKA (143), plus the enhanced signaling *via* exchange proteins directly activated by cAMP 2A-isoform (EPAC2A) pathways (120). However, a putative cAMP-independent pathway may also exist at physiological 1–10 pM [GLP-1] (231). Prolonged cAMP production could even be induced by internalized GLP1R, which partly potentiates GSIS (255). *Ex vivo*, GLP-1 was found to act at a low range of stimulating [glucose] 6–7.5 mM (5–6 mM in isolated β -cells) (65, 133, 177, 231), which paradoxically is equivalent to fasting glycemia in mice.

The PKA pathway activation leads to a surplus $[Ca^{2+}]_c$ above that of the net GSIS (*i.e.*, without any receptor stimulation) (151). This is achieved by the phosphorylation of K_V channels, leading to their deactivation. This prolongs the overall Ca^{2+} -stimulation signals and induces somewhat lower frequencies of Ca^{2+} oscillations, but with each spike lasting longer (231, 265). Also, the second phase of GSIS might be potentiated by such mechanisms. Speculatively, the PKA-pathway evoked $[Ca^{2+}]_c$ surplus may activate Cox4.1 in the ICS if the concentration therein would reflect $[Ca^{2+}]_c$. PKA also phosphorylates snapin, a protein of the exocytotic machinery. This promotes soluble N-ethylmaleimide-sensitive factor (NSF) attachment protein receptor (SNARE)-complex formation by the interaction of synaptosomal nerve-associated protein 25 (SNAP-25) with synaptogamins of IGVs. Thus, exocytosis is facilitated within the first GSIS phase (236, 237).

A parallel EPAC2A pathway activation by the GLP1R signaling stimulates TRPM2 channels (285), providing the essential shift in depolarization in synergy with K_{ATP} and thus triggers the action potential firing. EPAC2A also enhances K_{ATP} closing (40, 75, 121). The EPAC2A pathway also promotes the docking and priming of IGVs by allowing Rab3A interaction with Rim2 α (282); and a hypothetical interaction of EPAC2-Rim2 α -Picollo trimers with Rab3A, again facilitating IGV exocytosis (254). Also, Ca^{2+} -release is activated from the ER *via* the RyR-, which depends on Ca_V opening (120). A biased GLP1R stimulation *via* $G_{\alpha q/11}$ may also stimulate Ca^{2+} release from the ER now *via* IP3R (23) and *via* TRPM4 and TRPM5 activation due to phosphorylation by protein kinase C (PKC) (231).

Experiments using simultaneous electrophysiological and Ca^{2+} oscillation monitoring (with Ca^{2+} fluorescent probes) found that at 2 mM glucose, but with 200 μ M tolbutamide blocking K_{ATP} (265), the GLP-1 analog liraglutide decreased

the frequency of action potential spikes, which became individually wider. This reflects the PKA-mediated inactivation of $K_V2.1$ channels. With or without liraglutide, each action potential spike matched the triangular peak of the cytosolic Ca^{2+} rise. Its time-width increased from 2 s to about 5 s with liraglutide (265). The relative duration *versus* the active phase of Ca^{2+} spikes was $\sim 10\%$ at 4 mM, $\sim 50\%$ at 7 mM, and $\sim 80\%$ at 9 mM glucose (59). Earlier experiments at 7.7 mM glucose and with GLP-1 $_{(7-36)}$ amide (preproglucagon $_{78-107}$) also reported an increased duration of active and silent electrical activity (58).

Importantly, the observed delayed decay of Ca^{2+} -responses is not only determined by the prolonged action potential spikes but is also affected by Ca^{2+} , released from the intracellular stores, especially the ER, but also from mitochondria. The relay of these complex Ca^{2+} -responses onto the in-phase intermittent responses of proteins of the exocytotic machinery (formation of SNARE complexes) and the resulting pulsatile IGV exocytosis were also monitored by surveying the ATP-activated currents conducted by the artificially overexpressed P2X2 cation channels (145). This was possible due to IGVs containing a high ATP concentration.

Mitochondrial Metabolism of Pancreatic β -Cells

Redox shuttles provided by several mitochondrial anion carriers

Redox shuttles. NADPH has long been considered to be a facilitator of GSIS (107, 110, 112, 183, 193, 209). However, the NADPH increase was not known to activate NOX4 upon GSIS, and PPP was thought to be inactive due to the product-inhibition of G6P-dehydrogenase (227, 290). Later, metabolomics confirmed a significant diversion of G6P flux to PPP upon GSIS (147, 240). Besides the two PPP enzymes, G6P-dehydrogenase and 6-phosphogluconate dehydrogenase, there is a contribution of three metabolic redox shuttles to the increasing $[NADPH]_c$ upon GSIS (110), complying with the high pyruvate influx into the matrix (147). We recognize the pyruvate/malate, pyruvate/citrate, and pyruvate/isocitrate shuttle (Fig. 5).

Note also that metabolic pathways including metabolic shuttles are plastic, specifically when the key members are altered in their expression, such as identified upon glucotoxicity, lipotoxicity, and glucolipotoxicity in isolated human PIs (108). Therefore, the description below concerns with the most frequent schemes before and after glucose intake into intact pancreatic β -cells.

NADPH and NADH homeostasis in the cytosol and mitochondrial matrix upon GSIS. The redox shuttles, activated upon GSIS, do not allow maximum NADH to be produced in the mitochondrial matrix, but instead more NADPH is produced in the cell cytosol, representing a transfer of redox equivalents from the matrix to the cell cytosol (Fig. 5A, B). The shuttles concomitantly provide an independent, although minor NADPH source, supplying NOX4 to initiate redox signaling that enables insulin secretion upon elevated ATP. Mitochondrial malate dehydrogenase 2 (MDH2) produces less NADH, when compared with the situation of the 100% forward reaction, which proceeds at low [glucose].

Also, less NADH is produced, if isocitrate is not converted by the isocitrate dehydrogenase IDH3 to produce

NADH due to the truncated Krebs cycle owing to the citrate export from the matrix, or when the concurrent reaction direction exists so that isocitrate dehydrogenase 2, mitochondrial NADP⁺ dependent (IDH2) is switched to the inverse (reductive carboxylation) reaction. The exported isocitrate promotes NADPH formation by the cytosolic isocitrate dehydrogenase 1, cytosolic NADP⁺ dependent (IDH1). Thus again, instead of one NADH molecule produced in the matrix, one NADPH molecule is formed in the cytosol.

Decreasing matrix NADH ([NADH]_m) at high- *versus* low glucose conditions has one interesting consequence, a diminished matrix NADH/NAD⁺ ratio, which causes decreased superoxide formation, probably at the I_F flavin-site of Complex I (193). As a result, upon GSIS, we do have a dichotomic redox situation in the β -cell cytosol *versus* mitochondrial matrix. Whereas the cytosolic H₂O₂ elevation occurs due to NOX4 function, the matrix superoxide formation decreases (likewise H₂O₂ produced by superoxide dismutase MnSOD). Moreover, typical [NAD⁺]_m, estimated, for example, in HeLa cells, is up to two orders of magnitude higher than [NADH]_m. Values of 800 μ M [NAD⁺]_m and 5 μ M [NADH]_m were reported (33). During fast respiration upon GSIS, this difference actually leads to a situation in which each NADH molecule formed by the respective matrix dehydrogenases is instantly consumed by Complex I.

As for the matrix NADPH ([NADPH]_m), we found that it decreases with increasing glucose. Specifically, the operation of the pyruvate/isocitrate shuttle and reductive carboxylation by IDH2 consumes NADPH significantly in INS-1E cells (193), and this is not balanced by the increased NADPH formation by the matrix malic enzyme 3 (ME3) nor by the increasing forward (Δ p-consuming) mode of nicotinamide nucleotide transhydrogenase (NNT). The matrix ME3 forms pyruvate and NADPH from malate and NADP⁺ (85). The acute [NADPH]_m decrease could lead to a decrease in the reduced glutathione in the matrix, representing a resource sacrificed in exchange for the transfer of redox equivalents, ensuring elevations in cytosolic NADPH.

Other regulators of redox homeostasis

Nicotinamide nucleotide translocase in pancreatic β -cells.

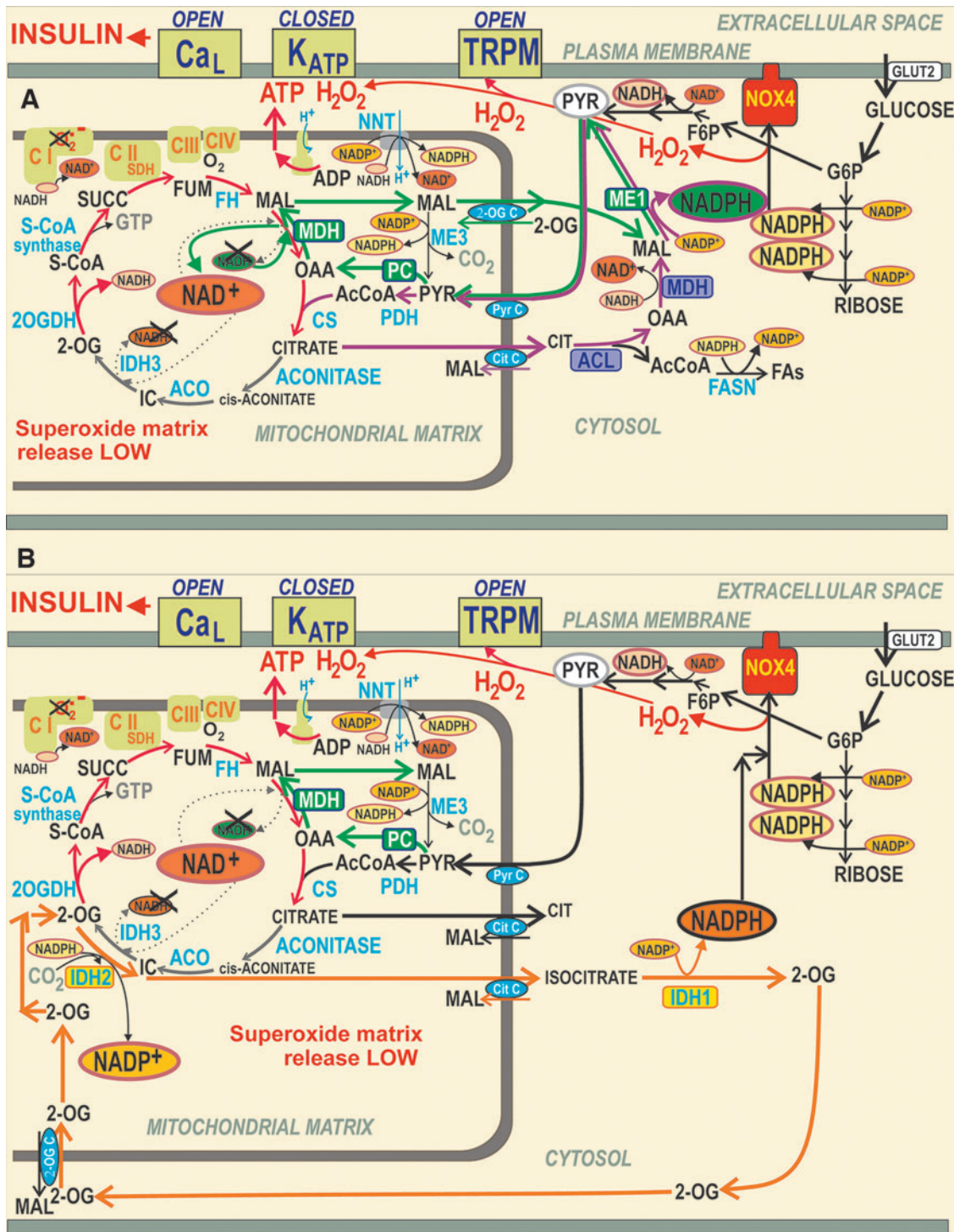
Contradictory findings were reported for the mitochondrial NNT in PIs (Fig. 6). This IMM enzyme exposes its active site to the mitochondrial matrix. In a thermodynamically favored forward mode upon GSIS, NNT consumes Δ p (Fig. 6B) by allowing H⁺ import into the matrix, tightly coupled with the conversion of NADP⁺ to NADPH and with the simultaneous NADH conversion to NAD⁺ (220). In this forward mode, NNT contributes to the matrix [NADPH]_m pool. Since NNT acts downstream of the redox shuttles, it cannot alter or affect them. Nevertheless, if all

FIG. 5. Pyruvate-based redox shuttles transfer matrix NADH equivalents to elevate cytosolic NADPH. (A) The *pyruvate/malate redox shuttle* (green arrows) and *pyruvate/citrate shuttle* (violet arrows). The pyruvate/malate redox shuttle bypasses PDH and the concomitant entry of the resulting acetyl-CoA into the Krebs cycle *via* the CS. This bypass exists due to the PC reaction producing OAA. Conditions upon glucose intake into pancreatic β -cells allow the reversed reaction of the matrix MDH2 that produces malate from oxaloacetate at the expense of NADH, which is converted to NAD⁺. That is why redox equivalents of NADH are transferred into cytosolic NADPH. The transfer is achieved by malate export *via* the “2-OGC” (SLC25A11) (183), where it is exchanged for 2OG, which is then imported to the matrix. The exported malate increases the cytosolic malate pool, which can be consumed by the ME1 reaction, driven by NADP⁺ and thus increasing the cytosolic NADPH pool (82, 195). This reaction direction is driven by an instant return of pyruvate to the mitochondrial matrix ensured by the pyruvate carrier (MPC1 and MPC2, providing pyruvate-H⁺ symport). In this way, the cycle is achieved. The *pyruvate/citrate shuttle* is enabled by the citrate export from the matrix after the CS reaction (54). This truncated Krebs cycle has been confirmed using ¹³C-tracing, demonstrating that high amounts of the cytosolic citrate originate from glucose-derived acetyl-CoA (146). Citrate is exported by the citrate carrier (“Cit C”; SLC25A1), enabling citrate antiport with malate. Together with the pyruvate/malate redox shuttle, malate cycling occurs. The exported citrate is split in the cytosol by the ACL with CoA, yielding oxaloacetate and acetyl-CoA. The cytosolic isoform of MDH1 then converts oxaloacetate into malate, which is again used by ME1 to produce NADPH and pyruvate, which is finally imported back to the matrix. The ACL reaction and hence shuttle operation is minor compared with the acetoacetate pathway operating upon GSIS (52). Under low glucose conditions, levels of short-chain acyl-CoA are preserved. (B) The *pyruvate/isocitrate shuttle* (orange arrows) exists when the reductive carboxylation reaction of matrix IDH2 takes place. Unlike IDH3, which is the regular Krebs cycle enzyme providing NADH, IDH2 in a “forward” oxidative decarboxylation mode uses NADP⁺ plus citrate and produces NADPH and 2OG in the matrix. At high [glucose], such conditions are established instead to facilitate the reverse IDH2 reaction, which is the NADPH-driven reductive carboxylation of 2OG in the presence of CO₂ (193). This is also facilitated by the Krebs cycle truncation, leaving a slow aconitase reaction and isocitrate formation so that the reverse IDH2 reaction occurs. The citrate carrier finally exports isocitrate to the cytosol, exchanging it for imported malate. The enhanced isocitrate pool in the β -cell cytosol is concomitantly consumed by the cytosolic IDH1, ensuring the NADP⁺-driven oxidative decarboxylation of isocitrate to 2OG, yielding NADPH (82). As a result, IDH1 within this shuttle contributes to another portion of the cytosolic NADPH increase upon GSIS (209). 2OG, as with the pyruvate/malate shuttle, is imported to the matrix, being exchanged for malate again by the oxoglutarate carrier. 2OG thus contributes to the mitochondrial matrix 2OG pool, consumed massively by the 2OGDH complex within the Krebs cycle. However, a portion of the matrix 2OG pool is used for another cycle of this shuttle, that is, for IDH2-mediated reductive carboxylation. 2OG, 2-oxoglutarate; 2OGC, 2-oxoglutarate carrier, mitochondrial; 2OGDH, 2-oxoglutarate dehydrogenase; ACL, ATP citrate lyase; ACO, aconitase; Cit C, citrate carrier, mitochondrial; CoA, coenzyme-A; CS, citrate synthase; F6P, fructose-6-phosphate; FASN, fatty acid synthase; FH, fumarate hydratase; IDH1, isocitrate dehydrogenase 1, cytosolic NADP⁺ dependent; IDH2, isocitrate dehydrogenase 2, mitochondrial NADP⁺ dependent; IDH3, isocitrate dehydrogenase 3, cytosolic NAD⁺ dependent; MDH, malate dehydrogenase; ME1, malic enzyme 1, cytosolic; OAA, oxaloacetate; PC, pyruvate carboxylase; PDH, pyruvate dehydrogenase; PyrC, pyruvate carrier, mitochondrial.

these shuttles operate, than IDH2 consumes NADPH and since ME3 cannot balance this consumption, matrix NADPH decreases upon GSIS (193).

Despite we could not indicate the reverse mode at low [glucose] (193), NNT was reported to function in the reverse mode (225), in which it pumps protons and thus provides a Δp surplus. This should be coupled with the consumption of NADPH and NAD^+ , yielding $NADP^+$ and NADH. Such a mode would be possible, since at low [glucose] respiration and ATP synthesis

exhibit somewhat slower rates, establishing a lower Δp , than with high [glucose]. The H^+ pumping against an intermediate Δp would be possible at rather high $NADPH/NADP^+$ ratio. In contrast, at high [glucose], NNT acts against the higher Δp . However, no direct observation of the actual H^+ flux direction was conducted (225). By comparing $\Delta\Psi_m$, monitored using fluorescent probes, we demonstrated $\Delta\Psi_m$ -increases in NNT-silenced INS-1E cells, supporting the existence of the forward NNT mode, which produces NADPH (193).



Neither experiments relying on the comparison of C57BL/6J *versus* C57BL/6N mice were conclusive. They reported that an in-frame five-exon deletion in the *Nnt* gene spontaneously occurred in C57BL/6J mice, thus removing exons 7–11, causing a complete absence of NNT protein (62, 63, 257).

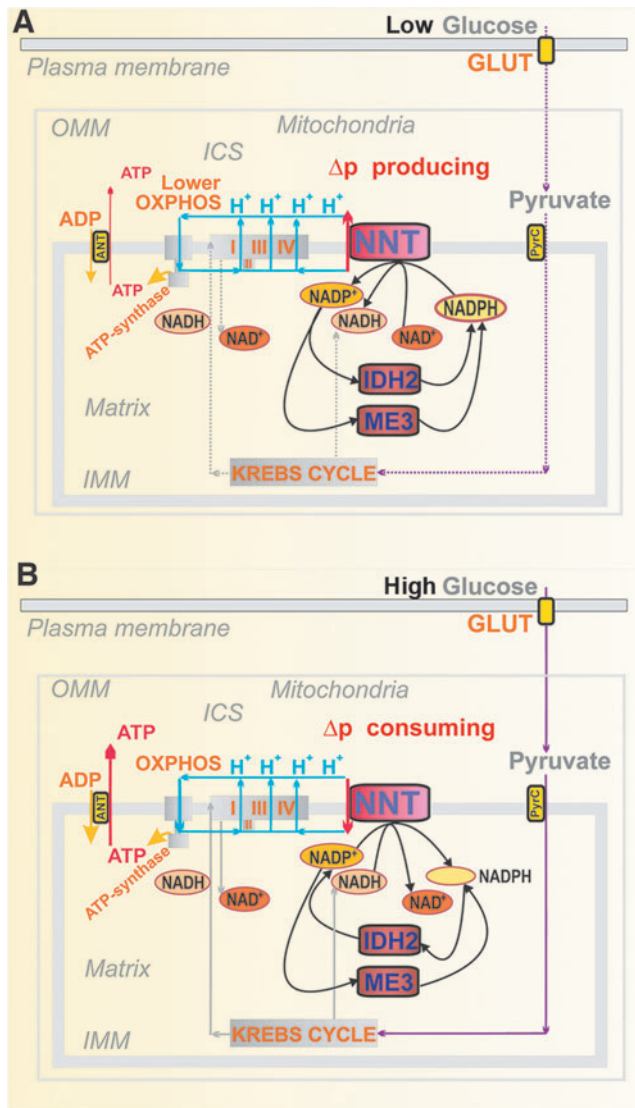


FIG. 6. Hypothetical reverse and forward mode of nicotinamide nucleotide translocase at low and high glucose, respectively. (A) Low glucose conditions: hypothetical reverse NNT mode is depicted, when NNT acts as a proton pump, using the energy of NADPH and NAD⁺, converting them to NADP⁺ and NADH, respectively. It would be possible, since under low glucose conditions in pancreatic β -cells, a lower Δp would allow the proton pumping against that Δp . Possible NADPH sources could be the matrix IDH2 providing oxidative decarboxylation and ME3. (B) High glucose conditions: forward NNT mode is possible (193) when NNT uses Δp to translocate H⁺ into the matrix and drives NADPH formation from NADP⁺ with the simultaneous conversion of NADH to NAD⁺. This mode is highly probable upon GSIS since a high Δp is established, thus driving the H⁺ influx *via* NNT. Also, since the pyruvate/isocitrate shuttle is activated upon GSIS, it switches the IDH2 reaction direction to reductive carboxylation and NADP⁺ production. ME3, malic enzyme 3; NNT, nicotinamide nucleotide transhydrogenase.

The C57BL/6J mouse strain was claimed to have a highly suppressed GSIS. However, other studies normally used knockouts backcrossed into the C57BL/6J-mice background as controls for GSIS and it exhibited high insulin secretion rates [*e.g.*, Plecita-Hlavata *et al.* (194) and Wong *et al.* (273)]. The discrepancy originates from the fact that initially only the quantitative trait loci were identified. Thus, a mere correlation with deletions in the *Nnt* gene was assumed, and verifications using the artificial *Nnt* expression can be regarded as inconclusive, since the *Nnt* expression *per se* could enhance insulin secretion. This could be subsequently interpreted as an apparent GSIS suppression in C57BL/6J mice (273).

Malate/aspartate shuttle in low and high glucose conditions. The malate/aspartate shuttle (MAS) was assumed to play a significant role in pancreatic β -cells (147, 240). However, interpretation of the relevant metabolomics data must be provided with caution since they mostly do not resolve metabolites of the mitochondrial matrix *versus* those from the cytosolic compartment (which is typically greater). One must consider that the metabolite transport direction within the active MAS is the opposite of the pyruvate redox shuttles (193) (Fig. 7). Their existence documented by numerous experiments over the last two decades (107, 110, 112, 183, 193, 209) thus excludes metabolite fluxes required for MAS operation at high [glucose].

The 2-oxoglutarate carrier (2OGC) mediates the malate efflux coupled with the 2-oxoglutarate (2OG) uptake to the matrix at high [glucose], whereas the malate import coupled with the 2OG export is required for MAS, if it exists. Unlike with pyruvate-based redox shuttles, at least one of two glutamate-aspartate antiporter isoforms is required for MAS, enabling the glutamate import in exchange for aspartate export from the matrix. In contrast, the aspartate needs to be imported as a part of the pyruvate/malate redox shuttle. However, glutamate formed in the matrix was suggested to be exported to the β -cell cytosol to facilitate IGV maturation and exocytosis (30, 72, 92, 93, 153, 155, 250). This would again require the opposite direction of glutamate flux.

At low [glucose], both aspartate–glutamate antiporters can participate in MAS, that is, SLC25A12/AGC1/aralar (18, 217) and SLC25A13/AGC2 (193). The existence of MAS was derived from the essential requirement of transaminases (aminotransferases) and aspartate–glutamate antiporters for β -cells (18, 217). Metabolomics studies evidenced a decrease in total cell aspartate at the initiation of GSIS, while aconitate, citrate, isocitrate, malate, or fumarate instantly rose, and elevations of 2OG and succinate were delayed until 15 min (241). Elevations in metabolites originate from the disbalance between producing *versus* consuming reactions, while the latter is slower; whereas for losses of metabolite, the producing reactions are slower. Hence, the observed aspartate losses reflect this disbalance.

Due to providing cytosolic glutamate, MAS was implicated in the GLP-1 amplification of GSIS, but not in GSIS itself (72). The ablation of cytosolic transaminase AST1/GOT1 reversibly transforming 2OG and aspartate to oxaloacetate plus L-glutamate led to the lack of GLP-1 effects. Further experiments are required to evaluate whether the three pyruvate-redox shuttles operate and interfere or not with MAS upon the GLP-1 amplification of GSIS, notably in the sustained second phase.

β -Hydroxybutyrate dehydrogenase and acetoacetate metabolism. β -Hydroxybutyrate dehydrogenase (β -OHBBDH) is exclusive to the matrix in rodent pancreatic β -cells, playing an important role in redox homeostasis (149, 178). In pioneering investigations with hepatocytes, the β -OHBBDH reaction was suggested to precisely reflect the matrix NAD^+/NADH ratio, which would therefore determine the ratio of (total) β -hydroxybutyrate/acetoacetate concentration (178). However, since the estimated order of magnitude for the matrix NAD^+/NADH ratio is >100 , such an excess of β -hydroxybutyrate is unlikely. Since we reported the increase in this ratio upon GSIS (193), one could speculate that also matrix β -hydroxybutyrate rises upon GSIS (Fig. 8). However, acetoacetate can also be exported to the cytosol, where it is utilized by other reactions (149, 178). This was thought to facilitate insulin secretion *via* the formation of various acyl-CoA derivatives (Fig. 8) (149), which could acetylate proteins thus speculatively enhancing GSIS (189, 190). β -Hydroxybutyrate (<https://www.brenda-enzymes.org/enzyme.php?ecno=1.1.1.30>) can also be formed in the cytosol of human β -cells.

Long-chain acyl-CoAs were also reported to bind to the KIR6.2 subunit of K_{ATP} (28), which potently activates

this channel (27, 77). Since upon GSIS, there is a reduction in total cell acyl-CoAs and malonyl-CoA (146, 198), such a reduction could facilitate K_{ATP} closure (146). Alternatively, FA β -oxidation (long-chain acyl-CoA shortening) could also provide the redox signaling toward K_{ATP} or TRPM2 (79, 123, 223), as with KIC (194) (see the Mitochondrial Contribution to Insulin Secretion Stimulated by BCKAs and FAS section).

Phosphoenolpyruvate cycle and role of pyruvate kinases. Another cycle, the phosphoenolpyruvate (PEP) cycle was suggested to act in the low glucose conditions. The PEP cycle is cataplerotic, beginning by the mitochondrial PEP-carboxykinase 2 (PEPCK2) conversion of oxaloacetate to PEP, which is exported by the citrate carrier (SLC25A1) from mitochondria. Cytosolic pyruvate kinases (PKs, isoforms constituent M1, recruitable M2 and L), existing in beta cells (167) use then the cytosolic PEP to convert it to pyruvate, which is coupled to ATP formation from ADP. Pyruvate enters mitochondria, where is metabolized either by PDH or by pyruvate carboxylase (PC). The PC flux completes the cycle by pyruvate conversion to oxaloacetate.

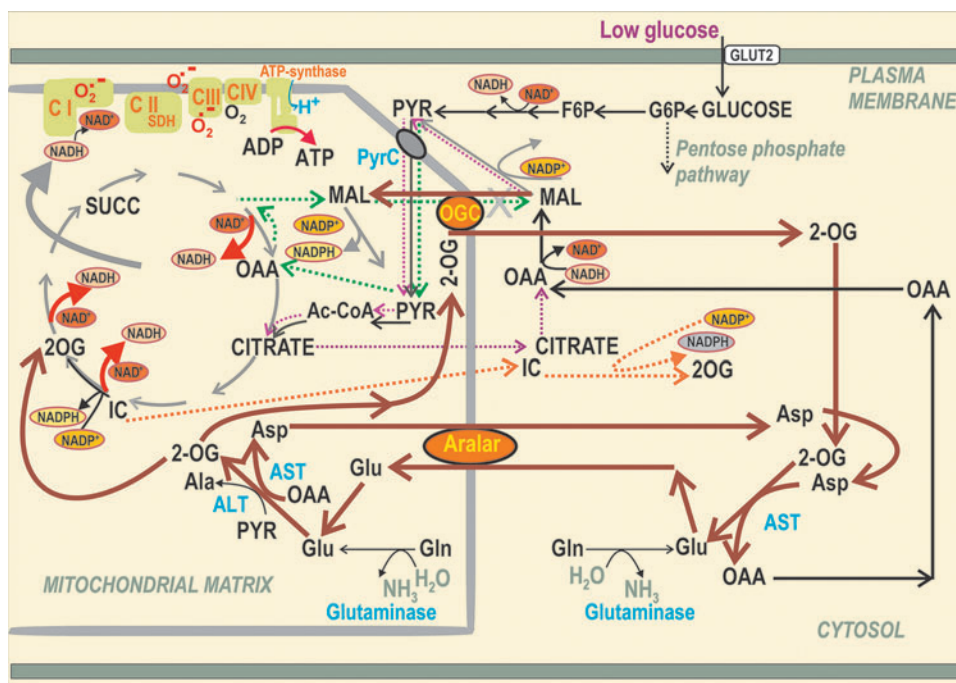


FIG. 7. MAS is plausible when pyruvate-based redox shuttles are not operating. The MAS (brown) could participate in metabolic fluxes in pancreatic β -cells at low nonstimulating [glucose], when the pyruvate-based redox shuttles do not provide the opposite malate fluxes for the 2OG. Moreover, the MAS transfers redox equivalents of NADH into the mitochondrial matrix; however, matrix NADH was found to decrease upon GSIS and relies on at least one of the two aspartate–glutamate antiporters, that is, SLC25A12/AGC1/aralar (18, 217) and SLC25A13/AGC2 (193) (data not shown). The key enzymes are alanine aminotransferases (cytosolic ALT1 and mitochondrial ALT2; also termed glutamate pyruvate transaminases, GPT1 and GPT2). Within MAS, ALT2 catalyzes the conversion of pyruvate plus L-glutamate to 2OG and L-alanine, whereas ALT1 (omitted for simplicity) would catalyze the reaction in the reverse mode. Analogously, there are aspartate aminotransferases, cytosolic AST1, and mitochondrial AST2 (also termed glutamate oxaloacetate transaminases, GOT1 and GOT2). In MAS, AST2 converts oxaloacetate plus L-glutamate to 2OG and L-aspartate, whereas AST1 should catalyze the opposite reaction to complete the cycle. Due to the reverse character of the aminotransferase reaction, its direction depends on the glutamate metabolism. AGC1, aspartate–glutamate antiporter SLC25A12 (Aralar); ALT, alanine aminotransferase; Aralar, aspartate–glutamate antiporter SLC25A12 (AGC1); AST, aspartate aminotransferase (aka glutamate oxaloacetate transaminase, GOT); GPT, glutamate pyruvate transaminase; MAS, malate/aspartate shuttle.

Pyruvate kinase isoform recruitable M2 (PKM2) and pyruvate kinase isoform L (PKL), allosterically activated by fructose 1,6-bisphosphate, were recently reported to aid K_{ATP} closure, as derived from patch-clamp experiments in excision mode combined with PK activation by a small-molecule activator (141). The authors exemplified PEP cycle switched on/off in the β -cell responses to intermediate 9 mM glucose, when V_p and or $[Ca^{2+}]_c$ bursts phases are interchanged with the interburst phases (Fig. 4). The decreased cytosolic ATP/ADP ratio was explained on the basis of the PEP cycle providing ATP synthesis by PK, that is, by “substrate” phosphorylation of ADP, independent of OXPHOS. Naturally low ATP sets K_{ATP} -channels open, which occurs before glucose elevation and/or after termination of the burst phase at 9 mM glucose. When OXPHOS continues to elevate ATP further, PEP cycle is less active and more importantly the Krebs cycle control strength overcomes that of PEP cycle. Consequently, the burst phase begins at 9 mM glucose. Also, PKM2 and PKL activator failed to improve GSIS in PEPCK2-knockout mice (1).

Glutamine and glutamate in pancreatic β -cells

Glutamine and glutamate metabolism. The reaction direction of mitochondrial glutamate dehydrogenase (GDH) in pancreatic β -cells was thought to favor the provision of glutamate and NAD^+ , while consuming 2OG, ammonium,

and NADH (30, 92, 153, 155, 250). This would also contribute to decreasing $[NADH]_m$, if acting upon GSIS. During fasting, GDH is activated by ADP and leucine, while at high [glucose], GDH is inhibited by GTP and ATP (67, 278).

Glutamate is exported from the matrix by the glutamate carrier GC1 (SLC25A22) (30, 92, 155). Also, pyruvate utilization by aminotransferases has a certain impact, despite being minor compared with the utilization by the matrix PDH complex and by the oxaloacetate anaplerosis provided by pyruvate carboxylase (6). Thus, cytosolic alanine aminotransferase (ALT1) and mitochondrial ALT2 [also termed glutamate pyruvate transaminases, GPT1 and GPT2 (188)] could catalyze the conversion of pyruvate plus L-glutamate to 2OG and L-alanine (279), which diminishes the matrix glutamate pool. The reverse GPT2 reaction would then produce glutamate and add pyruvate to its fast-consuming pool. Alternatively, AST1/GOT1 and mitochondrial AST2/GOT2 reversibly convert oxaloacetate plus L-glutamate to 2OG and aspartate.

Glutamine is also utilized in PIs, reportedly promoting leucine-stimulated insulin secretion at low [glucose], when phosphate-dependent glutaminase produces glutamate, which is further oxidized by GDH (67).

Glutamate regulation of insulin secretion. Glutamate was first suggested to facilitate GSIS (30, 92, 154, 155, 229), which was questioned by subsequent reports (24, 148). The

FIG. 8. β -OHB formation and FA metabolism in pancreatic β -cells. The scheme describes three selected metabolic branches: (i) β -OHB formation and its relationship to leucine metabolism; (ii) FA β -oxidation; and (iii) the cytosolic glycerol/FA cycle. As for (i), at high [glucose], succinate is interconverted with AcAcCoA to S-CoA and acetoacetate by SCoA:3oxoAcCoAT (52). As part of leucine metabolism during a series of oxidative reactions (“ β -like oxidation”) resembling FA β -oxidation, HMG-CoA is split by HMGCoAL into acetyl-CoA and acetoacetate. Besides being converted by β -OHBBDH, acetoacetate can escape to the cytosol. Distinct enzyme isoforms convert two molecules of acetyl-CoA into CoA and AcAcCoA in the mitochondrial matrix. The latter are ACAT1 and ACAA2, whereas in the cytosol, there are ACAT2 and ACAA1. Cytosolic acetyl-CoA was suggested to facilitate the acetylation of proteins, which might speculatively enhance GSIS (189, 190). (ii) FA β -oxidation: FA is imported via CD36 into β -cells, where AcylCoA-synthetase (ACSL), localized externally to the ER membrane and OMM, converts FAs to acyl-CoAs, whereas the cytosolic CAT1 (synonymous for carnitine palmitoyltransferase, CPT1) converts acyl-CoAs to acylcarnitines (207). The carnitine carrier (SLC25A20) provides the import of acylcarnitines into the matrix, exchanging them for carnitine. The matrix CAT2/CPT2 converts acyl carnitines to acyl-CoAs. The following chain of reactions, termed FA β -oxidation, shortens the FA-acyl chain by two carbons, involving acyl-CoA dehydrogenases, enoyl-CoA hydratase, 3-hydroxyacyl-CoA dehydrogenase, and β -thiolase. The product of a single cycle is just acyl-CoA shortened by two carbons plus acetyl-CoA. The FA β -oxidation is regulated via the inhibition of CAT1/CPT1 by malonyl-CoA, formed by ACC from acetyl-CoA. (iii) Cytosolic glycerol/FA cycle (197): elevated glucose is converted to glycerol3P, which is esterified by acyl-CoAs by GPATs (bound externally to ER and OMM) to LysoPhA. The latter is further esterified by AGPAT (bound to ER) to PhA. At the ER surface or lipid droplets, lipins transform PhA to 1,2-DAG, initiating PKC signaling and activating Munc13-1. DAG is also acylated there to TG, by diacylglycerol O-acyltransferase-1 and -2 (DGATs). Simultaneously, the lipolytic branch is provided by the cytosolic ATGL, hydrolyzing TG to DAG, upon the facilitation of perilipin (data not shown) and CGI-58 protein (CGI) on the lipid droplet surface. DAG is hydrolyzed to MAG by HSL, again facilitated by perilipin. The created MAGs can overactivate the GPR119 receptor (Fig. 10). The glycerol/FA cycle is completed by the hydrolysis of MAG to glycerol and FAs by the plasma membrane-associated ABHD6 (data not shown), whereas glycerol is exported from β -cells. β -OHB, β -hydroxybutyrate; β -OHBBDH, β -hydroxybutyrate dehydrogenase; ABHD6, alpha/beta-hydrolase domain containing 6, monoacylglycerol lipase; ACAA, acetyl-CoA acyltransferase; AcAcCoA, acetoacetyl-CoA; ACAT, acetyl-CoA acetyltransferase; ACC, acetyl-CoA carboxylase; ACSL, long-chain acyl-CoA synthetase; AGPAT, 1-acylglycerol-3-phosphate acyltransferase; ATGL, adipose triglyceride lipase; CAT, carnitine acyltransferase; CGI, comparative gene identification 58, ATGL co-activator (aka ABDH5); CPT, carnitine palmitoyltransferase; DAG, diacylglycerol; DAT, DGAT, diacylglycerol O-acyltransferase; FA, fatty acid; glycerol3P, glycerol-3-phosphate; GPAT1,2, glycerol-3-phosphate acyltransferase 1,2; GPAT3,4, glycerol-3-phosphate acyltransferase 3,4 (1-acylglycerol-3-phosphate O-acyltransferase); GPR, G-protein-coupled receptor; HMG-CoA, hydroxymethyl-glutaryl-CoA; HMGCoAL, hydroxymethyl-glutaryl-CoA lyase; HSL, hormone-sensitive lipase; LysoPhA, lysophosphatidic acid; MAG, monoacylglycerol; OMM, outer mitochondrial membrane; PhA, phosphatidic acid; PKC, protein kinase C; SCoA:3oxoAcCoAT, succinyl-CoA:3-ketoacid-CoA transferase; Succ-CoA, S-CoA, i.e. succinyl-CoA; TG, triglyceride.

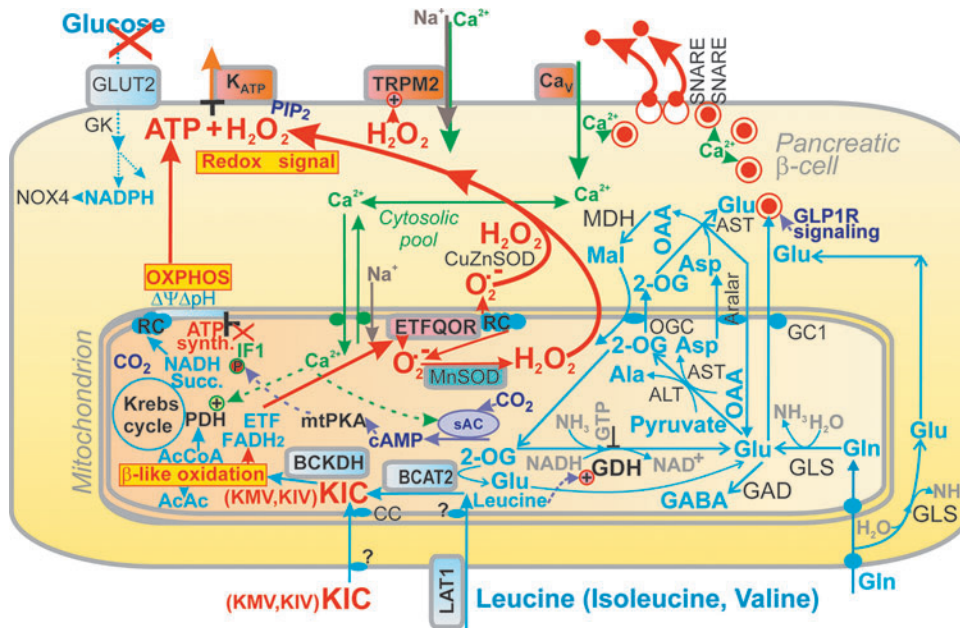


FIG. 9. Mitochondrial retrograde redox signaling determines insulin secretion by BCKAs. KIC, KMV, and KIV may arise from blood capillaries (imported into the matrix *via* the carnitine carrier, CC) or by being converted from leucine, isoleucine, and valine, respectively, by the branched-chain aminotransferase reaction in the mitochondrial matrix (BCAT2). The BCAA import is ensured by the plasma membrane LAT1 transporter. The BCKDH, which provides electrons to ETF, exists exclusively in β -cell mitochondria and initiates a series of reactions of β -like oxidation. ETF:QOR accepts electrons from two ETFs, when it converts Q to QH₂, and as side reactions produces superoxide together with its elevated production at sites I₀ and III₀ (cf. Fig. 11). In the mitochondrial matrix, superoxide is transformed to H₂O₂ by MnSOD, but by CuZnSOD in the intermembrane space and cytosol. The elevated mitochondrial/cytosolic H₂O₂ substantiates the retrograde redox signaling that targets K_{ATP} to ensure its closure together with ATP (and possibly also TRPM2). As a result, Ca_V channels are open, providing the Ca²⁺-signal for IGV exocytosis. The end products of the β -like oxidation of KIC contribute to OXPHOS. Thus, AcCoA enters the Krebs cycle to form citrate, whereas AcAc can be partly exported to the cytosol or converted to β -OHB by a reverse reaction of β -OHBBDH at the expense of NADH (Fig. 8). A link to glutamate and glutamine metabolism is also indicated, including the MAS (Fig. 7), which may exist together with BCKA-stimulated insulin secretion at low glucose, since at low glucose, the pyruvate-based redox shuttles are not highly active. AcAc, acetoacetate; AcCoA, acetyl-CoA; BCAA, branched-chain amino acid; BCAT2, branched/chain amino acid transferase 2, mitochondrial; BCKA, branched-chain ketoacid; BCKDH, branched-chain ketoacid dehydrogenase; ETF, electron transfer flavoprotein; ETF:QOR or ETF:QOR, electron transfer flavoprotein:quinone oxidoreductase; GAD, glutamate decarboxylase; GC1, glutamate carrier; GLS, glutaminase; IGV, insulin granule vesicle; KIC, 2-ketoisocaproate; KIV, 2-ketoisovalerate; KMV, 2-ketoisomethylvalerate; OXPHOS, oxidative phosphorylation; Q, ubiquinone; QH₂, ubiquinol.

Retrograde redox signaling (*i.e.*, from mitochondria to cell cytosol, nuclei, or other organelles) is provided when these BCKAs are oxidized in mitochondria (29). This is substantiated by the elevated mitochondrial superoxide formation due to BCKA oxidation, whereas superoxide is transformed to H₂O₂ either by the matrix MnSOD or by the intermembrane space CuZnSOD (Fig. 9).

Despite there being details missing on how BCAA or BCKA are transported to the mitochondrial matrix, a well-known exclusively matrix BCKDH complex converts CoA plus BCKAs to proper BCKA-CoAs, that is, to isovaleryl-CoA, isobutyryl-CoA, and methyl-isobutyryl-CoA from KIC, KIV, and KMV, respectively. The entire series of reactions, a β -like oxidation (resembling FA β -oxidation) continues, for example, for KIC *via* methylcrotonyl-CoA carboxylase (MCC), methyl-glutoconyl-CoA hydratase (MGCoAH), and 3-hydroxy-3-methylglutaryl-CoA lyase (HMGCoAL), leading to the end products acetyl-CoA, which drives the Krebs cycle, and acetoacetate.

Mechanism of superoxide formation upon oxidation of BCKAs. The BCKDH reaction includes FAD as an electron acceptor. Subsequently, two electron transfer flavoprotein (ETF) molecules reoxidize the resulting FADH₂ since each ETF is only a single-electron carrier. ETFs otherwise transfer electrons from 11 different mitochondrial flavoprotein dehydrogenases to the IMM ubiquinone (Q) pool. During BCKA oxidation, the transfer of electrons proceeds from one electron-reduced ETF one at a time to the lower potential FAD center of the electron transfer flavoprotein:quinone oxidoreductase (ETFQOR) (268). One electron is transferred to the iron cluster. ETF:QOR thus accepts two electrons, and this is coupled with the reduction of ubiquinone to ubiquinol (Q to QH₂) with a transient semiubiquinone formation (268). This is a clue to the enhanced superoxide formation upon BCKA oxidation.

Since QH₂ binds to the Complex I Q-binding site, the excessive supply of QH₂ by ETF:QOR causes a feedback inhibition of the ongoing Q reduction to QH₂ in Complex I.

As a result, mitochondrial superoxide formation is accelerated at the so-called I_Q site of superoxide formation (Fig. 11). The second possible source could be due to the ETF:QOR reaction itself, while electrons are leaking from flavin to oxygen at site E_F (Fig. 11), forming initially a radical pair and finally superoxide (25). The third possible source is given by the excessive acetyl-CoA (propionyl-CoA) entry or methylmalonyl and S-CoA entry into the Krebs cycle. Since such enhanced catabolism accelerates respiration, an enhanced superoxide formation can be expected at Complex I site I_F and site I_Q , and Complex III site III_{QO} , when the capacity of electron transfer is exceeded. Also, as discussed above, acetoacetate influences the established redox homeostasis.

Insulin secretion due to BCKAs. Insulin secretion upon elevated BCKA depends on increases in cytosolic ATP plus H_2O_2 , now both supplied by mitochondria (Fig. 9). Indeed, BCKDH silencing blocked KIC-stimulated insulin secretion, as did the mitochondrial-matrix-targeted antioxidant SkQ1

(194). In contrast, the transaminase inhibitor aminooxyacetate had no effect. The blockage correlated with the suppressed matrix superoxide release, which was otherwise elevated by KIC. So, the H_2O_2 diffusion from the matrix substantiates the retrograde redox signaling from mitochondria. We admit the KIC doses may be supraphysiological in these experiments. A magnitude of a minimum threshold should be further investigated, which still creates sufficient mitochondrial superoxide/ H_2O_2 *in vivo* to substantiate redox signaling reaching the plasma membrane and concomitant insulin exocytosis.

The most plausible terminal targets are located in the plasma membrane. They could be Cys residues of K_{ATP} , or an oxidizable Met residue of TRPM2 (223), or both. Note that TRPM2 or other NSCCs or chloride channels are essentially required to shift the depolarization to the -50 mV threshold required for the opening of Ca_V , and so for action potential firing (119, 221). This -50 mV threshold cannot be achieved without NSCCs or Cl^- channels, even when 100% of K_{ATP}

FIG. 10. Receptor and metabolic pathways determining FASIS. (A) Receptor component of stimulation is emphasized. (B) Metabolic component is emphasized. When present in islets capillaries, for example, in incoming chylomicrons, FAs are cleaved by lipoprotein lipase (ATGL being the most specific β -cell isoform) and may either (A) *act via receptor pathways* to stimulate the GPR40 metabotropic receptor (94), in parallel with the second product of the cleavage, MAG, which signals *via* GPR119. Alternatively, (B) *the metabolic pathway begins* by FA import into the cell by the CD36 transporter and by ACSL conversion to acyl-CoAs. As for (A), the activation of both receptors leads to Ca_V -mediated action potential spikes and concomitant pulsatile insulin secretion. GPR40 acts *via* the $G_{\alpha q/11}$, thus activating PLC, which leads to IP3 and DAG release (for DAG downstream pathway, see @). IP3 activates additional Ca^{2+} efflux from the ER *via* the IP3R, which is initiated either by the preceding Ca_V opening (95) or by PLC-TRPC-induced Ca^{2+} efflux from the ER (276). The most prominent pathway downstream of DAG involves the PKC-mediated phosphorylation of TRPM4 and TRPM5 to activate them. As a result, together with TRPM2, activated by Ca^{2+} and H_2O_2 , these channels strengthen the necessary shift to -50 mV depolarization at the 100% closed K_{ATP} ensemble. The K_{ATP} closure is ensured by the metabolic component of FASIS (B). The two components are mutually interrelated since the canonical GPR119 signaling and the biased GPR40 signaling leads to the cAMP-mediated activation of the PKA and EPAC2 pathways (65, 187, 287). PKA phosphorylates the $Ca_V\beta 2$ subunit to activate it, phosphorylates K_{ATP} (see legend of Fig. 2) and inhibits Kv channels, which prolongs the already more intensive Ca^{2+} influx (179). Snapin, which allows IGV docking to the plasma membrane, is also PKA-phosphorylated, enabling initiation of the snapin SNARE complex with a lipid-anchored protein, the SNAP-25 (236). The EPAC2 pathway is based on its guanine nucleotide exchange activity. This induces further TRPM2 activation (285), regulates K_{ATP} (121) plus priming of the interaction of Rim2a with Munc13-1, required for the syntaxin 1 interaction of IGV [which activates IGV exocytosis (282)] and, finally, the activation of RyR-mediated Ca^{2+} efflux from the ER (120). FAs imported by CD36 are converted to acyl-CoAs by AcylCoA-synthetase (ACSL), whereas CAT1 converts acyl-CoAs to acyl-carnitines (207). The carnitine carrier (SLC25A20) imports acylcarnitines into the matrix, exchanging them for carnitine. The matrix CAT2 converts acyl carnitines to acyl-CoAs, which is followed by FA β -oxidation (see also Fig. 8). As described in the Mechanisms of Insulin Secretion section, all the benefits of activation also occur for mitochondrial metabolism, that is, activations upon GSIS and its receptor-mediated amplification (cf. Fig. 4). Also, similar redox signaling due to the increased superoxide formation upon FA β -oxidation occurs during the metabolic branch of FASIS, as with BCKA-stimulated insulin secretion (cf. Fig. 9). Elevated ATP from OXPHOS fortified by FA β -oxidation and elevated cytosolic H_2O_2 due to the increased H_2O_2 -release from the matrix close the K_{ATP} channel (possibly also TRPM2), as they do upon GSIS. Overactivation of GPR40: pathways (A, B) are also interconnected because of the intramitochondrial redox signaling [elevated matrix superoxide/ H_2O_2 due to FA β -oxidation (Fig. 11) directly activates mitochondrial phospholipase $iPLA2\gamma/PNPLA8$ (98, 103, 105)]. The phospholipase $iPLA2\gamma$ cleaves both saturated and unsaturated FAs from the phospholipids of mitochondrial membranes. The cleaved free FAs diffuse up to the plasma membrane, where they activate GPR40 (103). FASIS in $iPLA2\gamma$ -knockout mice or its isolated islets yields $\sim 30\%$ insulin in the first fast phase of insulin secretion compared with wt mice (Holendová *et al.*, unpublished data). This supports the existence of such an acute mechanism *in vivo*. Overactivation of GPR119: FASIS in the presence of high [glucose] (which by itself would stimulate GSIS) also involves the so-called glycerol/FA cycle combining simultaneous lipogenesis and lipolysis, as suggested by Prentki *et al.* (197). Enzymes involved in this cycle are described in the legend of Figure 8. An important intermediate of the glycerol/FA cycle is 1,2-DAG, which initiates PKC signaling (and TRPM4,5 activation) and activates Munc13-1 to facilitate IGV exocytosis. Moreover, created MAGs (* indicates its diffusion toward GPR119) can diffuse to the plasma membrane and overactivate the GPR119 receptor there. ABDH6, alpha/beta-hydrolase domain containing 6, monoacylglycerol lipase; CaMKII, Ca^{2+} /calmodulin-dependent protein kinase II; FASIS, fatty acid-stimulated insulin secretion; IP3, inositol-1,4,5-triphosphate; IP3R, inositol-1,4,5-triphosphate receptor; $iPLA2\gamma$, Ca^{2+} -independent phospholipase A2 isoform γ ; Orai1, calcium release-activated calcium modulator 1; PLC, phospholipase C; Rap2, Ras-related protein 2; RC, respiratory chain; SNAP-25, synaptosomal nerve-associated protein 25; SNARE, soluble N-ethylmaleimide-sensitive factor (NSF) attachment protein receptor; tmAC, transmembrane adenylyl cyclase; TRPC, transient receptor potential canonical.

In vivo, there is always a concomitant parallel portion of insulin secretion stimulated by 2-monoacylglycerol (MAG), cleaved from postprandial chylomicrons in PI capillaries by lipoprotein lipase (Fig. 10) (37, 158, 182, 272). The resulting MAG and long-chain FAs (37, 158, 182, 272) stimulate their own receptors (171). Adipose triglyceride lipase (ATGL) is the major isoform that cleaves triglycerides in PI capillaries (192), besides secretory phospholipases A2 (64). MAG activates metabotropic receptor GPR119, providing signaling *via* *Gαs* and cAMP (76, 87, 94, 96, 157, 171). It has been questioned whether the levels of FAs bound to albumin can initiate FASIS (102, 261), but this could happen with metabolic syndrome and/or obesity and type 2 diabetes since circulating FA levels are then elevated.

The consensus view was that sufficient glucose must always be present for FAs to induce any insulin secretion (51, 76, 87, 94–96, 157, 206, 245, 276). However, FASIS was described to exist at low (insulin nonstimulating) [glucose] (32, 103, 106, 194), but not at zero glucose (32). Human islets perfused without glucose did not increase respiration with long-chain FAs, but released insulin (32), whereas both increasing respiration and insulin release were observed with long-chain FAs plus 5.5 mM glucose. FASIS was evidenced by FA triggering an action potential with a prolonged duration at low (insulin nonstimulating) [glucose] (57) and concomitantly increased Ca^{2+} influx and hence potentiation of insulin secretion (55, 184). As a result, FASIS should be based on the metabolic components plus metabotropic receptor GPR40 signaling (76, 87, 94, 96, 103, 106, 130, 157, 201, 222, 256, 281, 288). It has to be established whether these two branches are mutually independent.

The major receptor pathway of FASIS (Fig. 10A) includes the metabotropic receptor GPR40, as evidenced by its ablation or its point R258W mutation since both impaired FASIS (222). The major pathway downstream of GPR40 initiates signaling *via* the *Gαq/Gα11* (226), activating phospholipase C- β - (PLC- β -) mediated hydrolysis of phosphatidylinositol 4,5-bisphosphate into DAG and IP3 (23). The major axis involves the phosphorylation of TRPM4 (TRPM5) channels by PKC activated by DAG (231) or TRPC3 activation (276). As with TRPM2, the opening of TRPM4, TRPM5, or TRPC3 determines the necessary depolarization shift, despite the 100% closed K_{ATP} ensemble. The K_{ATP} closure is provided by the metabolic component of FASIS, that is, by FA β -oxidation providing ATP and H_2O_2 , which may also function under low glucose conditions.

Signaling along the axis of GPR40-*Gαq/Gα11*-PLC-IP3 promotes additional Ca^{2+} efflux from the ER (initiated by the Ca_v opening, Fig. 4) *via* the IP3R, forming a Ca^{2+} channel of ER membranes (13, 64). Alternatively, a synergy exists for the plasma membrane channel calcium release-activated calcium modulator 1 (Orai1) with IP3R1 and stromal interaction molecule 1 (STIM1), sensing ER Ca^{2+} (259). If biased GPR40-*Gαs* signaling occurs, also the EPAC2-RyR route of Ca^{2+} -release from ER might contribute to Ca^{2+} oscillations. GPR40 also initiates pathways of protein kinase D (PKD), activated by DAG (56), signal-regulated kinase 1 and 2 (ERK1/2) (201), and p21-activated kinase 4 (PAK4) (21). The latter regulates cytoskeletal dynamics, facilitating IGV exocytosis. Signaling downstream of GPR40 slightly increases respiration during 1-h incubations (130). Thus, PKC (224) and downstream ERK1/2 signaling stimulates OXPHOS, hence mitochondrial ATP synthesis (224).

Long-chain FAs are also imported into pancreatic β -cells by the sirtuin-activated CD36 FA transporter (125) (Fig. 10B). If short-chain FAs are present, they act *via* the GPR41 metabotropic receptor and contribute to the fine-tuning of insulin secretion in both fed and fasting states (200, 263). Similarly, the metabotropic receptor GPR120, having a different selectivity for agonists, mediates the amplification and/or stimulation of insulin secretion, by, for example, α -linolenic acid and polyunsaturated FAs (12, 172).

FA synthesis versus β -oxidation. During GSIS, due to the operation of pyruvate/isocitrate and pyruvate/citrate shuttles, conditions are set for FA synthesis. Metabolomics studies confirmed this, while observing an increase in free palmitic acid after transitions from low to high [glucose] (240). FA metabolism is even considered to be a prerequisite for GSIS since GSIS attenuation was observed in isolated PIs with inhibited triglyceride lipolysis (162, 176), in mice with deleted lipase specifically in β -cells (60) or in ATGL-knockout mice (192). But the net FASIS was not affected by the ATGL deletion. In contrast, at low [glucose] FA β -oxidation readily proceeds in pancreatic β -cells, supplying OXPHOS (Figs. 8 and 10B). Fifty to seventy percent of FAs generated by long-chain acyl-CoA synthetase (ACSL) are recycled into lipogenesis (197).

Retrograde redox signaling upon FASIS. FA β -oxidation is based on mitochondrial flavoprotein dehydrogenases, such as the short-chain acyl-CoA dehydrogenase (EC 1.3.8.1), medium-chain acyl-CoA dehydrogenase (EC 1.3.8.7), long-chain acyl-CoA dehydrogenase (EC 1.3.8.8), and very long-chain acyl-CoA dehydrogenase (EC 1.3.8.9). All of them donate electrons to ETF:QOR *via* ETF and therefore contribute to the mitochondrial superoxide formation, which after conversion to H_2O_2 serves as redox signaling (Fig. 11). Therefore, the mechanism is similar as for the β -like oxidation of BCKAs. Even at low [glucose], the ETF-ETF:QOR redox relay to Complex I and III of the mitochondrial respiratory chain serves as the electron acceptor for dehydrogenases of β -oxidation. Interestingly, GPR40 signaling also activated NOX2 (181).

Redox-sensitive mitochondrial phospholipase iPLA2 γ amplifies FASIS. Notably, the first FASIS phase (the second FASIS phase only moderately) was highly amplified by the action of mitochondrial phospholipase iPLA2 γ (Ca^{2+} -independent phospholipase A2 isoform γ [PNPLA8]), providing the cleaved mitochondrial FAs to GPR40 in insulinoma INS-1E cells (98, 103) and in mouse islets (Holeudová *et al.*, unpublished data). The iPLA2 γ is directly activated by H_2O_2 , and it is also activated by the intramitochondrial redox signaling resulting from FA β -oxidation (103). The activated iPLA2 γ cleaves free long-chain FAs from mitochondrial phospholipids. The cleaved long-chain FAs diffuse to the plasma membrane and subsequently stimulate GPR40 (Fig. 10A, B).

This was indicated by the direct observation of FA diffusion to the plasma membrane using the FA-sensitive fluorescent protein ADIFAB (103). Thus, the pool of free long-chain FAs generated by the glycerol/FA cycle (Figs. 8 and 10B) and CD36-mediated import is enriched by FAs cleaved from mitochondrial membranes. In this way, FAs

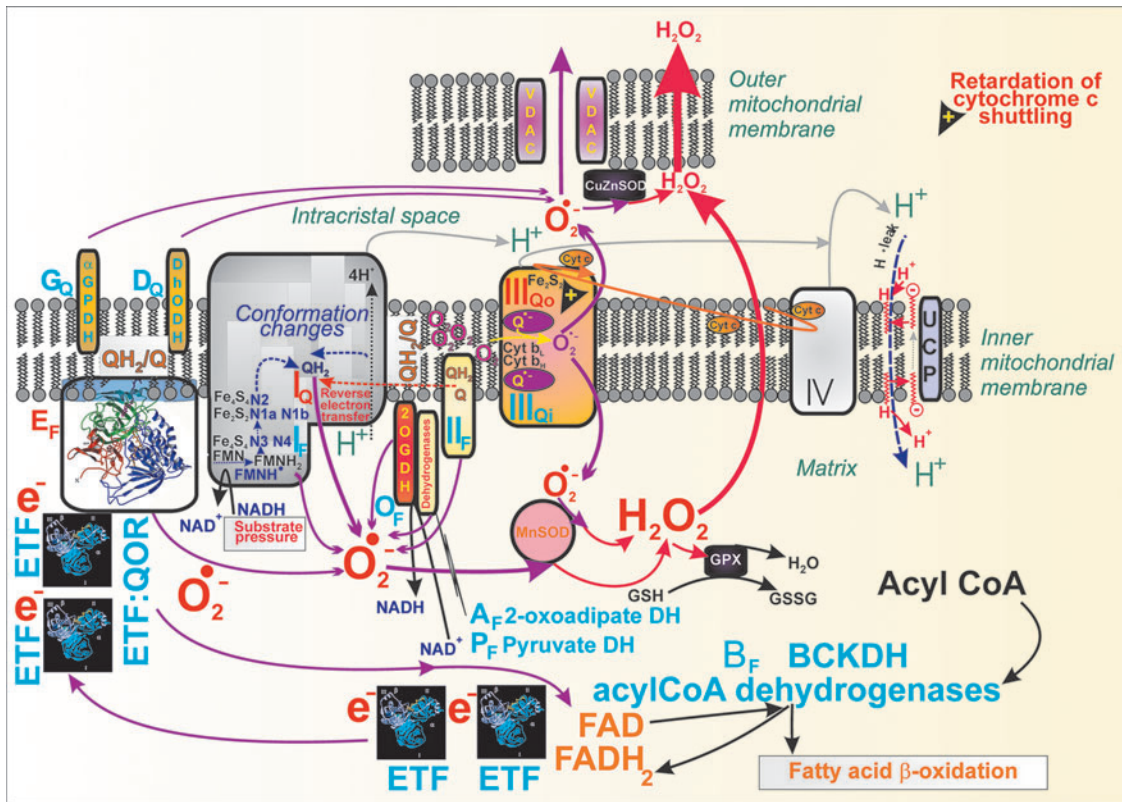


FIG. 11. Superoxide formation due to FA β -oxidation or oxidation of BCKAs. An overview of locations for mitochondrial superoxide sources (*blue capitalized fonts*), termed according to the nomenclature introduced by Brand (25) is shown with those which increase superoxide formation upon FA β -oxidation or the β -like oxidation of BCKAs emphasized (in *red*). The electron-transfer flavoprotein:ubiquinone oxidoreductase (ETFQOR) is a common key electron transfer link between the initial dehydrogenases of these reactions and the respiratory chain complexes III and IV (29, 268). ETFQOR accepts electrons sequentially from two ETFs as single-electron carriers, while converting ubiquinone (Q) from its IMM pool to QH₂. The electron leak from flavin to the oxygen leads to a radical pair formation and subsequent superoxide formation within the ETF:QOR itself (site E_F). Moreover, the requirement of ETF:QOR to react with Q effectively outcompetes Q as the Complex I substrate, resulting in relative electron transfer retardation over the whole respiratory chain, hence superoxide is formed at its sites I_Q and III_Q. Finally, due to the increasing acetyl-CoA entry (propionyl-CoA entry for KIV; through methylmalonyl and succinyl-CoA) and NADH entry into the Krebs cycle, the excessive formation of superoxide at site I_F may also contribute. After the conversion of superoxide to H₂O₂ by the matrix MnSOD and the intermembrane space CuZnSOD, the ongoing H₂O₂ efflux from mitochondria can be regarded as redox signaling. As in other types of mitochondria, there are in total six sites acting at the ~ 280 mV redox potential of the NADH/NAD⁺ isopotential pool (index F, flavin) and five sites acting at the ~ 20 mV redox potential of the QH₂/Q isopotential pool (index Q) (25). Of these, only the superoxide sources with more intensive production at higher $\Delta\Psi_m$ are attenuated by uncoupling proteins (103). This also involves the reverse electron transfer to the Complex I site I_Q. In turn, superoxide formation at site I_F increases with the increasing NADH/NAD⁺ ratio (“substrate pressure”). When cytochrome c shuttling (*orange elliptic arrow*) is retarded, then the Complex III site III_Q provides major superoxide formation, which cannot be attenuated by uncoupling. IMM, inner mitochondrial membrane.

self-accelerate the GPR40 signaling and hence insulin secretion. In INS-1E cells, $\sim 66\%$ of the FASIS first phase was dependent on GPR40, and nearly the same 66% of it was blocked upon the silencing of iPLA2 γ (or its ablation in mice, unpublished data). Hypothetically, the remaining part may depend on the elevation of ATP plus redox signaling from β -oxidation.

Mixed GSIS and FASIS. At high [glucose], triglyceride synthesis alternates with triglyceride hydrolysis in pancreatic β -cells (197). Because of ATP consumption, this cycling is futile. Since DAG is one of the intermediates of this cycle, it may provide all the above-specified signaling (Figs. 8 and

10B). Moreover, free FAs released during the cycle enrich the net GSIS with this supplemental FASIS. Indeed, the addition of FAs to β -cells and PIs at insulin-stimulating [glucose] amplifies GSIS, whereas β -cell acyl-CoA levels increase and appear to rapidly esterify glycerol-3-phosphate into lysophosphatidic acid and several different glycerolipids (51). This partly replenishes cytosolic NAD⁺. Also, glycerol-3-phosphatase produces glycerol and thus regulates glycolysis, the cellular redox state, ATP production, and other important branches of metabolism (175). The largest amount of insulin was secreted by INS-1E cells when palmitic acid plus 25 mM glucose were added, relative to either palmitic acid stimulation alone ($\sim 80\%$ of maximum) and GSIS alone ($\sim 30\%$ of maximum) (103).

Higher glucose decreases acyl-CoA levels in pancreatic β -cells (146). Previously, acyl-CoAs were suggested to activate K_{ATP} (26), hence declining acyl-CoAs would ease the K_{ATP} closure. Moreover, the metabolism of the remaining long-chain acyl-CoAs leads to superoxide/ H_2O_2 formation, which also aids the opening of Ca_v . In contrast, incoming higher glucose levels in pancreatic β -cells increase malonyl-CoA (81, 146), which inhibits carnitine palmitoyltransferase 1 (CPT1) and hence FA β -oxidation. This in turn opens the way for FA synthesis stemming from the ATP citrate lyase (ACL) reaction after the citrate efflux from the mitochondria (174). Nevertheless, the silencing of ACL and FA synthase in β -cells did not affect GSIS (113).

Upon increasing [glucose], glycerol-3-phosphate is also esterified, so the abundance of long-chain saturated monoacylglycerols increases (174, 291). These MAGs additionally stimulate insulin secretion *via* the GPR119 receptor and downstream PKA and EPAC2 pathway; the latter notably facilitates IGv priming by activating the protein Munc13-1 (291) (Figs. 8 and 10A). Note that this is similar to the GPR40 activation by the FAs cleaved in the cell interior, that is, from the mitochondrial membranes by mitochondrial phospholipase iPLA2 γ .

Acknowledgment

The authors gratefully acknowledge the precise frequent renumbering of references during the article preparation and molecular modeling for Figure 2 by B.H.

Authors' Contributions

Conceptualization, P.J.; resources, B.H.; writing—original draft preparation, P.J.; writing—review and editing, P.J., B.H., A.D., M.J., and L.P.-H.; funding acquisition, P.J.

Author Disclosure Statement

The authors declare no conflicts of interest.

Funding Information

This research was funded by the Grant Agency of the Czech Republic (Grantová Agentura České Republiky, GAČR), grant number 20-00408S.

References

1. Abulizi A, Cardone RL, Stark R, Lewandowski SL, Zhao X, Hillion J, Ma L, Sehgal R, Alves TC, Thomas C, Kung C, Wang B, Siebel S, Andrews ZB, Mason GF, Rinehart J, Merrins MJ, and Kibbey RG. Multi-tissue acceleration of the mitochondrial phosphoenolpyruvate cycle improves whole-body metabolic health. *Cell Metab* 32: 751.e11–766.e11, 2020.
2. Acin-Perez R, Russwurm M, Günnewig K, Gertz M, Zoidl G, Ramos L, Buck J, Levin LR, Rassow J, Manfredi G, and Steegborn C. A phosphodiesterase 2A isoform localized to mitochondria regulates respiration. *J Biol Chem* 286: 30423–30432, 2011.
3. Agnes RS, Jernigan F, Shell JR, Sharma V, and Lawrence DS. Suborganelle sensing of mitochondrial cAMP-dependent protein kinase activity. *J Am Chem Soc* 132: 6075–6080, 2010.
4. Alam MR, Groschner LN, Parichatikanond W, Kuo L, Bondarenko AI, Rost R, Waldeck-Weiermair M, Malli R, and Graier WF. Mitochondrial Ca^{2+} uptake 1 (MICU1) and mitochondrial Ca^{2+} uniporter (MCU) contribute to metabolism-secretion coupling in clonal pancreatic β -cells. *J Biol Chem* 287: 34445–34454, 2012.
5. Alejandro EU, Gregg B, Blandino-Rosano M, Cras-Méneur C, and Bernal-Mizrachi E. Natural history of β -cell adaptation and failure in type 2 diabetes. *Mol Aspects Med* 42: 19–41, 2015.
6. Alves TC, Pongratz RL, Zhao X, Yarborough O, Sereda S, Shirihai O, Cline GW, Mason G, and Kibbey RG. Integrated, step-wise, mass-isotopomeric flux analysis of the TCA cycle. *Cell Metab* 22: 936–947, 2015.
7. Ashcroft FM, Ashcroft SJ, and Harrison DE. Effects of 2-ketoisocaproate on insulin release and single potassium channel activity in dispersed rat pancreatic beta-cells. *J Physiol* 385: 517–529, 1987.
8. Ashcroft FM, Harrison DE, and Ashcroft SJ. Glucose induces closure of single potassium channels in isolated rat pancreatic beta-cells. *Nature* 312: 446–448, 1984.
9. Ashcroft FM, Puljung MC, and Vedovato N. Neonatal diabetes and the K(ATP) channel: from mutation to therapy. *Trends Endocrinol Metab* 28: 377–387, 2017.
10. Aspinwall CA, Brooks SA, Kennedy RT, and Lakey JR. Effects of intravesicular H^+ and extracellular H^+ and Zn^{2+} on insulin secretion in pancreatic beta cells. *J Biol Chem* 272: 31308–31314, 1997.
11. Babenko AP and Vaxillaire M. Mechanism of K_{ATP} hyperactivity and sulfonyleurea tolerance due to a diabetogenic mutation in L0 helix of sulfonyleurea receptor 1 (ABCC8). *FEBS Lett* 585: 3555–3559, 2011.
12. Bai T, Yang H, Wang H, Zhi L, Liu T, Cui L, Liu W, Wang Y, Zhang M, Liu Y, and Zhang Y. Inhibition of voltage-gated K(+) channels mediates docosahexaenoic acid-stimulated insulin secretion in rat pancreatic β -cells. *Food Funct* 11: 8893–8904, 2020.
13. Barker CJ and Berggren PO. New horizons in cellular regulation by inositol polyphosphates: insights from the pancreatic β -cell. *Pharmacol Rev* 65: 641–669, 2013.
14. Baukowitz T, Schulte U, Oliver D, Herlitz S, Krauter T, Tucker SJ, Ruppertsberg JP, and Fakler B. PIP2 and PIP as determinants for ATP inhibition of K_{ATP} channels. *Science* 282: 1141–1144, 1998.
15. Beauvois MC, Merezak C, Jonas JC, Ravier MA, Henquin JC, and Gilon P. Glucose-induced mixed $[Ca^{2+}]_c$ oscillations in mouse beta-cells are controlled by the membrane potential and the SERCA3 Ca^{2+} -ATPase of the endoplasmic reticulum. *Am J Physiol Cell Physiol* 290: C1503–C1511, 2006.
16. Béguin P, Nagashima K, Nishimura M, Gono T, and Seino S. PKA-mediated phosphorylation of the human K(ATP) channel: separate roles of Kir6.2 and SUR1 subunit phosphorylation. *EMBO J* 18: 4722–4732, 1999.
17. Benáková Š, Holendová B, and Plecítá-Hlavatá L. Redox homeostasis in pancreatic β -cells: from development to failure. *Antioxidants (Basel)* 10: 526, 2021.
18. Bender K, Maechler P, McClenaghan NH, Flatt PR, and Newsholme P. Overexpression of the malate-aspartate NADH shuttle member Aralar1 in the clonal beta-cell line BRIN-BD11 enhances amino-acid-stimulated insulin secretion and cell metabolism. *Clin Sci (Lond)* 117: 321–330, 2009.

19. Bennett K, James C, and Hussain K. Pancreatic β -cell K_{ATP} channels: hypoglycaemia and hyperglycaemia. *Rev Endocr Metab Disord* 11: 157–163, 2010.
20. Bensellam M, Jonas JC, and Laybutt DR. Mechanisms of β -cell dedifferentiation in diabetes: recent findings and future research directions. *J Endocrinol* 236: R109–R143, 2018.
21. Bergeron V, Ghislain J, and Poirier V. The P21-activated kinase PAK4 is implicated in fatty-acid potentiation of insulin secretion downstream of free fatty acid receptor 1. *Islets* 8: 157–164, 2016.
22. Bermont F, Hermant A, Benninga R, Chabert C, Jacot G, Santo-Domingo J, Kraus MR, Feige JN, and De Marchi U. Targeting mitochondrial calcium uptake with the natural flavonol kaempferol, to promote metabolism/secretion coupling in pancreatic β -cells. *Nutrients* 12: 538, 2020.
23. Berridge MJ. The inositol trisphosphate/calcium signaling pathway in health and disease. *Physiol Rev* 96: 1261–1296, 2016.
24. Bertrand G, Ishiyama N, Nenquin M, Ravier MA, and Henquin JC. The elevation of glutamate content and the amplification of insulin secretion in glucose-stimulated pancreatic islets are not causally related. *J Biol Chem* 277: 32883–32891, 2002.
25. Brand MD. Mitochondrial generation of superoxide and hydrogen peroxide as the source of mitochondrial redox signaling. *Free Radic Biol Med* 100: 14–31, 2016.
26. Bränström R, Aspinwall CA, Välimäki S, Ostensson CG, Tibell A, Eckhard M, Brandhorst H, Corkey BE, Berggren PO, and Larsson O. Long-chain CoA esters activate human pancreatic beta-cell K_{ATP} channels: potential role in type 2 diabetes. *Diabetologia* 47: 277–283, 2004.
27. Bränström R, Corkey BE, Berggren PO, and Larsson O. Evidence for a unique long chain acyl-CoA ester binding site on the ATP-regulated potassium channel in mouse pancreatic beta cells. *J Biol Chem* 272: 17390–17394, 1997.
28. Bränström R, Leibiger IB, Leibiger B, Corkey BE, Berggren PO, and Larsson O. Long chain coenzyme A esters activate the pore-forming subunit (Kir6. 2) of the ATP-regulated potassium channel. *J Biol Chem* 273: 31395–31400, 1998.
29. Bunik VI. Redox-driven signaling: 2-oxo acid dehydrogenase complexes as sensors and transmitters of metabolic imbalance. *Antioxid Redox Signal* 30: 1911–1947, 2019.
30. Casimir M, Lasorsa FM, Rubi B, Caille D, Palmieri F, Meda P, and Maechler P. Mitochondrial glutamate carrier GC1 as a newly identified player in the control of glucose-stimulated insulin secretion. *J Biol Chem* 284: 25004–25014, 2009.
31. Catterall WA. Structure and regulation of voltage-gated Ca^{2+} channels. *Annu Rev Cell Dev Biol* 16: 521–555, 2000.
32. Cen J, Sargsyan E, and Bergsten P. Fatty acids stimulate insulin secretion from human pancreatic islets at fasting glucose concentrations via mitochondria-dependent and -independent mechanisms. *Nutr Metab (Lond)* 13: 59, 2016.
33. Chen WW, Freinkman E, Wang T, Birsoy K, and Sabatini DM. Absolute quantification of matrix metabolites reveals the dynamics of mitochondrial metabolism. *Cell* 166: 1324.e11–1337.e11, 2016.
34. Chen Y, Cann MJ, Litvin TN, Iourgenko V, Sinclair ML, Levin LR, and Buck J. Soluble adenylyl cyclase as an evolutionarily conserved bicarbonate sensor. *Science* 289: 625–628, 2000.
35. Cook DL and Hales CN. Intracellular ATP directly blocks K^{+} channels in pancreatic B-cells. *Nature* 311: 271–273, 1984.
36. Craig TJ, Ashcroft FM, and Proks P. How ATP inhibits the open $K(ATP)$ channel. *J Gen Physiol* 132: 131–144, 2008.
37. Cruz WS, Kwon G, Marshall CA, McDaniel ML, and Semenkovich CF. Glucose and insulin stimulate heparin-releasable lipoprotein lipase activity in mouse islets and INS-1 cells. A potential link between insulin resistance and beta-cell dysfunction. *J Biol Chem* 276: 12162–12168, 2001.
38. De Marchi U, Galindo AN, Thevenet J, Hermant A, Bermont F, Lassueur S, Domingo JS, Kussmann M, Dayon L, and Wiederkehr A. Mitochondrial lysine deacetylation promotes energy metabolism and calcium signaling in insulin-secreting cells. *FASEB J* 33: 4660–4674, 2019.
39. De Rasmio D, Micelli L, Santeramo A, Signorile A, Lattanzio P, and Papa S. cAMP regulates the functional activity, coupling efficiency and structural organization of mammalian FOF1 ATP synthase. *Biochim Biophys Acta* 1857: 350–358, 2016.
40. de Rooij J, Zwartkruis FJ, Verheijen MH, Cool RH, Nijman SM, Wittinghofer A, and Bos JL. Epac is a Rap1 guanine-nucleotide-exchange factor directly activated by cyclic AMP. *Nature* 396: 474–477, 1998.
41. De Stefani D, Raffaello A, Teardo E, Szabò I, and Rizzuto R. A forty-kilodalton protein of the inner membrane is the mitochondrial calcium uniporter. *Nature* 476: 336–340, 2011.
42. Denton RM. Regulation of mitochondrial dehydrogenases by calcium ions. *Biochim Biophys Acta* 1787: 1309–1316, 2009.
43. Detimary P, Dejonghe S, Ling Z, Pipeleers D, Schuit F, and Henquin JC. The changes in adenine nucleotides measured in glucose-stimulated rodent islets occur in beta cells but not in alpha cells and are also observed in human islets. *J Biol Chem* 273: 33905–33908, 1998.
44. Di Benedetto G, Scalzotto E, Mongillo M, and Pozzan T. Mitochondrial Ca^{2+} uptake induces cyclic AMP generation in the matrix and modulates organelle ATP levels. *Cell Metab* 17: 965–975, 2013.
45. Di Fulvio M and Aguilar-Bryan L. Chloride transporters and channels in β -cell physiology: revisiting a 40-year-old model. *Biochem Soc Trans* 47: 1843–1855, 2019.
46. DiPilato LM, Cheng X, and Zhang J. Fluorescent indicators of cAMP and Epac activation reveal differential dynamics of cAMP signaling within discrete subcellular compartments. *Proc Natl Acad Sci U S A* 101: 16513–16518, 2004.
47. Doliba NM, Qin W, Najafi H, Liu C, Buettger CW, Sotiris J, Collins HW, Li C, Stanley CA, Wilson DF, Grimsby J, Sarabu R, Naji A, and Matschinsky FM. Glucokinase activation repairs defective bioenergetics of islets of Langerhans isolated from type 2 diabetics. *Am J Physiol Endocrinol Metab* 302: E87–E102, 2012.
48. Drews G, Bauer C, Edalat A, Düfer M, and Krippeit-Drews P. Evidence against a Ca^{2+} -induced potentiation of dehydrogenase activity in pancreatic beta-cells. *Pflügers Arch* 467: 2389–2397, 2015.
49. Drews G, Krippeit-Drews P, and Düfer M. Electrophysiology of Islet Cells. In: Islam M. (ed). The Islets of

- Langerhans. *Advances in Experimental Medicine and Biology*, vol. 654. Springer, Dordrecht. https://doi.org/10.1007/978-90-481-3271-3_7.
50. Düfer M, Gier B, Wolpers D, Krippeit-Drews P, Ruth P, and Drews G. Enhanced glucose tolerance by SK4 channel inhibition in pancreatic beta-cells. *Diabetes* 58: 1835–1843, 2009.
 51. El-Azzouny M, Evans CR, Treutelaar MK, Kennedy RT, and Burant CF. Increased glucose metabolism and glycerolipid formation by fatty acids and GPR40 receptor signaling underlies the fatty acid potentiation of insulin secretion. *J Biol Chem* 289: 13575–13588, 2014.
 52. El Azzouny M, Longacre MJ, Ansari IH, Kennedy RT, Burant CF, and MacDonald MJ. Knockdown of ATP citrate lyase in pancreatic beta cells does not inhibit insulin secretion or glucose flux and implicates the acetoacetate pathway in insulin secretion. *Mol Metab* 5: 980–987, 2016.
 53. Esparza-Moltó PB and Cuezva JM. Reprogramming oxidative phosphorylation in cancer: a role for RNA-binding proteins. *Antioxid Redox Signal* 33: 927–945, 2020.
 54. Farfari S, Schulz V, Corkey B, and Prentki M. Glucose-regulated anaplerosis and cataplerosis in pancreatic beta-cells: possible implication of a pyruvate/citrate shuttle in insulin secretion. *Diabetes* 49: 718–726, 2000.
 55. Feng DD, Luo Z, Roh SG, Hernandez M, Tawadros N, Keating DJ, and Chen C. Reduction in voltage-gated K⁺ currents in primary cultured rat pancreatic beta-cells by linoleic acids. *Endocrinology* 147: 674–682, 2006.
 56. Ferdaoussi M, Bergeron V, Zarrouki B, Kolic J, Cantley J, Fielitz J, Olson EN, Prentki M, Biden T, MacDonald PE, and Poitout V. G protein-coupled receptor (GPR)40-dependent potentiation of insulin secretion in mouse islets is mediated by protein kinase D1. *Diabetologia* 55: 2682–2692, 2012.
 57. Fernandez J and Valdeolmillos M. Increased levels of free fatty acids in fasted mice stimulate in vivo beta-cell electrical activity. *Diabetes* 47: 1707–1712, 1998.
 58. Fernandez J and Valdeolmillos M. Glucose-dependent stimulatory effect of glucagon-like peptide 1(7–36) amide on the electrical activity of pancreatic beta-cells recorded in vivo. *Diabetes* 48: 754–757, 1999.
 59. Fernandez J and Valdeolmillos M. Synchronous glucose-dependent [Ca(2+)](i) oscillations in mouse pancreatic islets of Langerhans recorded in vivo. *FEBS Lett* 477: 33–36, 2000.
 60. Fex M, Haemmerle G, Wierup N, Dekker-Nitert M, Rehn M, Ristow M, Zechner R, Sundler F, Holm C, Eliasson L, and Mulder H. A beta cell-specific knockout of hormone-sensitive lipase in mice results in hyperglycaemia and disruption of exocytosis. *Diabetologia* 52: 271–280, 2009.
 61. Frayn KN. *Metabolic Regulation: A Human Perspective*. Chichester, UK: A John Wiley & Sons, Ltd., 2010, pp. 53–76; 144–168; 169–212; 306–328.
 62. Freeman H, Shimomura K, Cox RD, and Ashcroft FM. Nicotinamide nucleotide transhydrogenase: a link between insulin secretion, glucose metabolism and oxidative stress. *Biochem Soc Trans* 34: 806–810, 2006.
 63. Freeman HC, Huggill A, Dear NT, Ashcroft FM, and Cox RD. Deletion of nicotinamide nucleotide transhydrogenase: a new quantitative trait locus accounting for glucose intolerance in C57BL/6J mice. *Diabetes* 55: 2153–2156, 2006.
 64. Fujiwara K, Maekawa F, and Yada T. Oleic acid interacts with GPR40 to induce Ca²⁺ signaling in rat islet beta-cells: mediation by PLC and L-type Ca²⁺ channel and link to insulin release. *Am J Physiol Endocrinol Metab* 289: E670–E677, 2005.
 65. Furman B, Ong WK, and Pyne NJ. Cyclic AMP signaling in pancreatic islets. *Adv Exp Med Biol* 654: 281–304, 2010.
 66. Gammelsaeter R, Coppola T, Marcaggi P, Storm-Mathisen J, Chaudhry FA, Attwell D, Regazzi R, and Gundersen V. A role for glutamate transporters in the regulation of insulin secretion. *PLoS One* 6: e22960, 2011.
 67. Gao ZY, Li G, Najafi H, Wolf BA, and Matschinsky FM. Glucose regulation of glutaminolysis and its role in insulin secretion. *Diabetes* 48: 1535–1542, 1999.
 68. García-Aguilar A and Cuezva JM. A review of the inhibition of the mitochondrial ATP synthase by IF1 in vivo: reprogramming energy metabolism and inducing mitohormesis. *Front Physiol* 9: 1322, 2018.
 69. García-Bermúdez J, Sánchez-Aragó M, Soldevilla B, Del Arco A, Nuevo-Tapióles C, and Cuezva JM. PKA phosphorylates the ATPase inhibitory factor 1 and inactivates its capacity to bind and inhibit the mitochondrial H(+)-ATP synthase. *Cell Rep* 12: 2143–2155, 2015.
 70. Georgiadou E, Haythorne E, Dickerson MT, Lopez-Noriega L, Pullen TJ, da Silva Xavier G, Davis SPX, Martinez-Sanchez A, Semplici F, Rizzuto R, McGinty JA, French PM, Cane MC, Jacobson DA, Leclerc I, and Rutter GA. The pore-forming subunit MCU of the mitochondrial Ca(2+) uniporter is required for normal glucose-stimulated insulin secretion in vitro and in vivo in mice. *Diabetologia* 63: 1368–1381, 2020.
 71. Georgiadou E and Rutter GA. Control by Ca(2+) of mitochondrial structure and function in pancreatic β -cells. *Cell Calcium* 91: 102282, 2020.
 72. Ghenni G, Ogura M, Iwasaki M, Yokoi N, Minami K, Nakayama Y, Harada K, Hastoy B, Wu X, Takahashi H, Kimura K, Matsubara T, Hoshikawa R, Hatano N, Sugawara K, Shibasaki T, Inagaki N, Bamba T, Mizoguchi A, Fukusaki E, Rorsman P, and Seino S. Glutamate acts as a key signal linking glucose metabolism to incretin/cAMP action to amplify insulin secretion. *Cell Rep* 9: 661–673, 2014.
 73. Gilon P, Ravier MA, Jonas JC, and Henquin JC. Control mechanisms of the oscillations of insulin secretion in vitro and in vivo. *Diabetes* 51(Suppl 1): S144–S151, 2002.
 74. Gledhill JR, Montgomery MG, Leslie AG, and Walker JE. How the regulatory protein, IF(1), inhibits F(1)-ATPase from bovine mitochondria. *Proc Natl Acad Sci U S A* 104: 15671–15676, 2007.
 75. Gloerich M and Bos JL. Epac: defining a new mechanism for cAMP action. *Annu Rev Pharmacol Toxicol* 50: 355–375, 2010.
 76. Graciano MF, Valle MM, Curi R, and Carpinelli AR. Evidence for the involvement of GPR40 and NADPH oxidase in palmitic acid-induced superoxide production and insulin secretion. *Islets* 5: 139–148, 2013.
 77. Gribble FM, Proks P, Corkey BE, and Ashcroft FM. Mechanism of cloned ATP-sensitive potassium channel activation by oleoyl-CoA. *J Biol Chem* 273: 26383–26387, 1998.
 78. Grimsrud PA, Carson JJ, Hebert AS, Hubler SL, Niemi NM, Bailey DJ, Jochem A, Stapleton DS, Keller MP, Westphall MS, Yandell BS, Attie AD, Coon JJ, and Paggiarini DJ. A quantitative map of the liver mitochondrial phosphoproteome reveals posttranslational control of ketogenesis. *Cell Metab* 16: 672–683, 2012.

79. Grupe M, Myers G, Penner R, and Fleig A. Activation of store-operated I(CRAC) by hydrogen peroxide. *Cell Calcium* 48: 1–9, 2010.
80. Gu J, Zhang L, Zong S, Guo R, Liu T, Yi J, Wang P, Zhuo W, and Yang M. Cryo-EM structure of the mammalian ATP synthase tetramer bound with inhibitory protein IF1. *Science* 364: 1068–1075, 2019.
81. Guay C, Joly E, Pepin E, Barbeau A, Hentsch L, Pineda M, Madiraju SR, Brunengraber H, and Prentki M. A role for cytosolic isocitrate dehydrogenase as a negative regulator of glucose signaling for insulin secretion in pancreatic β -cells. *PLoS One* 8: e77097, 2013.
82. Guay C, Madiraju SR, Aumais A, Joly E, and Prentki M. A role for ATP-citrate lyase, malic enzyme, and pyruvate/citrate cycling in glucose-induced insulin secretion. *J Biol Chem* 282: 35657–35665, 2007.
83. Gurgul-Convey E, Kaminski MT, and Lenzen S. Physiological characterization of the human EndoC- β H1 β -cell line. *Biochem Biophys Res Commun* 464: 13–19, 2015.
84. Hara Y, Wakamori M, Ishii M, Maeno E, Nishida M, Yoshida T, Yamada H, Shimizu S, Mori E, Kudoh J, Shimizu N, Kurose H, Okada Y, Imoto K, and Mori Y. LTRPC2 Ca²⁺-permeable channel activated by changes in redox status confers susceptibility to cell death. *Mol Cell* 9: 163–173, 2002.
85. Hasan NM, Longacre MJ, Stoker SW, Kendrick MA, and MacDonald MJ. Mitochondrial malic enzyme 3 is important for insulin secretion in pancreatic β -cells. *Mol Endocrinol* 29: 396–410, 2015.
86. Hashim M, Yokoi N, Takahashi H, Gheni G, Okechi OS, Hayami T, Murao N, Hidaka S, Minami K, Mizoguchi A, and Seino S. Inhibition of SNAT5 induces incretin-responsive state from incretin-unresponsive state in pancreatic β -cells: study of β -cell spheroid clusters as a model. *Diabetes* 67: 1795–1806, 2018.
87. Hauge M, Vestmar MA, Husted AS, Ekberg JP, Wright MJ, Di Salvo J, Weinglass AB, Engelstoft MS, Madsen AN, Luckmann M, Müller MW, Trujillo ME, Frimurer TM, Holst B, Howard AD, and Schwartz TW. GPR40 (FFAR1)—combined Gs and Gq signaling in vitro is associated with robust incretin secretagogue action ex vivo and in vivo. *Mol Metab* 4: 3–14, 2015.
88. Heissig H, Urban KA, Hastedt K, Zünkler BJ, and Panten U. Mechanism of the insulin-releasing action of alpha-ketoisocaproate and related alpha-keto acid anions. *Mol Pharmacol* 68: 1097–1105, 2005.
89. Henquin JC, Dufrene D, and Nenquin M. Nutrient control of insulin secretion in isolated normal human islets. *Diabetes* 55: 3470–3477, 2006.
90. Hodson DJ, Tarasov AI, Gimeno Brias S, Mitchell RK, Johnston NR, Haghollahi S, Cane MC, Bugliani M, Marchetti P, Bosco D, Johnson PR, Hughes SJ, and Rutter GA. Incretin-modulated beta cell energetics in intact islets of Langerhans. *Mol Endocrinol* 28: 860–871, 2014.
91. Hoppa MB, Collins S, Ramracheya R, Hodson L, Amisten S, Zhang Q, Johnson P, Ashcroft FM, and Rorsman P. Chronic palmitate exposure inhibits insulin secretion by dissociation of Ca(2+) channels from secretory granules. *Cell Metab* 10: 455–465, 2009.
92. Høy M, Maechler P, Efanov AM, Wollheim CB, Berggren PO, and Gromada J. Increase in cellular glutamate levels stimulates exocytosis in pancreatic beta-cells. *FEBS Lett* 531: 199–203, 2002.
93. Hull J, Hindy ME, Kehoe PG, Chalmers K, Love S, and Conway ME. Distribution of the branched chain aminotransferase proteins in the human brain and their role in glutamate regulation. *J Neurochem* 123: 997–1009, 2012.
94. Husted AS, Trauelsen M, Rudenko O, Hjorth SA, and Schwartz TW. GPCR-mediated signaling of metabolites. *Cell Metab* 25: 777–796, 2017.
95. Itoh K, Moriguchi R, Yamada Y, Fujita M, Yamato T, Oumi M, Holst JJ, and Seino Y. High saturated fatty acid intake induces insulin secretion by elevating gastric inhibitory polypeptide levels in healthy individuals. *Nutr Res* 34: 653–660, 2014.
96. Itoh Y, Kawamata Y, Harada M, Kobayashi M, Fujii R, Fukusumi S, Ogi K, Hosoya M, Tanaka Y, Uejima H, Tanaka H, Maruyama M, Satoh R, Okubo S, Kizawa H, Komatsu H, Matsumura F, Noguchi Y, Shinohara T, Hinuma S, Fujisawa Y, and Fujino M. Free fatty acids regulate insulin secretion from pancreatic β cells through GPR40. *Nature* 422: 173–176, 2003.
97. Ivarsson R, Quintens R, Dejonghe S, Tsukamoto K, in 't Veld P, Renström E, and Schuit FC. Redox control of exocytosis: regulatory role of NADPH, thioredoxin, and glutaredoxin. *Diabetes* 54: 2132–2142, 2005.
98. Jabůrek M, Průchová P, Holendová B, Galkin A, and Ježek P. Antioxidant synergy of mitochondrial phospholipase PNPLA8/iPLA2 γ with fatty acid-conducting SLC25 gene family transporters. *Antioxidants (Basel)* 10: 678, 2021.
99. Jacob S, Köhler M, Tröster P, Visa M, García-Prieto CF, Alanentalo T, Moede T, Leibiger B, Leibiger IB, and Berggren PO. In vivo Ca(2+) dynamics in single pancreatic β cells. *FASEB J* 34: 945–959, 2020.
100. Jacobson DA, Kuznetsov A, Lopez JP, Kash S, Ammälä CE, and Philipson LH. Kv2.1 ablation alters glucose-induced islet electrical activity, enhancing insulin secretion. *Cell Metab* 6: 229–235, 2007.
101. Jacobson DA and Shyng SL. Ion channels of the islets in type 2 diabetes. *J Mol Biol* 432: 1326–1346, 2020.
102. Jensen MD and Nielsen S. Insulin dose response analysis of free fatty acid kinetics. *Metabolism* 56: 68–76, 2007.
103. Ježek J, Dlasková A, Zelenka J, Jabůrek M, and Ježek P. H₂O₂-activated mitochondrial phospholipase iPLA2 γ prevents lipotoxic oxidative stress in synergy with UCP2, amplifies signaling via g-protein-coupled receptor GPR40, and regulates insulin secretion in pancreatic β -cells. *Antioxid Redox Signal* 23: 958–972, 2015.
104. Ježek P, Holendová B, Jabůrek M, Tauber J, Dlasková A, and Plecítá-Hlavatá L. The pancreatic β -cell: the perfect redox system. *Antioxidants (Basel)* 10: 197, 2021.
105. Ježek P, Holendova B, and Plecítá-Hlavata L. Redox signaling from mitochondria: signal propagation and its targets. *Biomolecules* 10: 93, 2020.
106. Ježek P, Jaburek M, Holendova B, and Plecítá-Hlavata L. Fatty acid-stimulated insulin secretion vs. lipotoxicity. *Molecules* 23: 1483, 2018.
107. Ježek P, Jabůrek M, and Plecítá-Hlavatá L. Contribution of oxidative stress and impaired biogenesis of pancreatic β -cells to type 2 diabetes. *Antioxid Redox Signal* 31: 722–751, 2019.
108. Jimenez-Sánchez C, Brun T, and Maechler P. Mitochondrial carriers regulating insulin secretion profiled in human islets upon metabolic stress. *Biomolecules* 10: 1543, 2020.

109. Jing X, Li DQ, Olofsson CS, Salehi A, Surve VV, Caballero J, Ivarsson R, Lundquist I, Pereverzev A, Schneider T, Rorsman P, and Renström E. $Ca_v2.3$ calcium channels control second-phase insulin release. *J Clin Invest* 115: 146–154, 2005.
110. Jitrapakdee S, Wutthisathapornchai A, Wallace JC, and MacDonald MJ. Regulation of insulin secretion: role of mitochondrial signalling. *Diabetologia* 53: 1019–1032, 2010.
111. Johnston NR, Mitchell RK, Haythorne E, Pessoa MP, Semplici F, Ferrer J, Piemonti L, Marchetti P, Bugliani M, Bosco D, Berishvili E, Duncanson P, Watkinson M, Broichhagen J, Trauner D, Rutter GA, and Hodson DJ. Beta cell hubs dictate pancreatic islet responses to glucose. *Cell Metab* 24: 389–401, 2016.
112. Joseph JW, Jensen MV, Ilkayeva O, Palmieri F, Alárcon C, Rhodes CJ, and Newgard CB. The mitochondrial citrate/isocitrate carrier plays a regulatory role in glucose-stimulated insulin secretion. *J Biol Chem* 281: 35624–35632, 2006.
113. Joseph JW, Odegaard ML, Ronnebaum SM, Burgess SC, Muehlbauer J, Sherry AD, and Newgard CB. Normal flux through ATP-citrate lyase or fatty acid synthase is not required for glucose-stimulated insulin secretion. *J Biol Chem* 282: 31592–31600, 2007.
114. Kadenbach B. Regulation of cytochrome c oxidase contributes to health and optimal life. *World J Biol Chem* 11: 52–61, 2020.
115. Kahancová A, Sklenář F, Ježek P, and Dlasková A. Regulation of glucose-stimulated insulin secretion by ATPase inhibitory factor 1 (IF1). *FEBS Lett* 592: 999–1009, 2018.
116. Kahancová A, Sklenář F, Ježek P, and Dlasková A. Overexpression of native IF1 downregulates glucose-stimulated insulin secretion by pancreatic INS-1E cells. *Sci Rep* 10: 1551, 2020.
117. Kahn SE, Hull RL, and Utzschneider KM. Mechanisms linking obesity to insulin resistance and type 2 diabetes. *Nature* 444: 840–846, 2006.
118. Kakei M, Kelly RP, Ashcroft SJ, and Ashcroft FM. The ATP-sensitivity of K^+ channels in rat pancreatic B-cells is modulated by ADP. *FEBS Lett* 208: 63–66, 1986.
119. Kakei M, Yoshida M, Dezaki K, Ito K, Yamada H, Funazaki S, Kawakami M, Sugawara H, and Yada T. Glucose and GTP-binding protein-coupled receptor cooperatively regulate transient receptor potential-channels to stimulate insulin secretion [review]. *Endocr J* 63: 867–876, 2016.
120. Kang G, Joseph JW, Chepurny OG, Monaco M, Wheeler MB, Bos JL, Schwede F, Genieser HG, and Holz GG. Epac-selective cAMP analog 8-pCPT-2'-O-Me-cAMP as a stimulus for Ca^{2+} -induced Ca^{2+} release and exocytosis in pancreatic beta-cells. *J Biol Chem* 278: 8279–8285, 2003.
121. Kang G, Leech CA, Chepurny OG, Coetzee WA, and Holz GG. Role of the cAMP sensor Epac as a determinant of K_{ATP} channel ATP sensitivity in human pancreatic beta-cells and rat INS-1 cells. *J Physiol* 586: 1307–1319, 2008.
122. Kanno T, Suga S, Wu J, Kimura M, and Wakui M. Intracellular cAMP potentiates voltage-dependent activation of L-type Ca^{2+} channels in rat islet beta-cells. *Pflugers Arch* 435: 578–580, 1998.
123. Kashio M and Tominaga M. Redox signal-mediated enhancement of the temperature sensitivity of transient receptor potential melastatin 2 (TRPM2) elevates glucose-induced insulin secretion from pancreatic islets. *J Biol Chem* 290: 12435–12442, 2015.
124. Kennedy ED, Rizzuto R, Theler JM, Pralong WF, Bastianutto C, Pozzan T, and Wollheim CB. Glucose-stimulated insulin secretion correlates with changes in mitochondrial and cytosolic Ca^{2+} in aequorin-expressing INS-1 cells. *J Clin Invest* 98: 2524–2538, 1996.
125. Khan S and Kowluru A. CD36 mediates lipid accumulation in pancreatic beta cells under the duress of glucolipotoxic conditions: novel roles of lysine deacetylases. *Biochem Biophys Res Commun* 495: 2221–2226, 2018.
126. Kibbey RG, Pongratz RL, Romanelli AJ, Wollheim CB, Cline GW, and Shulman GI. Mitochondrial GTP regulates glucose-stimulated insulin secretion. *Cell Metab* 5: 253–264, 2007.
127. Klec C, Ziomek G, Pichler M, Malli R, and Graier WF. Calcium signaling in β -cell physiology and pathology: a revisit. *Int J Mol Sci* 20: 6110, 2019.
128. Koster JC, Cadario F, Peruzzi C, Colombo C, Nichols CG, and Barbetti F. The G53D mutation in Kir6.2 (KCNJ11) is associated with neonatal diabetes and motor dysfunction in adulthood that is improved with sulfonylurea therapy. *J Clin Endocrinol Metab* 93: 1054–1061, 2008.
129. Kostic M, Katoshevski T, and Sekler I. Allosteric regulation of NCLX by mitochondrial membrane potential links the metabolic state and $Ca(2+)$ signaling in mitochondria. *Cell Rep* 25: 3465.e4–3475.e4, 2018.
130. Kristinsson H, Bergsten P, and Sargsyan E. Free fatty acid receptor 1 (FFAR1/GPR40) signaling affects insulin secretion by enhancing mitochondrial respiration during palmitate exposure. *Biochim Biophys Acta* 1853: 3248–3257, 2015.
131. Lee KPK, Chen J, and MacKinnon R. Molecular structure of human K_{ATP} in complex with ATP and ADP. *Elife* 6: e32481, 2017.
132. Lefkimmiatis K, Leronna D, and Hofer AM. The inner and outer compartments of mitochondria are sites of distinct cAMP/PKA signaling dynamics. *J Cell Biol* 202: 453–462, 2013.
133. Lefkimmiatis K and Zaccolo M. cAMP signaling in sub-cellular compartments. *Pharmacol Ther* 143: 295–304, 2014.
134. Leguina-Ruzzi A, Vodičková A, Holendová B, Pavluch V, Tauber J, Engstová H, Dlasková A, and Ježek P. Glucose-induced expression of DAPIT in pancreatic β -cells. *Biomolecules* 10: 1026, 2020.
135. Lenzen S. Oxidative stress: the vulnerable beta-cell. *Biochem Soc Trans* 36: 343–347, 2008.
136. Lenzen S. Chemistry and biology of reactive species with special reference to the antioxidative defence status in pancreatic β -cells. *Biochim Biophys Acta Gen Subj* 1861: 1929–1942, 2017.
137. Lenzen S, Drinkgern J, and Tiedge M. Low antioxidant enzyme gene expression in pancreatic islets compared with various other mouse tissues. *Free Radic Biol Med* 20: 463–466, 1996.
138. Lenzen S, Formanek H, and Panten U. Signal function of metabolism of neutral amino acids and 2-keto acids for initiation of insulin secretion. *J Biol Chem* 257: 6631–6633, 1982.
139. Lenzen S, Schmidt W, and Panten U. Transamination of neutral amino acids and 2-keto acids in pancreatic B-cell mitochondria. *J Biol Chem* 260: 12629–12634, 1985.

140. Lenzen S, Schmidt W, Rustenbeck I, and Panten U. 2-ketoglutarate generation in pancreatic B-cell mitochondria regulates insulin secretory action of amino acids and 2-keto acids. *Biosci Rep* 6: 163–169, 1986.
141. Lewandowski SL, Cardone RL, Foster HR, Ho T, Potapenko E, Poudel C, VanDeusen HR, Sdao SM, Alves TC, Zhao X, Capozzi ME, de Souza AH, Jahan I, Thomas CJ, Nunemaker CS, Davis DB, Campbell JE, Kibbey RG, and Merrins MJ. Pyruvate kinase controls signal strength in the insulin secretory pathway. *Cell Metab* 32: 736.e5–750.e5, 2020.
142. Li N, Wu JX, Ding D, Cheng J, Gao N, and Chen L. Structure of a pancreatic ATP-sensitive potassium channel. *Cell* 168: 101.e10–110.e10, 2017.
143. Light PE, Manning Fox JE, Riedel MJ, and Wheeler MB. Glucagon-like peptide-1 inhibits pancreatic ATP-sensitive potassium channels via a protein kinase A- and ADP-dependent mechanism. *Mol Endocrinol* 16: 2135–2144, 2002.
144. Lin YF, Jan YN, and Jan LY. Regulation of ATP-sensitive potassium channel function by protein kinase A-mediated phosphorylation in transfected HEK293 cells. *EMBO J* 19: 942–955, 2000.
145. Liu T, Li H, Gouko NV, Zhou Z, Xu A, Hong W, and Han W. Detection of insulin granule exocytosis by an electrophysiology method with high temporal resolution reveals enlarged insulin granule pool in BIG3-knockout mice. *Am J Physiol Endocrinol Metab* 307: E611–E618, 2014.
146. Lorenz MA, El Azzouny MA, Kennedy RT, and Burant CF. Metabolome response to glucose in the β -cell line INS-1 832/13. *J Biol Chem* 288: 10923–10935, 2013.
147. Lu D, Mulder H, Zhao P, Burgess SC, Jensen MV, Kamzolova S, Newgard CB, and Sherry AD. ¹³C NMR isotopomer analysis reveals a connection between pyruvate cycling and glucose-stimulated insulin secretion (GSIS). *Proc Natl Acad Sci U S A* 99: 2708–2713, 2002.
148. MacDonald MJ and Fahien LA. Glutamate is not a messenger in insulin secretion. *J Biol Chem* 275: 34025–34027, 2000.
149. MacDonald MJ, Hasan NM, and Longacre MJ. Studies with leucine, beta-hydroxybutyrate and ATP citrate lyase-deficient beta cells support the acetoacetate pathway of insulin secretion. *Biochim Biophys Acta* 1780: 966–972, 2008.
150. MacDonald PE. Signal integration at the level of ion channel and exocytotic function in pancreatic β -cells. *Am J Physiol Endocrinol Metab* 301: E1065–E1069, 2011.
151. MacDonald PE, Salapatek AM, and Wheeler MB. Glucagon-like peptide-1 receptor activation antagonizes voltage-dependent repolarizing K(+) currents in beta-cells: a possible glucose-dependent insulinotropic mechanism. *Diabetes* 51(Suppl 3): S443–S447, 2002.
152. Maechler P. Mitochondrial function and insulin secretion. *Mol Cell Endocrinol* 379: 12–18, 2013.
153. Maechler P. Glutamate pathways of the beta-cell and the control of insulin secretion. *Diabetes Res Clin Pract* 131: 149–153, 2017.
154. Maechler P, Kennedy ED, Pozzan T, and Wollheim CB. Mitochondrial activation directly triggers the exocytosis of insulin in permeabilized pancreatic beta-cells. *EMBO J* 16: 3833–3841, 1997.
155. Maechler P and Wollheim CB. Mitochondrial glutamate acts as a messenger in glucose-induced insulin exocytosis. *Nature* 402: 685–689, 1999.
156. Maechler P and Wollheim CB. Mitochondrial function in normal and diabetic beta-cells. *Nature* 414: 807–812, 2001.
157. Mancini AD, Bertrand G, Vivot K, Carpentier É, Tremblay C, Ghislain J, Bouvier M, and Poitout V. β -Arrestin recruitment and biased agonism at free fatty acid receptor 1. *J Biol Chem* 290: 21131–21140, 2015.
158. Marshall BA, Tordjman K, Host HH, Ensor NJ, Kwon G, Marshall CA, Coleman T, McDaniel ML, and Semenkovich CF. Relative hypoglycemia and hyperinsulinemia in mice with heterozygous lipoprotein lipase (LPL) deficiency. Islet LPL regulates insulin secretion. *J Biol Chem* 274: 27426–27432, 1999.
159. Martin GM, Yoshioka C, Rex EA, Fay JF, Xie Q, Whorton MR, Chen JZ, and Shyng SL. Cryo-EM structure of the ATP-sensitive potassium channel illuminates mechanisms of assembly and gating. *Elife* 6: e24149, 2017.
160. Masgrau R, Churchill GC, Morgan AJ, Ashcroft SJ, and Galione A. NAADP: a new second messenger for glucose-induced Ca²⁺ responses in clonal pancreatic beta cells. *Curr Biol* 13: 247–251, 2003.
161. Masia R, Koster JC, Tumini S, Chiarelli F, Colombo C, Nichols CG, and Barbetti F. An ATP-binding mutation (G334D) in KCNJ11 is associated with a sulfonyleurea-insensitive form of developmental delay, epilepsy, and neonatal diabetes. *Diabetes* 56: 328–336, 2007.
162. Masiello P, Novelli M, Bombara M, Fierabracci V, Vittorini S, Prentki M, and Bergamini E. The antilipolytic agent 3,5-dimethylpyrazole inhibits insulin release in response to both nutrient secretagogues and cyclic adenosine monophosphate agonists in isolated rat islets. *Metabolism* 51: 110–114, 2002.
163. McClenaghan NH and Flatt PR. Glucose and non-glucidic nutrients exert permissive effects on 2-keto acid regulation of pancreatic beta-cell function. *Biochim Biophys Acta* 1426: 110–118, 1999.
164. McCormack JG, Halestrap AP, and Denton RM. Role of calcium ions in regulation of mammalian intramitochondrial metabolism. *Physiol Rev* 70: 391–425, 1990.
165. McKenna JP, Ha J, Merrins MJ, Satin LS, Sherman A, and Bertram R. Ca²⁺ effects on ATP production and consumption have regulatory roles on oscillatory islet activity. *Biophys J* 110: 733–742, 2016.
166. Mikhailov MV, Campbell JD, de Wet H, Shimomura K, Zadek B, Collins RF, Sansom MS, Ford RC, and Ashcroft FM. 3-D structural and functional characterization of the purified K_{ATP} channel complex Kir6.2-SUR1. *EMBO J* 24: 4166–4175, 2005.
167. Mitok KA, Freiburger EC, Schueler KL, Rabaglia ME, Stapleton DS, Kwiecien NW, Malec PA, Hebert AS, Broman AT, Kennedy RT, Keller MP, Coon JJ, and Attie AD. Islet proteomics reveals genetic variation in dopamine production resulting in altered insulin secretion. *J Biol Chem* 293: 5860–5877, 2018.
168. Miyahonara J, Kakae M, Nagayasu K, Nakagawa T, Mori Y, Arai K, Shirakawa H, and Kaneko S. TRPM2 channel aggravates CNS inflammation and cognitive impairment via activation of microglia in chronic cerebral hypoperfusion. *J Neurosci* 38: 3520–3533, 2018.
169. Montrose-Rafizadeh C, Avdonin P, Garant MJ, Rodgers BD, Kole S, Yang H, Levine MA, Schwindinger W, and Bernier M. Pancreatic glucagon-like peptide-1 receptor

- couples to multiple G proteins and activates mitogen-activated protein kinase pathways in Chinese hamster ovary cells. *Endocrinology* 140: 1132–1140, 1999.
170. Moon MJ, Park S, Kim DK, Cho EB, Hwang JI, Vaudry H, and Seong JY. Structural and molecular conservation of glucagon-like Peptide-1 and its receptor confers selective ligand-receptor interaction. *Front Endocrinol (Lausanne)* 3: 141, 2012.
 171. Moran BM, Abdel-Wahab YH, Flatt PR, and McKillop AM. Activation of GPR119 by fatty acid agonists augments insulin release from clonal β -cells and isolated pancreatic islets and improves glucose tolerance in mice. *Biol Chem* 395: 453–464, 2014.
 172. Moran BM, Abdel-Wahab YH, Flatt PR, and McKillop AM. Evaluation of the insulin-releasing and glucose-lowering effects of GPR120 activation in pancreatic β -cells. *Diabetes Obes Metab* 16: 1128–1139, 2014.
 173. Moss CE, Glass LL, Diakogiannaki E, Pais R, Lenaghan C, Smith DM, Wedin M, Bohlooly YM, Gribble FM, and Reimann F. Lipid derivatives activate GPR119 and trigger GLP-1 secretion in primary murine L-cells. *Peptides* 77: 16–20, 2016.
 174. Mugabo Y, Zhao S, Lamontagne J, Al-Mass A, Peyot ML, Corkey BE, Joly E, Madiraju SRM, and Prentki M. Metabolic fate of glucose and candidate signaling and excess-fuel detoxification pathways in pancreatic β -cells. *J Biol Chem* 292: 7407–7422, 2017.
 175. Mugabo Y, Zhao S, Seifried A, Gezzar S, Al-Mass A, Zhang D, Lamontagne J, Attane C, Poursharifi P, Iglesias J, Joly E, Peyot ML, Gohla A, Madiraju SR, and Prentki M. Identification of a mammalian glycerol-3-phosphate phosphatase: role in metabolism and signaling in pancreatic β -cells and hepatocytes. *Proc Natl Acad Sci U S A* 113: E430–E439, 2016.
 176. Mulder H, Yang S, Winzell MS, Holm C, and Ahrén B. Inhibition of lipase activity and lipolysis in rat islets reduces insulin secretion. *Diabetes* 53: 122–128, 2004.
 177. Müller TD, Finan B, Bloom SR, D'Alessio D, Drucker DJ, Flatt PR, Fritsche A, Gribble F, Grill HJ, Habener JF, Holst JJ, Langhans W, Meier JJ, Nauck MA, Perez-Tilve D, Pocai A, Reimann F, Sandoval DA, Schwartz TW, Seeley RJ, Stemmer K, Tang-Christensen M, Woods SC, DiMarchi RD, and Tschöp MH. Glucagon-like peptide 1 (GLP-1). *Mol Metab* 30: 72–130, 2019.
 178. Newman JC and Verdin E. β -Hydroxybutyrate: a signaling metabolite. *Annu Rev Nutr* 37: 51–76, 2017.
 179. Nichols CG. K_{ATP} channels as molecular sensors of cellular metabolism. *Nature* 440: 470–476, 2006.
 180. Noguchi S, Kondo Y, Ito R, Katayama T, Kazama S, Kadota Y, Kitaura Y, Harris RA, and Shimomura Y. Ca(2+)-dependent inhibition of branched-chain α -ketoacid dehydrogenase kinase by thiamine pyrophosphate. *Biochem Biophys Res Commun* 504: 916–920, 2018.
 181. Nunes Marsiglio-Libraires G, Aparecida Vilas-Boas E, Carlein C, Hoffmann MDA, Roma LP, and Carpinelli AR. Evidence for NADPH oxidase activation by GPR40 in pancreatic β -cells. *Redox Rep* 25: 41–50, 2020.
 182. Nyrén R, Chang CL, Lindström P, Barmina A, Vorrösjö E, Ali Y, Juntti-Berggren L, Bensadoun A, Young SG, Olivecrona T, and Olivecrona G. Localization of lipoprotein lipase and GPIHBP1 in mouse pancreas: effects of diet and leptin deficiency. *BMC Physiol* 12: 14, 2012.
 183. Odegaard ML, Joseph JW, Jensen MV, Lu D, Ilkayeva O, Ronnebaum SM, Becker TC, and Newgard CB. The mitochondrial 2-oxoglutarate carrier is part of a metabolic pathway that mediates glucose- and glutamine-stimulated insulin secretion. *J Biol Chem* 285: 16530–16537, 2010.
 184. Olofsson CS, Salehi A, Holm C, and Rorsman P. Palmitate increases L-type Ca^{2+} currents and the size of the readily releasable granule pool in mouse pancreatic beta-cells. *J Physiol* 557: 935–948, 2004.
 185. Ortiz D, Voyvodic P, Gossack L, Quast U, and Bryan J. Two neonatal diabetes mutations on transmembrane helix 15 of SUR1 increase affinity for ATP and ADP at nucleotide binding domain 2. *J Biol Chem* 287: 17985–17995, 2012.
 186. Ostapchenko VG, Chen M, Guzman MS, Xie YF, Lavine N, Fan J, Beraldo FH, Martyn AC, Belrose JC, Mori Y, MacDonald JF, Prado VF, Prado MA, and Jackson MF. The transient receptor potential melastatin 2 (TRPM2) channel contributes to β -amyloid oligomer-related neurotoxicity and memory impairment. *J Neurosci* 35: 15157–15169, 2015.
 187. Ould Amer Y and Hebert-Chatelain E. Mitochondrial cAMP-PKA signaling: what do we really know? *Biochim Biophys Acta Bioenerg* 1859: 868–877, 2018.
 188. Ouyang Q, Nakayama T, Baytas O, Davidson SM, Yang C, Schmidt M, Lizarraga SB, Mishra S, Ei-Quessny M, Niaz S, Gul Butt M, Imran Murtaza S, Javed A, Chaudhry HR, Vaughan DJ, Hill RS, Partlow JN, Yoo SY, Lam AT, Nasir R, Al-Saffar M, Barkovich AJ, Schwede M, Nagpal S, Rajab A, DeBerardinis RJ, Housman DE, Mochida GH, and Morrow EM. Mutations in mitochondrial enzyme GPT2 cause metabolic dysfunction and neurological disease with developmental and progressive features. *Proc Natl Acad Sci U S A* 113: E5598–E5607, 2016.
 189. Panten U, Früh E, Reckers K, and Rustenbeck I. Acute metabolic amplification of insulin secretion in mouse islets: role of cytosolic acetyl-CoA. *Metabolism* 65: 1225–1229, 2016.
 190. Panten U, Willenborg M, Schumacher K, Hamada A, Ghaly H, and Rustenbeck I. Acute metabolic amplification of insulin secretion in mouse islets is mediated by mitochondrial export of metabolites, but not by mitochondrial energy generation. *Metabolism* 62: 1375–1386, 2013.
 191. Pathak T and Trebak M. Mitochondrial Ca(2+) signaling. *Pharmacol Ther* 192: 112–123, 2018.
 192. Peyot ML, Guay C, Latour MG, Lamontagne J, Lussier R, Pineda M, Ruderman NB, Haemmerle G, Zechner R, Joly E, Madiraju SR, Poirout V, and Prentki M. Adipose triglyceride lipase is implicated in fuel- and non-fuel-stimulated insulin secretion. *J Biol Chem* 284: 16848–16859, 2009.
 193. Plecítá-Hlavatá L, Engstová H, Holendová B, Tauber J, Špaček T, Petrásková L, Křen V, Špačková J, Gotvaldová K, Ježek J, Dlasková A, Smolková K, and Ježek P. Mitochondrial superoxide production decreases on glucose-stimulated insulin secretion in pancreatic β cells due to decreasing mitochondrial matrix NADH/NAD(+) ratio. *Antioxid Redox Signal* 33: 789–815, 2020.
 194. Plecítá-Hlavatá L, Jaburek M, Holendová B, Tauber J, Pavluch V, Berkova Z, Cahova M, Schroeder K, Brandes RP, Siemen D, and Ježek P. Glucose-stimulated insulin secretion fundamentally requires H_2O_2 signaling by NADPH oxidase 4. *Diabetes* 69: 1341–1354, 2020.
 195. Pongratz RL, Kibbey RG, Shulman GI, and Cline GW. Cytosolic and mitochondrial malic enzyme isoforms dif-

- ferentially control insulin secretion. *J Biol Chem* 282: 200–207, 2007.
196. Prentki M, Joly E, El-Assaad W, and Roduit R. Malonyl-CoA signaling, lipid partitioning, and glucolipotoxicity: role in beta-cell adaptation and failure in the etiology of diabetes. *Diabetes* 51(Suppl 3): S405–S413, 2002.
 197. Prentki M, Matschinsky Franz M, and Madiraju SRM. Metabolic signaling in fuel-induced insulin secretion. *Cell Metab* 18: 162–185, 2013.
 198. Prentki M, Vischer S, Glennon MC, Regazzi R, Deeney JT, and Corkey BE. Malonyl-CoA and long chain acyl-CoA esters as metabolic coupling factors in nutrient-induced insulin secretion. *J Biol Chem* 267: 5802–5810, 1992.
 199. Proks P, Antcliff JF, Lippiat J, Gloyn AL, Hattersley AT, and Ashcroft FM. Molecular basis of Kir6.2 mutations associated with neonatal diabetes or neonatal diabetes plus neurological features. *Proc Natl Acad Sci U S A* 101: 17539–17544, 2004.
 200. Pujol JB, Christinat N, Ratinaud Y, Savoia C, Mitchell SE, and Dioum EHM. Coordination of GPR40 and ketogenesis signaling by medium chain fatty acids regulates beta cell function. *Nutrients* 10: 473, 2018.
 201. Qian J, Gu Y, Wu C, Yu F, Chen Y, Zhu J, Yao X, Bei C, and Zhu Q. Agonist-induced activation of human FFA1 receptor signals to extracellular signal-regulated kinase 1 and 2 through Gq- and Gi-coupled signaling cascades. *Cell Mol Biol Lett* 22: 13, 2017.
 202. Quan X, Nguyen TT, Choi SK, Xu S, Das R, Cha SK, Kim N, Han J, Wiederkehr A, Wollheim CB, and Park KS. Essential role of mitochondrial Ca²⁺ uniporter in the generation of mitochondrial pH gradient and metabolism-secretion coupling in insulin-releasing cells. *J Biol Chem* 290: 4086–4096, 2015.
 203. Ramzan R, Rhiel A, Weber P, Kadenbach B, and Vogt S. Reversible dimerization of cytochrome c oxidase regulates mitochondrial respiration. *Mitochondrion* 49: 149–155, 2019.
 204. Reinbothe TM, Ivarsson R, Li D-Q, Niazi O, Jing X, Zhang E, Stenson L, Bryborn U, and Renström E. Glutaredoxin-1 mediates NADPH-dependent stimulation of calcium-dependent insulin secretion. *Mol Endocrinol* 23: 893–900, 2009.
 205. Remedi MS, Koster JC, Patton BL, and Nichols CG. ATP-sensitive K⁺ channel signaling in glucokinase-deficient diabetes. *Diabetes* 54: 2925–2931, 2005.
 206. Remizov O, Jakubov R, Düfer M, Krippel Drews P, Drews G, Waring M, Brabant G, Wienbergen A, Rustenbeck I, and Schöfl C. Palmitate-induced Ca²⁺-signaling in pancreatic beta-cells. *Mol Cell Endocrinol* 212: 1–9, 2003.
 207. Ribas GS and Vargas CR. Evidence that oxidative imbalance and mitochondrial dysfunction are involved in the pathophysiology of fatty acid oxidation disorders. *Cell Mol Neurobiol* 2020, Sep 2. doi: 10.1007/s10571-020-00955-7.
 208. Roma LP and Jonas JC. Nutrient metabolism, subcellular redox state, and oxidative stress in pancreatic islets and beta-cells. *J Mol Biol* 432: 1461–1493, 2020.
 209. Ronnebaum SM, Ilkayeva O, Burgess SC, Joseph JW, Lu D, Stevens RD, Becker TC, Sherry AD, Newgard CB, and Jensen MV. A pyruvate cycling pathway involving cytosolic NADP-dependent isocitrate dehydrogenase regulates glucose-stimulated insulin secretion. *J Biol Chem* 281: 30593–30602, 2006.
 210. Rorsman P and Ashcroft FM. Pancreatic β -cell electrical activity and insulin secretion: of mice and men. *Physiol Rev* 98: 117–214, 2018.
 211. Rorsman P and Braun M. Regulation of insulin secretion in human pancreatic islets. *Annu Rev Physiol* 75: 155–179, 2013.
 212. Rorsman P, Braun M, and Zhang Q. Regulation of calcium in pancreatic α - and β -cells in health and disease. *Cell Calcium* 51: 300–308, 2012.
 213. Rorsman P, Eliasson L, Kanno T, Zhang Q, and Gopel S. Electrophysiology of pancreatic β -cells in intact mouse islets of Langerhans. *Prog Biophys Mol Biol* 107: 224–235, 2011.
 214. Rorsman P and Renström E. Insulin granule dynamics in pancreatic beta cells. *Diabetologia* 46: 1029–1045, 2003.
 215. Rorsman P and Trube G. Calcium and delayed potassium currents in mouse pancreatic beta-cells under voltage-clamp conditions. *J Physiol* 374: 531–550, 1986.
 216. Rosca M, Minkler P, and Hoppel CL. Cardiac mitochondria in heart failure: normal cardiolipin profile and increased threonine phosphorylation of complex IV. *Biochim Biophys Acta* 1807: 1373–1382, 2011.
 217. Rubi B, del Arco A, Bartley C, Satrustegui J, and Maechler P. The malate-aspartate NADH shuttle member Aralar1 determines glucose metabolic fate, mitochondrial activity, and insulin secretion in beta cells. *J Biol Chem* 279: 55659–55666, 2004.
 218. Rutter GA, Hodson DJ, Chabosseau P, Haythorne E, Pullen TJ, and Leclerc I. Local and regional control of calcium dynamics in the pancreatic islet. *Diabetes Obes Metab* 19(Suppl 1): 30–41, 2017.
 219. Rutter GA, Pralong WF, and Wollheim CB. Regulation of mitochondrial glycerol-phosphate dehydrogenase by Ca²⁺ within electroporated insulin-secreting cells (INS-1). *Biochim Biophys Acta* 1175: 107–113, 1992.
 220. Rydstrom J. Mitochondrial NADPH, transhydrogenase and disease. *Biochim Biophys Acta* 1757: 721–726, 2006.
 221. Sabourin J and Allagnat F. Store-operated Ca²⁺ entry: a key component of the insulin secretion machinery. *J Mol Endocrinol* 57: F35–F39, 2016.
 222. Sabrautzi S, Kaiser G, Przemek GKH, Gerst F, Lorza-Gil E, Panse M, Sartorius T, Hoene M, Marschall S, Haring HU, Hrabe de Angelis M, and Ullrich S. Point mutation of Ffar1 abrogates fatty acid-dependent insulin secretion, but protects against HFD-induced glucose intolerance. *Mol Metab* 6: 1304–1312, 2017.
 223. Sakaguchi R and Mori Y. Transient receptor potential (TRP) channels: biosensors for redox environmental stimuli and cellular status. *Free Radic Biol Med* 146: 36–44, 2020.
 224. Santo-Domingo J, Chareyron I, Dayon L, Núñez Galindo A, Cominetti O, Pilar Giner Giménez M, De Marchi U, Canto C, Kussmann M, and Wiederkehr A. Coordinated activation of mitochondrial respiration and exocytosis mediated by PKC signaling in pancreatic β cells. *FASEB J* 31: 1028–1045, 2017.
 225. Santos LRB, Muller C, de Souza AH, Takahashi HK, Spégel P, Sweet IR, Chae H, Mulder H, and Jonas J-C. NNT reverse mode of operation mediates glucose control of mitochondrial NADPH and glutathione redox state in mouse pancreatic β -cells. *Mol Metab* 6: 535–547, 2017.
 226. Sassmann A, Gier B, Gröne HJ, Drews G, Offermanns S, and Wettchurck N. The Gq/G11-mediated signaling

- pathway is critical for autocrine potentiation of insulin secretion in mice. *J Clin Invest* 120: 2184–2193, 2010.
227. Schuit F, De Vos A, Farfari S, Moens K, Pipeleers D, Brun T, and Prentki M. Metabolic fate of glucose in purified islet cells. Glucose-regulated anaplerosis in beta cells. *J Biol Chem* 272: 18572–18579, 1997.
 228. Schulla V, Renström E, Feil R, Feil S, Franklin I, Gjinovci A, Jing XJ, Laux D, Lundquist I, Magnuson MA, Obermüller S, Olofsson CS, Salehi A, Wendt A, Klugbauer N, Wollheim CB, Rorsman P, and Hofmann F. Impaired insulin secretion and glucose tolerance in beta cell-selective Ca(v)1.2 Ca²⁺ channel null mice. *EMBO J* 22: 3844–3854, 2003.
 229. Sener A, Conget I, Rasschaert J, Leclercq-Meyer V, Villanueva-Peñacarrillo ML, Valverde I, and Malaisse WJ. Insulinotropic action of glutamic acid dimethyl ester. *Am J Physiol* 267: E573–E584, 1994.
 230. Shen L, Zhi L, Hu W, and Wu MX. IEX-1 targets mitochondrial F1Fo-ATPase inhibitor for degradation. *Cell Death Differ* 16: 603–612, 2009.
 231. Shigeto M, Ramracheya R, Tarasov AI, Cha CY, Chibalina MV, Hastoy B, Philippaert K, Reinbothe T, Rorsman N, Salehi A, Sones WR, Vergari E, Weston C, Gorelik J, Katsura M, Nikolaev VO, Vennekens R, Zaccolo M, Galione A, Johnson PR, Kaku K, Ladds G, and Rorsman P. GLP-1 stimulates insulin secretion by PKC-dependent TRPM4 and TRPM5 activation. *J Clin Invest* 125: 4714–4728, 2015.
 232. Shimomura K, de Nancrales GP, Foutinou C, Caimari M, Castaño L, and Ashcroft FM. The first clinical case of a mutation at residue K185 of Kir6.2 (KCNJ11): a major ATP-binding residue. *Diabet Med* 27: 225–229, 2010.
 233. Shyng S, Ferrigni T, and Nichols CG. Regulation of K_{ATP} channel activity by diazoxide and MgADP. Distinct functions of the two nucleotide binding folds of the sulfonylurea receptor. *J Gen Physiol* 110: 643–654, 1997.
 234. Shyng SL and Nichols CG. Membrane phospholipid control of nucleotide sensitivity of K_{ATP} channels. *Science* 282: 1138–1141, 1998.
 235. Smith PA, Ashcroft FM, and Rorsman P. Simultaneous recordings of glucose dependent electrical activity and ATP-regulated K(+) currents in isolated mouse pancreatic beta-cells. *FEBS Lett* 261: 187–190, 1990.
 236. Somanath S, Partridge CJ, Marshall C, Rowe T, and Turner MD. Snapin mediates insulin secretory granule docking, but not trans-SNARE complex formation. *Biochem Biophys Res Commun* 473: 403–407, 2016.
 237. Song WJ, Seshadri M, Ashraf U, Mdluli T, Mondal P, Keil M, Azevedo M, Kirschner LS, Stratakis CA, and Hussain MA. Snapin mediates incretin action and augments glucose-dependent insulin secretion. *Cell Metab* 13: 308–319, 2011.
 238. Sonoda N, Imamura T, Yoshizaki T, Babendure JL, Lu JC, and Olefsky JM. Beta-Arrestin-1 mediates glucagon-like peptide-1 signaling to insulin secretion in cultured pancreatic beta cells. *Proc Natl Acad Sci U S A* 105: 6614–6619, 2008.
 239. Soty M, Visa M, Soriano S, del Carmen Carmona M, Nadal Á, and Novials A. Involvement of ATP-sensitive potassium (K_{ATP}) channels in the loss of beta-cell function induced by human islet amyloid polypeptide. *J Biol Chem* 286: 40857–40866, 2011.
 240. Spégel P and Mulder H. Metabolomics analysis of nutrient metabolism in β -cells. *J Mol Biol* 432: 1429–1445, 2020.
 241. Spégel P, Sharoyko VV, Goehring I, Danielsson AP, Malmgren S, Nagorny CL, Andersson LE, Koeck T, Sharp GW, Straub SG, Wollheim CB, and Mulder H. Time-resolved metabolomics analysis of β -cells implicates the pentose phosphate pathway in the control of insulin release. *Biochem J* 450: 595–605, 2013.
 242. Speier S, Yang SB, Sroka K, Rose T, and Rupnik M. K_{ATP}-channels in beta-cells in tissue slices are directly modulated by millimolar ATP. *Mol Cell Endocrinol* 230: 51–58, 2005.
 243. Srinivasan S, Spear J, Chandran K, Joseph J, Kalyanaraman B, and Avadhani NG. Oxidative stress induced mitochondrial protein kinase A mediates cytochrome c oxidase dysfunction. *PLoS One* 8: e77129, 2013.
 244. Stegink LD, Filer LJ, Jr., and Baker GL. Plasma amino acid concentrations in normal adults fed meals with added monosodium L-glutamate and aspartame. *J Nutr* 113: 1851–1860, 1983.
 245. Stein DT, Stevenson BE, Chester MW, Basit M, Daniels MB, Turley SD, and McGarry JD. The insulinotropic potency of fatty acids is influenced profoundly by their chain length and degree of saturation. *J Clin Invest* 100: 398–403, 1997.
 246. Stuhlmann T, Planells-Cases R, and Jentsch TJ. LRRC8/VRAC anion channels enhance β -cell glucose sensing and insulin secretion. *Nat Commun* 9: 1974, 2018.
 247. Sumoza-Toledo A and Penner R. TRPM2: a multifunctional ion channel for calcium signalling. *J Physiol* 589: 1515–1525, 2011.
 248. Swisa A, Glaser B, and Dor Y. Metabolic stress and compromised identity of pancreatic beta cells. *Front Genet* 8: 21, 2017.
 249. Szollosi A, Nenquin M, and Henquin J. Pharmacological stimulation and inhibition of insulin secretion in mouse islets lacking ATP-sensitive K⁺ channels. *Br J Pharmacol* 159: 669–677, 2010.
 250. Takahashi H, Yokoi N, and Seino S. Glutamate as intracellular and extracellular signals in pancreatic islet functions. *Proc Jpn Acad Ser B Phys Biol Sci* 95: 246–260, 2019.
 251. Tarasov AI, Girard CA, and Ashcroft FM. ATP sensitivity of the ATP-sensitive K⁺ channel in intact and permeabilized pancreatic beta-cells. *Diabetes* 55: 2446–2454, 2006.
 252. Tarasov AI, Semplici F, Li D, Rizzuto R, Ravier MA, Gilon P, and Rutter GA. Frequency-dependent mitochondrial Ca(2+) accumulation regulates ATP synthesis in pancreatic β cells. *Pflugers Arch* 465: 543–554, 2013.
 253. Tarasov AI, Semplici F, Ravier MA, Bellomo EA, Pullen TJ, Gilon P, Sekler I, Rizzuto R, and Rutter GA. The mitochondrial Ca²⁺ uniporter MCU is essential for glucose-induced ATP increases in pancreatic β -cells. *PLoS One* 7: e39722, 2012.
 254. Teraoku H and Lenzen S. Dynamics of insulin secretion from EndoC- β H1 β -cell pseudoislets in response to glucose and other nutrient and nonnutrient secretagogues. *J Diabetes Res* 2017: 2309630, 2017.
 255. Thompson A and Kanamarlapudi V. Agonist-induced internalisation of the glucagon-like peptide-1 receptor is mediated by the G α_q pathway. *Biochem Pharmacol* 93: 72–84, 2015.
 256. Tomita T, Hosoda K, Fujikura J, Inagaki N, and Nakao K. The G-protein-coupled long-chain fatty acid receptor GPR40 and glucose metabolism. *Front Endocrinol (Lausanne)* 5: 152, 2014.

257. Toye AA, Lippiat JD, Proks P, Shimomura K, Bentley L, Hugill A, Mijat V, Goldsworthy M, Moir L, Haynes A, Quarterman J, Freeman HC, Ashcroft FM, and Cox RD. A genetic and physiological study of impaired glucose homeostasis control in C57BL/6J mice. *Diabetologia* 48: 675–686, 2005.
258. Tsuboi T, da Silva Xavier G, Holz GG, Jouaville LS, Thomas AP, and Rutter GA. Glucagon-like peptide-1 mobilizes intracellular Ca²⁺ and stimulates mitochondrial ATP synthesis in pancreatic MIN6 beta-cells. *Biochem J* 369: 287–299, 2003.
259. Usui R, Yabe D, Fauzi M, Goto H, Botagarova A, Tokumoto S, Tatsuoka H, Tahara Y, Kobayashi S, Manabe T, Baba Y, Kurosaki T, Herrera PL, Ogura M, Nagashima K, and Inagaki N. GPR40 activation initiates store-operated Ca(2+) entry and potentiates insulin secretion via the IP3R1/STIM1/Orai1 pathway in pancreatic β -cells. *Sci Rep* 9: 15562, 2019.
260. Vakilian M, Tahamtani Y, and Ghaedi K. A review on insulin trafficking and exocytosis. *Gene* 706: 52–61, 2019.
261. van der Vusse GJ. Albumin as fatty acid transporter. *Drug Metab Pharmacokinet* 24: 300–307, 2009.
262. Vedovato N, Rorsman O, Hennis K, Ashcroft FM, and Proks P. Role of the C-terminus of SUR in the differential regulation of β -cell and cardiac K(ATP) channels by MgADP and metabolism. *J Physiol* 596: 6205–6217, 2018.
263. Veprik A, Laufer D, Weiss S, Rubins N, and Walker MD. GPR41 modulates insulin secretion and gene expression in pancreatic β -cells and modifies metabolic homeostasis in fed and fasting states. *FASEB J* 30: 3860–3869, 2016.
264. Vierra NC, Dadi PK, Jeong I, Dickerson M, Powell DR, and Jacobson DA. Type 2 diabetes-associated K⁺ channel TALK-1 modulates β -cell electrical excitability, second-phase insulin secretion, and glucose homeostasis. *Diabetes* 64: 3818–3828, 2015.
265. Vierra NC, Dickerson MT, Philipson LH, and Jacobson DA. Simultaneous real-time measurement of the β -cell membrane potential and Ca(2+) influx to assess the role of potassium channels on β -cell function. *Methods Mol Biol* 1684: 73–84, 2018.
266. Vollmer K, Holst JJ, Baller B, Ellrichmann M, Nauck MA, Schmidt WE, and Meier JJ. Predictors of incretin concentrations in subjects with normal, impaired, and diabetic glucose tolerance. *Diabetes* 57: 678–687, 2008.
267. Walker JN, Ramracheya R, Zhang Q, Johnson PR, Braun M, and Rorsman P. Regulation of glucagon secretion by glucose: paracrine, intrinsic or both? *Diabetes Obes Metab* 13(Suppl 1): 95–105, 2011.
268. Watmough NJ and Frerman FE. The electron transfer flavoprotein: ubiquinone oxidoreductases. *Biochim Biophys Acta* 1797: 1910–1916, 2010.
269. Weissert V, Rieger B, Morris S, Arroum T, Psathaki OE, Zobel T, Perkins G, and Busch KB. Inhibition of the mitochondrial ATPase function by IF1 changes the spatiotemporal organization of ATP synthase. *Biochim Biophys Acta Bioenerg* 1862: 148322, 2021.
270. Welsh N, Margulis B, Borg LA, Wiklund HJ, Saldeen J, Flodström M, Mello MA, Andersson A, Pipeleers DG, and Hellerström C. Differences in the expression of heat-shock proteins and antioxidant enzymes between human and rodent pancreatic islets: implications for the pathogenesis of insulin-dependent diabetes mellitus. *Mol Med* 1: 806–820, 1995.
271. Wiederkehr A, Szanda G, Akhmedov D, Matakı C, Heizmann CW, Schoonjans K, Pozzan T, Spät A, and Wollheim CB. Mitochondrial matrix calcium is an activating signal for hormone secretion. *Cell Metab* 13: 601–611, 2011.
272. Winzell MS, Ström K, Holm C, and Ahrén B. Glucose-stimulated insulin secretion correlates with beta-cell lipolysis. *Nutr Metab Cardiovasc Dis* 16(Suppl 1): S11–S16, 2006.
273. Wong N, Blair AR, Morahan G, and Andrikopoulos S. The deletion variant of nicotinamide nucleotide transhydrogenase (Nnt) does not affect insulin secretion or glucose tolerance. *Endocrinology* 151: 96–102, 2010.
274. Woo HA, Yim SH, Shin DH, Kang D, Yu DY, and Rhee SG. Inactivation of peroxiredoxin I by phosphorylation allows localized H₂O₂ accumulation for cell signaling. *Cell* 140: 517–528, 2010.
275. Wooten D, Reynolds CA, Smith KJ, Mobarec JC, Koole C, Savage EE, Pabreja K, Simms J, Sridhar R, Furness SGB, Liu M, Thompson PE, Miller LJ, Christopoulos A, and Sexton PM. The extracellular surface of the GLP-1 receptor is a molecular trigger for biased agonism. *Cell* 165: 1632–1643, 2016.
276. Yamada H, Yoshida M, Ito K, Dezaki K, Yada T, Ishikawa SE, and Kakei M. Potentiation of glucose-stimulated insulin secretion by the GPR40-PLC-TRPC pathway in pancreatic β -cells. *Sci Rep* 6: 25912, 2016.
277. Yang HQ, Martinez-Ortiz W, Hwang J, Fan X, Cardozo TJ, and Coetzee WA. Palmitoylation of the K(ATP) channel Kir6.2 subunit promotes channel opening by regulating PIP(2) sensitivity. *Proc Natl Acad Sci U S A* 117: 10593–10602, 2020.
278. Yang J, Chi Y, Burkhardt BR, Guan Y, and Wolf BA. Leucine metabolism in regulation of insulin secretion from pancreatic beta cells. *Nutr Rev* 68: 270–279, 2010.
279. Yang RZ, Park S, Reagan WJ, Goldstein R, Zhong S, Lawton M, Rajamohan F, Qian K, Liu L, and Gong DW. Alanine aminotransferase isoenzymes: molecular cloning and quantitative analysis of tissue expression in rats and serum elevation in liver toxicity. *Hepatology* 49: 598–607, 2009.
280. Yang SN, Shi Y, Yang G, Li Y, Yu J, and Berggren PO. Ionic mechanisms in pancreatic β cell signaling. *Cell Mol Life Sci* 71: 4149–4177, 2014.
281. Yashiro H, Tsujihata Y, Takeuchi K, Hazama M, Johnson PR, and Rorsman P. The effects of TAK-875, a selective G protein-coupled receptor 40/free fatty acid 1 agonist, on insulin and glucagon secretion in isolated rat and human islets. *J Pharmacol Exp Ther* 340: 483–489, 2012.
282. Yasuda T, Shibasaki T, Minami K, Takahashi H, Mizoguchi A, Uriu Y, Numata T, Mori Y, Miyazaki J, Miki T, and Seino S. Rim2alpha determines docking and priming states in insulin granule exocytosis. *Cell Metab* 12: 117–129, 2010.
283. Yasui S, Mawatari K, Morizumi R, Furukawa H, Shimohata T, Harada N, Takahashi A, and Nakaya Y. Hydrogen peroxide inhibits insulin-induced ATP-sensitive potassium channel activation independent of insulin signaling pathway in cultured vascular smooth muscle cells. *J Med Invest* 59: 36–44, 2012.
284. Yoshida M, Dezaki K, Yamato S, Aoki A, Sugawara H, Toyoshima H, Ishikawa SE, Kawakami M, Nakata M, Yada T, and Kakei M. Regulation of voltage-gated K⁺ channels by glucose metabolism in pancreatic beta-cells. *FEBS Lett* 583: 2225–2230, 2009.

285. Yosida M, Dezaki K, Uchida K, Kodera S, Lam NV, Ito K, Rita RS, Yamada H, Shimomura K, Ishikawa SE, Sugawara H, Kawakami M, Tominaga M, Yada T, and Kakei M. Involvement of cAMP/EPAC/TRPM2 activation in glucose- and incretin-induced insulin secretion. *Diabetes* 63: 3394–3403, 2014.
286. Zhang F, Qi Y, Zhou K, Zhang G, Linask K, and Xu H. The cAMP phosphodiesterase Prune localizes to the mitochondrial matrix and promotes mtDNA replication by stabilizing TFAM. *EMBO Rep* 16: 520–527, 2015.
287. Zhang F, Zhang L, Qi Y, and Xu H. Mitochondrial cAMP signaling. *Cell Mol Life Sci* 73: 4577–4590, 2016.
288. Zhang L, Duan X, Sun W, and Sun H. Perfluorooctane sulfonate acute exposure stimulates insulin secretion via GPR40 pathway. *Sci Total Environ* 726: 138498, 2020.
289. Zhang Q, Chibalina MV, Bengtsson M, Groschner LN, Ramracheya R, Rorsman NJ, Leiss V, Nassar MA, Welling A, Gribble FM, Reimann F, Hofmann F, Wood JN, Ashcroft FM, and Rorsman P. Na⁺ current properties in islet α - and β -cells reflect cell-specific Scn3a and Scn9a expression. *J Physiol* 592: 4677–4696, 2014.
290. Zhang Z, Liew CW, Handy DE, Zhang Y, Leopold JA, Hu J, Guo L, Kulkarni RN, Loscalzo J, and Stanton RC. High glucose inhibits glucose-6-phosphate dehydrogenase, leading to increased oxidative stress and beta-cell apoptosis. *FASEB J* 24: 1497–1505, 2010.
291. Zhao S, Mugabo Y, Iglesias J, Xie L, Delghingaro-Augusto V, Lussier R, Peyot ML, Joly E, Taib B, Davis MA, Brown JM, Abousalham A, Gaisano H, Madiraju SR, and Prentki M. α/β -Hydrolase domain-6-accessible monoacylglycerol controls glucose-stimulated insulin secretion. *Cell Metab* 19: 993–1007, 2014.
292. Zhao X, León IR, Bak S, Mogensen M, Wrzesinski K, Højlund K, and Jensen ON. Phosphoproteome analysis of functional mitochondria isolated from resting human muscle reveals extensive phosphorylation of inner membrane protein complexes and enzymes. *Mol Cell Proteomics* 10: M110.000299, 2011.

Address correspondence to:

Dr. Petr Ježek

Department of Mitochondrial Physiology

Institute of Physiology of the Czech Academy of Sciences

No. 75, Vídeňská 1083, Prague 14220

Czech Republic

E-mail: jezek@biomed.cas.cz

Date of first submission to ARS Central, May 27, 2021; date of acceptance, June 16, 2021.

Abbreviations Used

2OG = 2-oxoglutarate
 2OGC = 2-oxoglutarate carrier, mitochondrial
 2OGDH = 2-oxoglutarate dehydrogenase
 β -OHB = β -hydroxybutyrate
 β -OHBHDH = β -hydroxybutyrate dehydrogenase
 ABHD6 = alpha/beta-hydrolase domain containing 6, monoacylglycerol lipase

ACAA = acetyl-CoA acyltransferase
 AcAc = acetoacetate
 AcAcCoA = acetoacetyl-CoA
 ACAT = acetyl-CoA acetyltransferase
 ACC = acetyl-CoA carboxylase
 AcCoA = acetyl-CoA
 ACL = ATP citrate lyase
 ACO = aconitase
 ACSL = long-chain acyl-CoA synthetase
 AGC1 = aspartate–glutamate antiporter SLC25A12 (Aralar)
 AGPAT = 1-acylglycerol-3-phosphate acyltransferase
 ALT = alanine aminotransferase (aka glutamate pyruvate transaminase, GPT)
 Aralar = aspartate–glutamate antiporter SLC25A12 (AGC1)
 AST = aspartate aminotransferase (aka glutamate oxaloacetate transaminase, GOT)
 ATGL = adipose triglyceride lipase
 BCAA = branched-chain amino acid
 BCAT2 = branched-chain amino acid transferase 2, mitochondrial
 BCKA = branched-chain ketoacid
 BCKDH = branched-chain ketoacid dehydrogenase
 Ca_L = voltage-dependent Ca²⁺ channels of L-type
 CaMKII = Ca²⁺/calmodulin-dependent protein kinase II
 CAT = carnitine acyl transferase
 Ca_V = voltage-dependent Ca²⁺ channels
 CGI = comparative gene identification 58, ATGL co-activator (aka ABDH5)
 Cit C = citrate carrier, mitochondrial
 CoA = coenzyme-A
 CS = citrate synthase
 DAG = diacylglycerol
 DAT, DGAT = diacylglycerol O-acyltransferase
 EPAC = exchange proteins directly activated by cAMP
 ER = endoplasmic reticulum
 ERK = extracellular regulated kinase
 ETF = electron transfer flavoprotein
 ETF:QOR = electron transfer flavoprotein: quinone oxidoreductase
 F6P = fructose-6-phosphate
 FA = fatty acid
 FASIS = fatty acid-stimulated insulin secretion
 FASN = fatty acid synthase
 FH = fumarate hydratase
 FUM = fumarate
 G6P = glucose-6-phosphate
 G6PDH = glucose-6-phosphate dehydrogenase
 GAD = glutamate decarboxylase
 GC1 = glutamate carrier
 GDH = glutamate dehydrogenase
 GLP-1 = glucagon-like peptide 1
 GLPIR = glucagon-like peptide 1 receptor

Abbreviations Used (Cont.)

GLS = glutaminase
 GLUT = glucose transporter
 glycerol3P = glycerol-3-phosphate
 GPAT1,2 = glycerol-3-phosphate acyltransferase 1,2
 GPAT3,4 = glycerol-3-phosphate acyltransferase 3,4 (1-acylglycerol-3-phosphate O-acyltransferase)
 GPR = G-protein-coupled receptor
 GPT = glutamate pyruvate transaminase
 GSIS = glucose-stimulated insulin secretion
 HMG-CoA = hydroxymethyl-glutaryl-CoA
 HMGCAL = hydroxymethyl-glutaryl-CoA lyase
 HSL = hormone-sensitive lipase
 IC = isocitrate
 ICS = intracrystal space
 IDH1 = isocitrate dehydrogenase 1, cytosolic NADP⁺ dependent
 IDH2 = isocitrate dehydrogenase 2, mitochondrial NADP⁺ dependent
 IDH3 = isocitrate dehydrogenase 3, cytosolic NAD⁺ dependent
 IF1 = ATPase inhibitory factor 1 (*i.e.*, ATP synthase inhibitory factor 1)
 IGV = insulin granule vesicle
 IMM = inner mitochondrial membrane
 IP3 = inositol-1,4,5-triphosphate
 IP3R = inositol-1,4,5-triphosphate receptor
 iPLA2 γ = Ca²⁺-independent phospholipase A2 isoform γ (PNPLA8)
 K_{ATP} = ATP-sensitive K⁺ channel
 KIC = 2-ketoisocaproate
 KIV = 2-ketoisovalerate
 KMV = 2-ketoisomethylvalerate
 LysoPhA = lysophosphatidic acid
 MAG = monoacylglycerol
 MAL = malate
 MAS = malate/aspartate shuttle
 MCU = mitochondrial calcium uniporter
 MDH = malate dehydrogenase
 ME1 = malic enzyme 1, cytosolic
 ME3 = malic enzyme 3, mitochondrial
 MODY = maturity-onset diabetes of the young
 NBF = nucleotide-binding fold
 NCLX = mitochondrial sodium calcium exchanger
 NNT = nicotinamide nucleotide transhydrogenase

NOX4 = NADPH oxidase 4
 NSCC = nonspecific calcium channels
 OAA = oxaloacetate
 OCR = oxygen consumption rate
 OMM = outer mitochondrial membrane
 Orai1 = calcium release-activated calcium modulator 1
 OXPHOS = oxidative phosphorylation
 PC = pyruvate carboxylase
 PDH = pyruvate dehydrogenase
 PEP = phosphoenolpyruvate
 PEPCK2 = phosphoenolpyruvate-carboxykinase 2
 PhA = phosphatidic acid
 PI = pancreatic islets
 PIP₂ = phosphatidylinositol 4,5-bisphosphate
 PK = pyruvate kinase
 PKA = protein kinase A
 PKC = protein kinase C
 PKL = pyruvate kinase isoform L
 PKM2 = pyruvate kinase isoform recruitable M2
 PLC = phospholipase C
 PMCA = plasma membrane Ca²⁺ATPase
 PPP = pentose phosphate pathway
 PyrC = pyruvate carrier, mitochondrial
 Q = ubiquinone
 QH₂ = ubiquinol
 Rap2 = Ras-related protein 2
 RC = respiratory chain
 RyR = ryanodine receptor
 sAC = soluble adenylyl cyclase
 S-CoA = succinyl-CoA
 SCoA:3oxoAcCoAT = succinyl-CoA:3-ketoacid-CoA transferase
 SERCA = sarco/endoplasmic reticulum Ca²⁺-ATPase
 SNAP-25 = synaptosomal nerve-associated protein 25
 SNARE = soluble N-ethylmaleimide-sensitive factor (NSF) attachment protein receptor
 SUCC = succinate
 SUR1 = sulfonylurea receptor 1
 TG = triglycerides
 tmAC = transmembrane adenylyl cyclase
 TRPC = transient receptor potential canonical
 TRPM = transient receptor potential melastin
 TRPV = transient receptor potential vanilloid